Structural and Vibrational Properties of Lanthanide Lindqvist Polyoxometalate Complexes

Primadi J. Subintoro[1] and Korey P. Carter[1*]
[1]Department of Chemistry, University of Iowa, Iowa City, IA 52242, United States

Table of Contents

Supporting Information

Table S1. Crystallographic parameters for complexes **1-14** (LaW_{10} – LuW_{10}).

Formula	$Na_9LaW_{10}O_{36}$ •$34H_2O$ (**1**)	$Na_9CeW_{10}O_{36}$ •$28H_2O$ (**2**)	$Na_9PrW_{10}O_{36}$ •$29H_2O$ (**3**)	$Na_9NdW_{10}O_{36}$ •$32H_2O$ (**4**)	$Na_9SmW_{10}O_{36}$ •$36H_2O$ (**5**)	$Na_9EuW_{10}O_{36}$ •$36H_2O$ (**6**)	$Na_9GdW_{10}O_{36}$ •$36H_2O$ (**7**)
Mr	3304.32	3209.53	3228.72	3269.65	3347.76	3349.37	3354.66
SG	P-1	P-1	P-1	P-1	P-1	P-1	P-1
a (Å)	12.8892 (13)	12.8331 (6)	12.8137 (6)	12.7722 (5)	12.9063 (17)	12.9037 (5)	12.8985 (5)
b (Å)	12.9526 (12)	12.9660 (6)	12.9517 (7)	13.0343 (6)	13.1156 (15)	13.1129 (5)	13.1035 (3)
c (Å)	20.1296 (19)	20.1117 (10)	20.0978 (12)	19.6802 (8)	20.911 (3)	20.8991 (7)	20.9180 (8)
α (°)	102.062 (4)	101.615 (2)	101.581 (2)	98.160 (2)	76.931 (5)	77.072 (1)	77.025 (1)
β (°)	97.834 (4)	98.179 (2)	98.253 (2)	102.820 (2)	83.975 (5)	83.923 (2)	83.922 (1)
γ (°)	101.546 (4)	101.864 (2)	101.755 (2)	101.538 (2)	77.418 (5)	77.463 (2)	77.519 (1)
V(Å^3)	3163.8 (5)	3148.5 (3)	3139.3 (3)	3070.0 (2)	3359.4 (7)	3358.3 (2)	3357.7 (2)
R_{int}	0.0839	0.0969	0.0878	0.1081	0.0945	0.0861	0.0703
R1	0.0512	0.0489	0.0451	0.0339	0.0361	0.0426	0.0412
wR2	0.1202	0.1264	0.1181	0.0899	0.0865	0.1012	0.0882
GooF	1.200	1.075	1.115	1.041	1.121	1.100	1.148
Mu (mm^{-1})	18.947	19.071	19.18	19.670	18.086	18.151	18.208
F000	2912	2818	2838	2878	2954	2956	2958
Z	2	2	2	2	2	2	2
Density (g/cm^3)	3.469	3.385	3.416	3.537	3.310	3.312	3.318
Temperature (K)	100 (2)	100 (2)	100 (2)	100 (2)	100 (2)	100 (2)	100 (2)
Wavelength (Å)	0.71073	0.71073	0.71073	0.71073	0.71073	0.71073	0.71073

Formula	$Na_9TbW_{10}O_{36}$ •$37H_2O$ (**8**)	$Na_9DyW_{10}O_{36}$ •$35H_2O$ (**9**)	$Na_9HoW_{10}O_{36}$ •$35H_2O$ (**10**)	$Na_9ErW_{10}O_{36}$ •$35H_2O$ (**11**)	$Na_9TmW_{10}O_{36}$ •$35H_2O$ (**12**)	$Na_9YbW_{10}O_{36}$ •$37H_2O$ (**13**)	$Na_9LuW_{10}O_{36}$ •$32H_2O$ (**14**)
Mr	3372.33	3343.91	3346.34	3364.67	3350.34	3387.25	3356.38
SG	P-1	P-1	P-1	P-1	P-1	P-1	P-1
a (Å)	12.8721 (6)	12.7414 (5)	12.727 (3)	12.7343 (9)	12.8752 (9)	12.8747 (6)	12.7347 (7)
b (Å)	13.0881 (7)	13.0651 (5)	13.063 (5)	13.0518 (8)	13.0761 (9)	13.0649 (6)	13.0458 (7)
c (Å)	20.8876 (11)	20.4611 (9)	20.465 (7)	20.4813 (15)	20.8761 (12)	20.9095 (9)	20.4697 (12)
α (°)	77.102 (2)	82.874 (2)	82.848 (7)	82.805 (3)	77.097 (2)	77.190 (2)	82.887 (2)
β (°)	83.865 (2)	74.520 (2)	74.548 (8)	74.496 (3)	83.853 (2)	83.860 (2)	74.479 (2)
γ (°)	77.384 (2)	88.910 (2)	88.878 (11)	88.750 (3)	77.351 (3)	77.461 (2)	88.659 (2)
V (Å^3)	3341.1 (3)	3256.8 (2)	3253.4 (18)	3254.2 (4)	3336.5 (4)	3341.3 (3)	3251.3 (3)
R_{int}	0.1072	0.0933	0.0898	0.0967	0.0953	0.0608	0.0895
R1	0.0471	0.0267	0.0326	0.0758	0.0359	0.0315	0.0360
wR2	0.1143	0.0585	0.0764	0.1600	0.0848	0.0745	0.0807
GooF	1.1129	1.021	1.111	1.230	1.105	1.135	1.100
Mu (mm^{-1})	18.366	18.899	18.986	19.058	18.657	18.706	19.300
F000	2976	2946	2948	2966	2952	2987	2956
Z	2	2	2	2	2	2	2
Density (g/cm^3)	3.352	3.410	3.416	3.434	3.335	3.367	3.428
Temperature (K)	100 (2)	100 (2)	100 (2)	100 (2)	100 (2)	100 (2)	100 (2)
Wavelength (Å)	0.71073	0.71073	0.71073	0.71073	0.71073	0.71073	0.71073

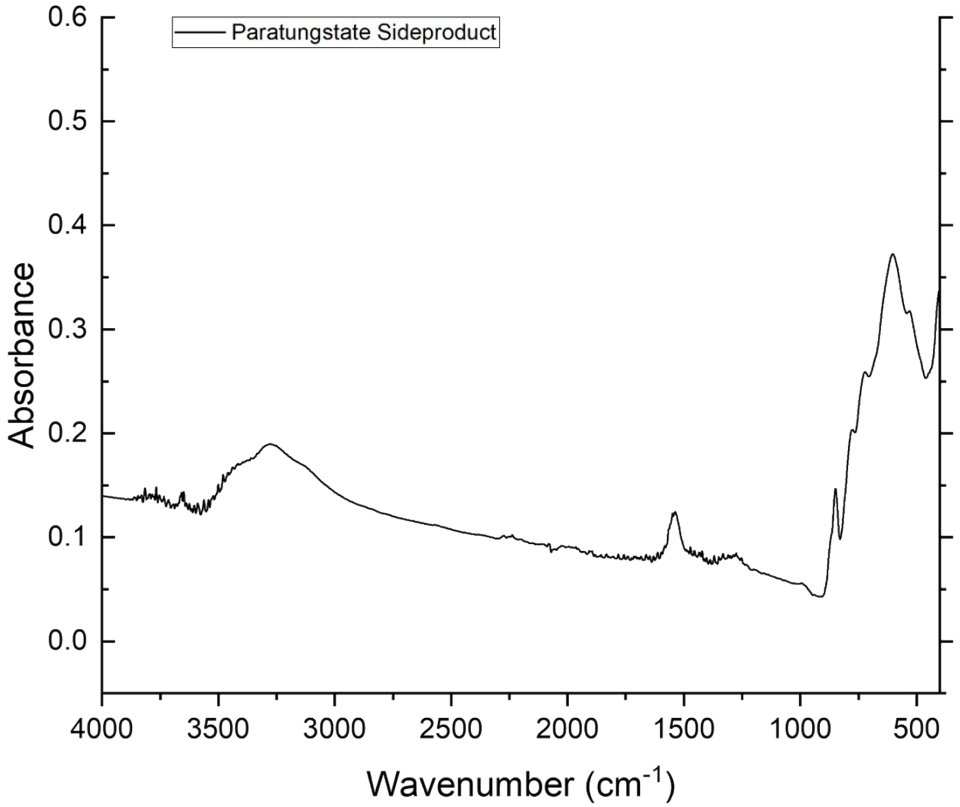

Figure S1. MIR spectra of sodium paratungstate ($Na_{10}H_2W_{12}O_{40}$•XH_2O) side product formed during synthesis of LnW_{10} complexes using method from Peacock and Weakly.

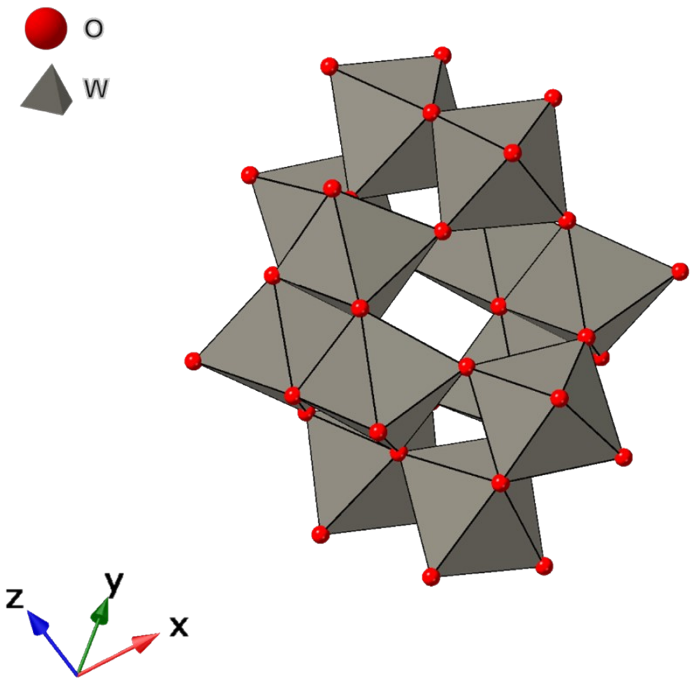

Figure S2. Polyhedral representation of sodium paratungstate ($Na_{10}W_{12}O_{40}$•$21H_2O$), the byproduct of the LnW_{10} synthesis formed when using the protocol from Peacock and Weakley. Sodium cations and lattice water molecules have been excluded for clarity.

Table S2. Crystallographic parameters for sodium paratungstate.

Formula	$Na_{10}W_{12}O_{40}$•$21H_2O$
Mr	3411.98
SG	P-1
a(Å)	11.772
b(Å)	12.428
c(Å)	22.015
α	86.357
β	86.659
γ	66.438
V(Å^3)	2944.4
Rint	0.0505
R1	0.1153
wR2	0.2852
GooF	1.182
Mu	23.525
F000	2972
Z	2
Dx (g/cm^3)	3.848

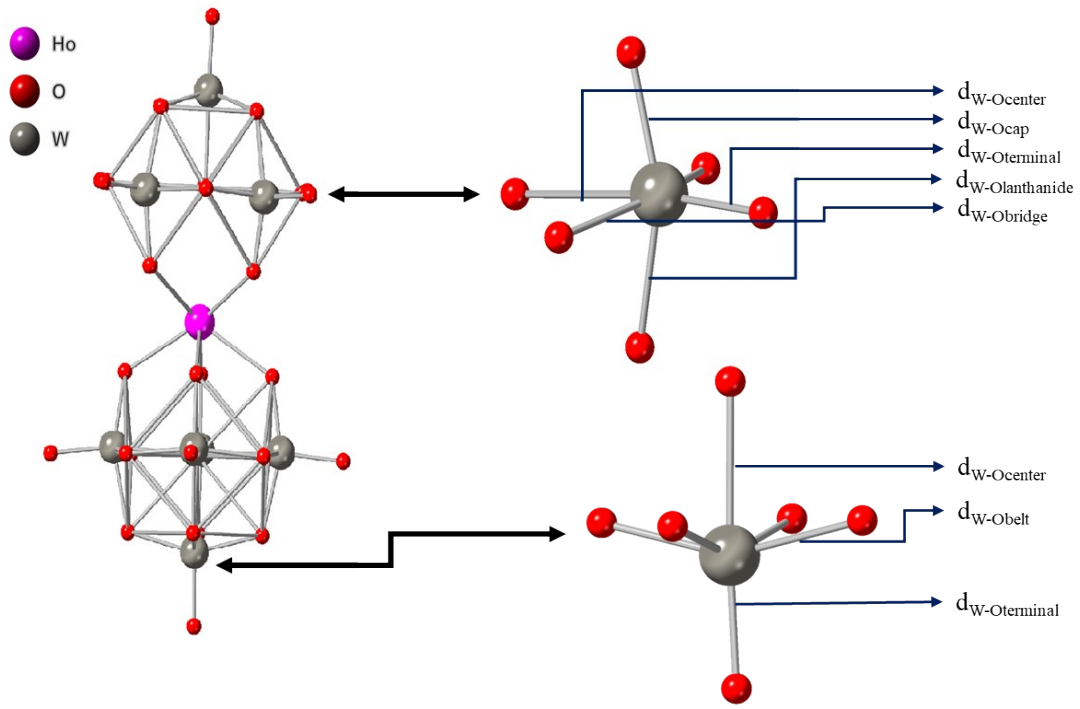

Figure S3. Ball and stick representation of complex **10** (HoW_{10}) highlighting WO_6 belt and cap moieties. The WO_6 belt moiety possesses five different types of W-O bonds: W-O_{center}, W-O_{cap}, W-$O_{terminal}$, W-$O_{lanthanide}$, and W-O_{bridge} whereas the WO_6 cap moiety includes three unique types of W-O bonds: W-O_{center}, W-O_{belt}, and W-$O_{terminal}$.

Methodology for Acquiring Structural Distortion Parameters.

The plane angle (PA) is the angle between the two coordinating planes (red planes) as shown in **Figure S4** (**Top**). The plane distance (PD) is the difference in distance between the top coordinating plane with the metal center and the bottom coordinating plane with the metal center (**Figure S4**, **Top**). The skew angle (SA) is calculated by measuring the angle between a perpendicular plane constructed out of the metal center and two oxygen atoms that are approximately 180 º from one another from the top coordinating plane (black planes—**Figure S4**, **Bottom**) and a perpendicular plane constructed out of the metal center and two oxygen atoms that are approximately 180 º from one another from the bottom coordinating plane (blue planes—**Figure S4**, **Bottom)**. This method produces four different SAs which are then averaged and subtracted from 45 º. The absolute value of this calculation produces the final SA values. Generation of coordinating planes as well as distance and angle measurements were done using the Mercury software package.

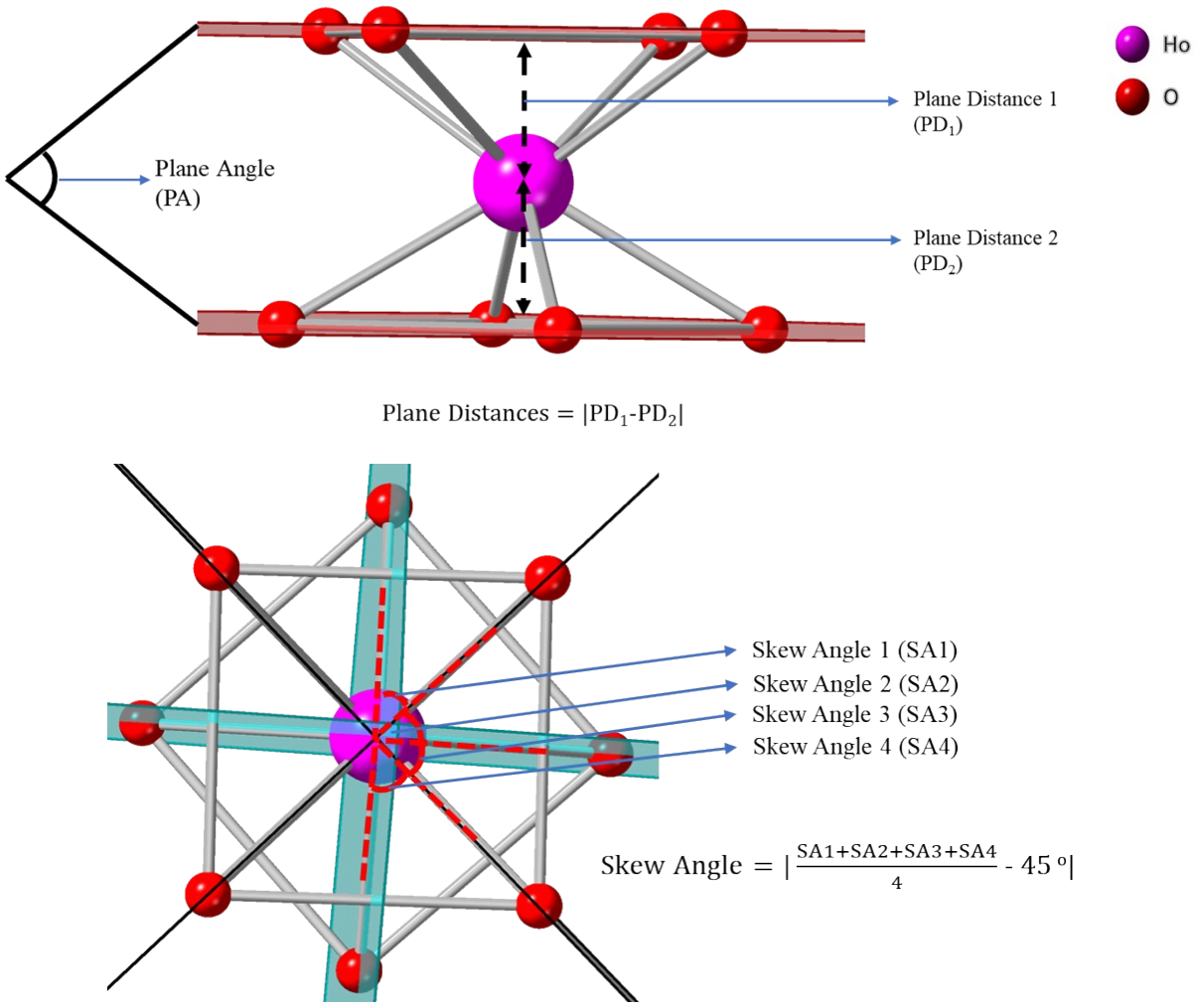

Figure S4. Ball and stick representation of the HoO_8 moiety from the side (**Top**) and a top-down view (**Bottom**) along with calculated planes used to determine structural distortion parameters.

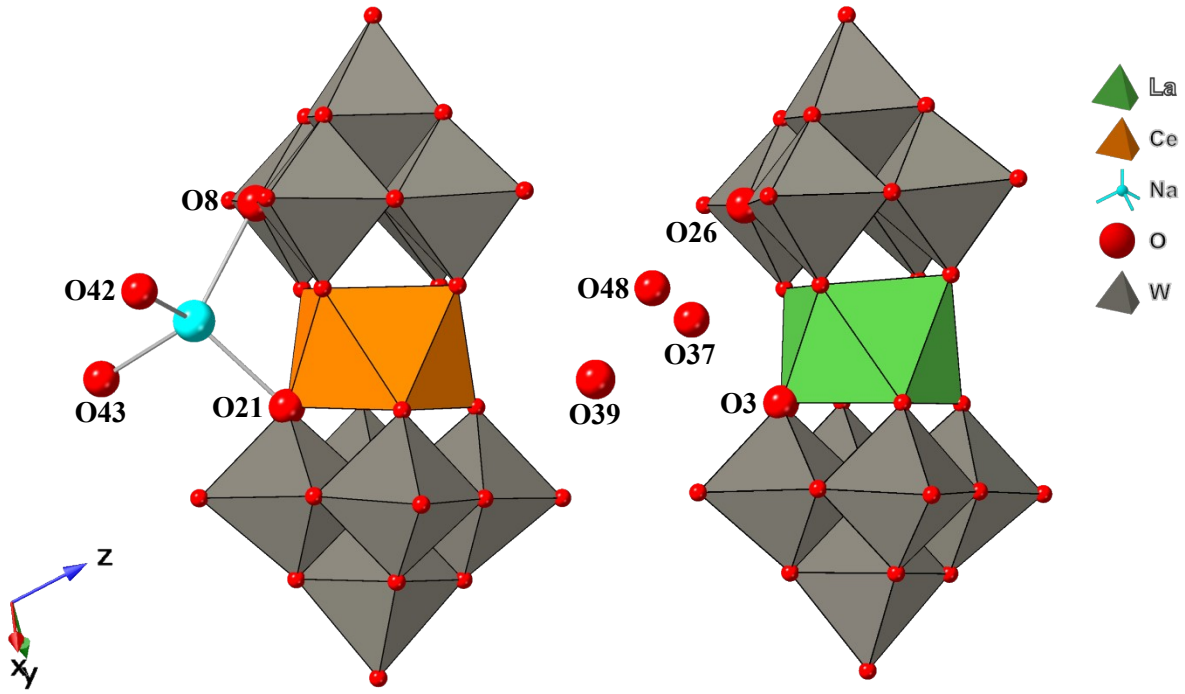

Figure S5. Polyhedral representations of complexes **2** (CeW_{10}) and **1** (LaW_{10}) that highlight the unusual tetrahedral coordination geometry of the Na(I) cation in **2** and the replacement of this Na(I) cation with a lattice water molecule in **1**.

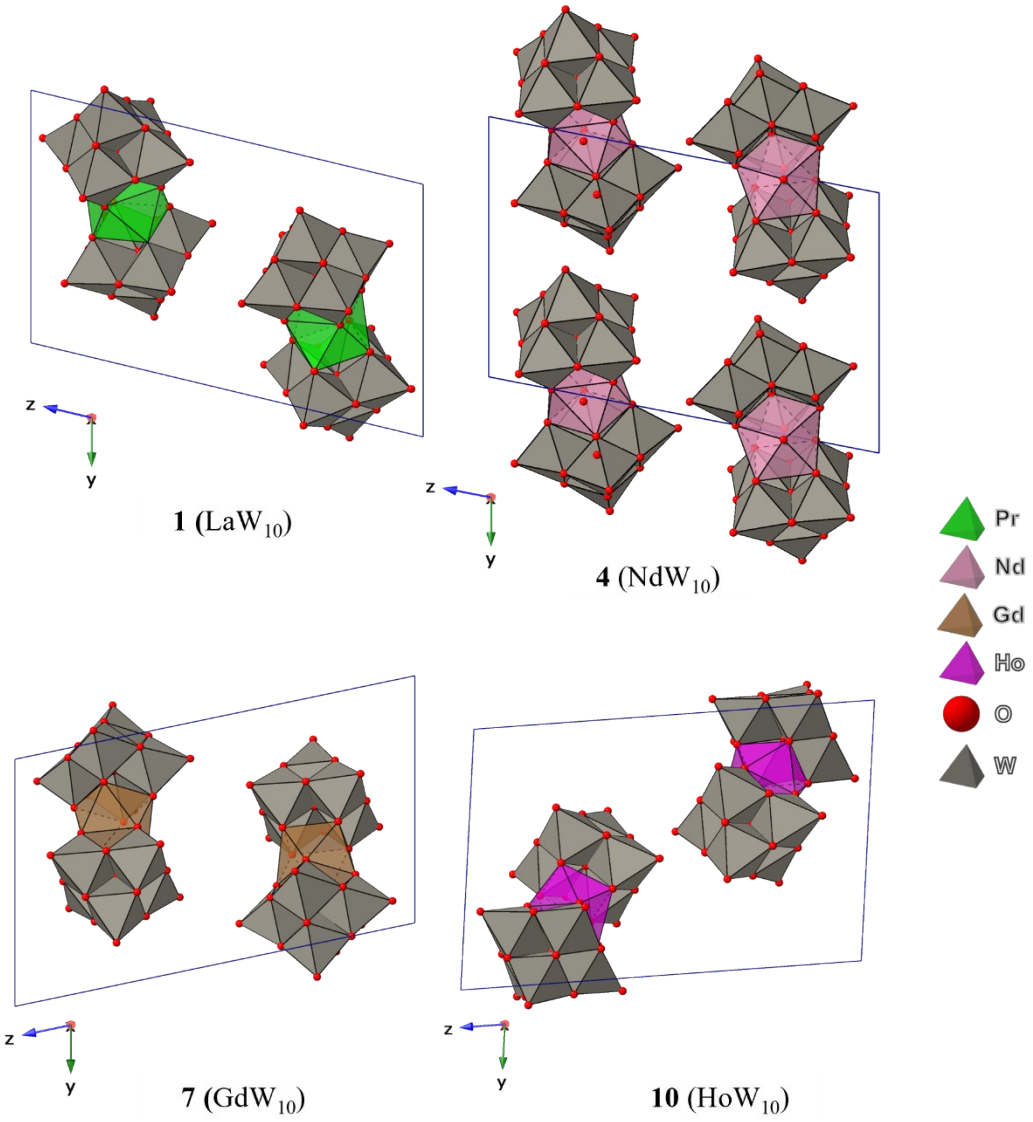

Figure S6. Polyhedral representations of **1** (LaW_{10}), **4** (NdW_{10}), **7** (GdW_{10}), and **10** (HoW_{10}) to illustrate cell packing in the different LnW_{10} polymorphs. Complex **1** is a representative example of polymorph 1, complex **4** is the only example of polymorph 2, complex **7** is a representative example of polymorph 3, and complex **10** is a representative example of polymorph 4.

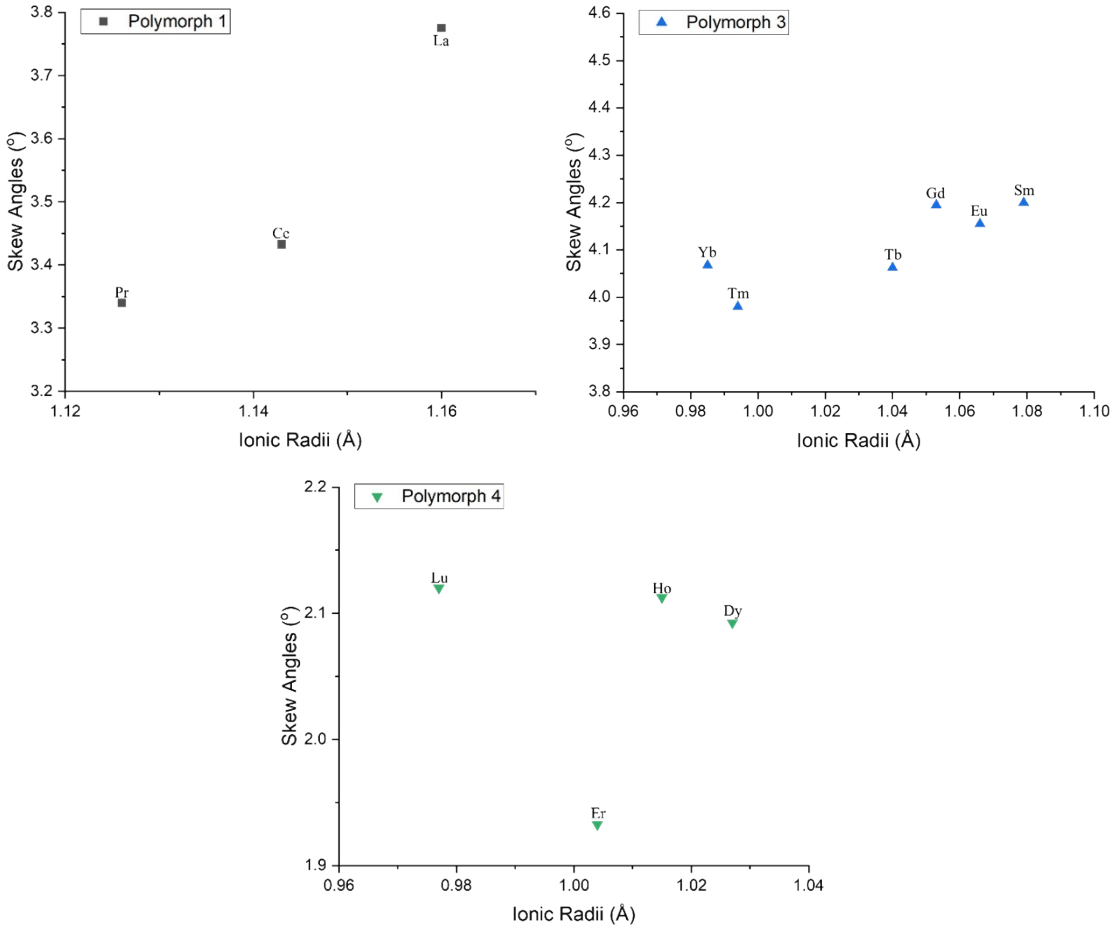

Figure S7. Plots of SAs vs. lanthanide ionic radii separated by LnW_{10} structural polymorph.

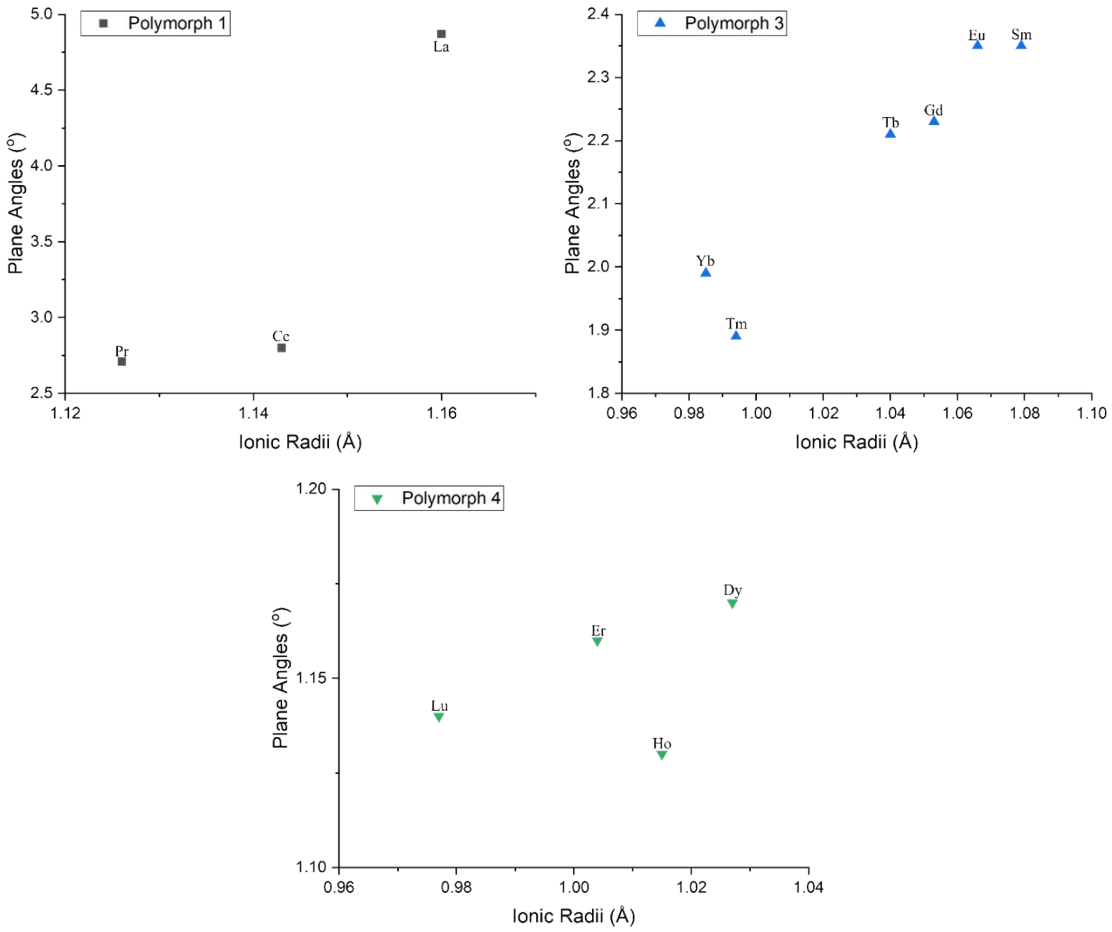

Figure S8. Plots of PAs vs. lanthanide ionic radii separated by LnW_{10} structural polymorph.

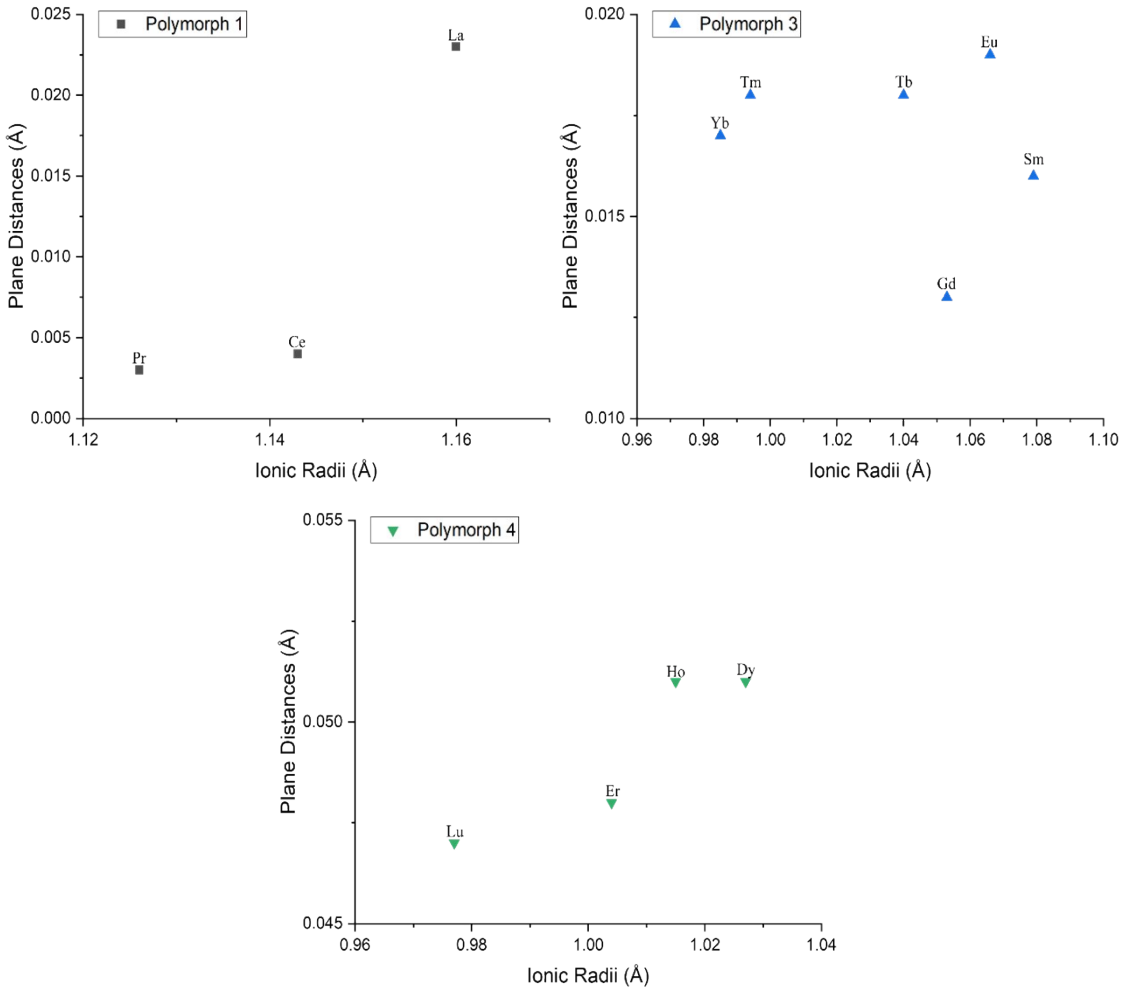

Figure S9. Plots of PDs vs. lanthanide ionic radii separated by LnW_{10} structural polymorph.

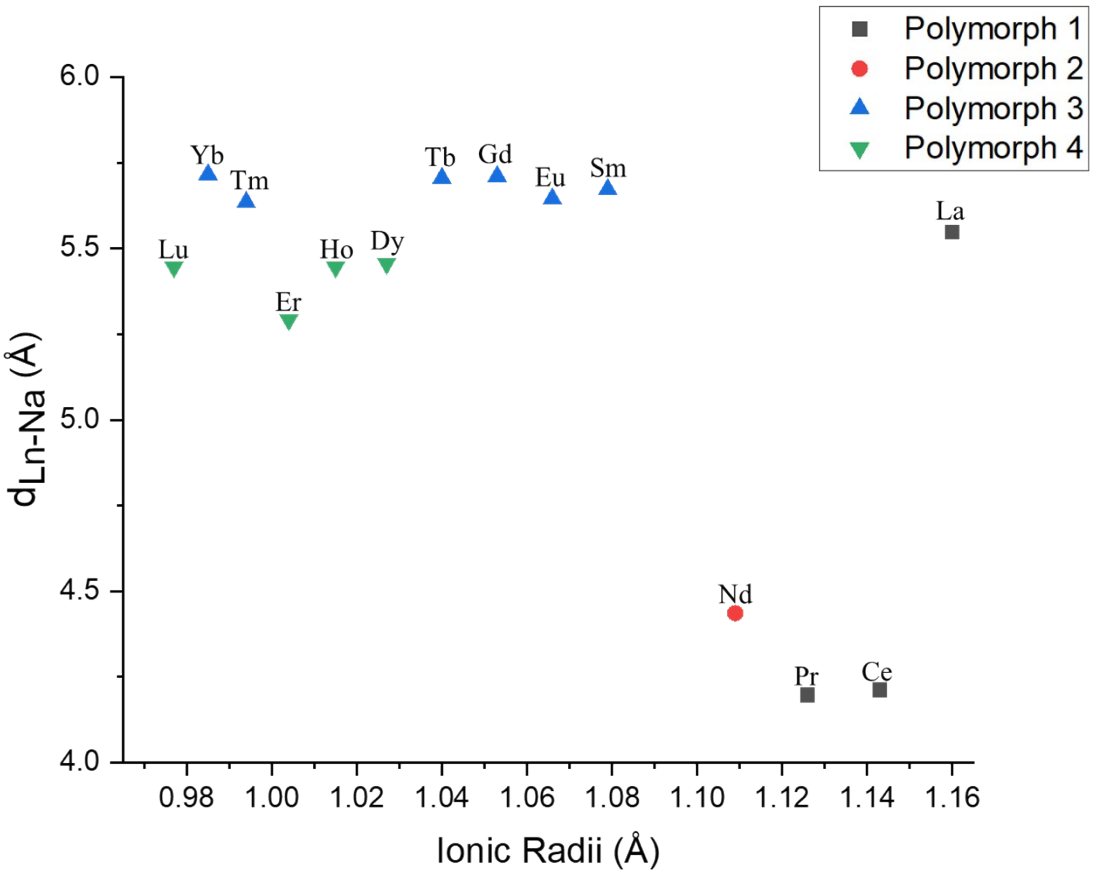

Figure S10. Plot of d_{Ln-Na} vs. lanthanide ionic radii depicting clear polymorph driven trends in Ln(III)-Na(I) distances.

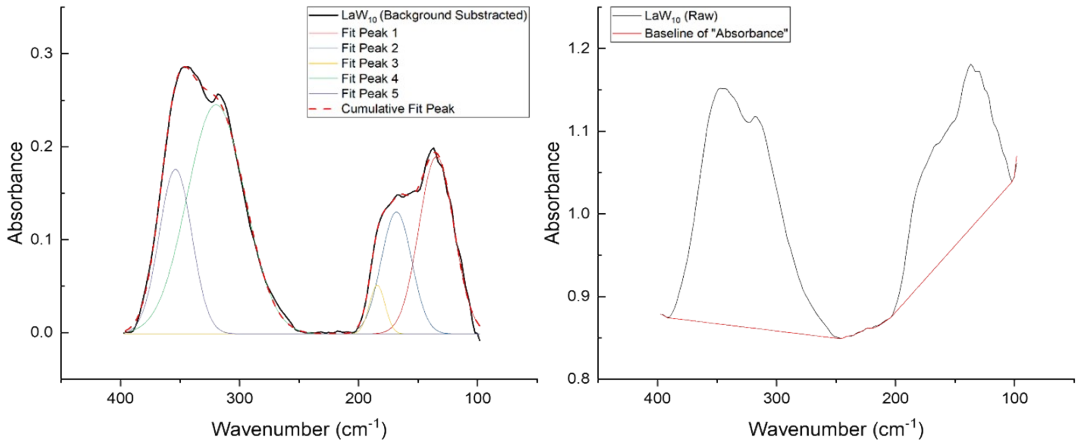

Figure S11. (**Left**) Background subtracted FIR spectrum of complex **1** (LaW_{10}) fit to Gaussian functions. (**Right**) Raw FIR spectrum for complex **1** and baseline used for background subtraction.

Table S3. Peak fitting parameters for FIR spectrum of complex **1**.

Model	Gauss				
Equation	y=y0 + (A/(w*sqrt(pi/2)))*exp(-2*((x-xc)/w)^2)				
Plot	Peak1 (Absorbance)	Peak2 (Absorbance)	Peak3 (Absorbance)	Peak4 (Absorbance)	Peak5 (Absorbance)
y0	-0.0014 ± 8.84422E-4	-0.0014 ± 8.84422E-4	-0.0014 ± 8.84422E-4	-0.0014 ± 8.84422E-4	-0.0014 ± 8.84422E-4
xc	134.60314 ± 0.63564	168.18858 ± 1.46285	184.39212 ± 0.60924	319.75397 ± 0.96246	353.85273 ± 0.36267
w	29.3108 ± 0.80281	25.59368 ± 2.79547	13.24783 ± 2.32961	48.46464 ± 1.23053	27.46196 ± 0.76501
A	7.00134 ± 0.28039	4.20582 ± 0.6668	0.8696 ± 0.45422	14.97735 ± 0.56918	6.09223 ± 0.50338
Reduced Chi-Sqr	2.13E-05				
R-Square (COD)	0.99789				
Adj. R-Square	0.99766				

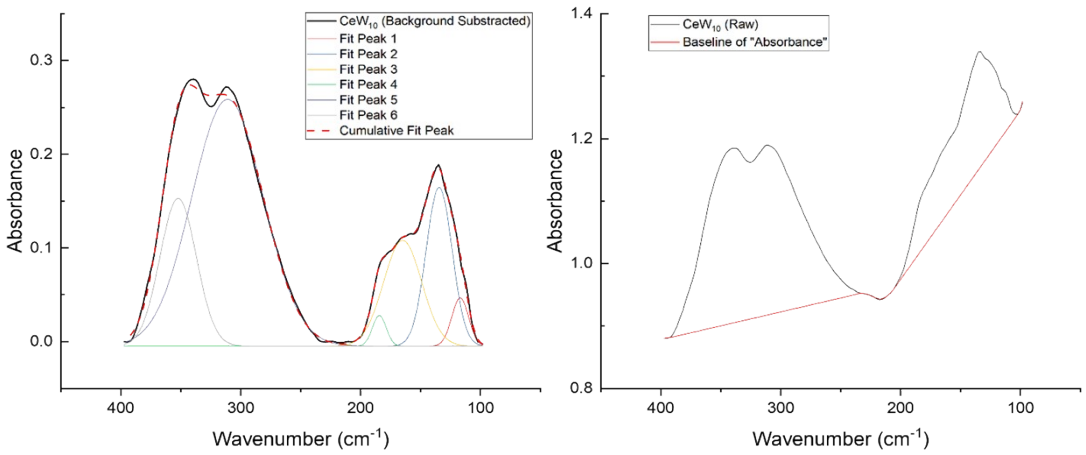

Figure S12. (**Left**) Background subtracted FIR spectrum of complex **2** (CeW_{10}) fit to Gaussian functions. (**Right**) Raw FIR spectrum for complex **2** and baseline used for background subtraction.

Table S4. Peak fitting parameters for FIR spectrum of complex **2**.

Model	Gauss					
Equation	y=y0 + (A/(w*sqrt(pi/2)))*exp(-2*((x-xc)/w)^2)					
Plot	Peak1 (Absorbance)	Peak2 (Absorbance)	Peak3 (Absorbance)	Peak4 (Absorbance)	Peak5 (Absorbance)	Peak6 (Absorbance)
y0	-0.00474 ± 0.0012	-0.00474 ± 0.0012	-0.00474 ± 0.0012	-0.00474 ± 0.0012	-0.00474 ± 0.0012	-0.00474 ± 0.0012
xc	116.98744 ± 1.49648	134.52474 ± 0.81322	164.95805 ± 2.04858	184.42907 ± 0.66011	311.03222 ± 0.7547	352.22405 ± 0.29375
w	14.04169 ± 2.05722	21.67149 ± 2.5111	31.80234 ± 2.45201	11.42623 ± 1.78541	59.51296 ± 1.16467	30.34262 ± 0.7528
A	0.90283 ± 0.47704	4.59578 ± 0.8435	4.49624 ± 0.46849	0.46714 ± 0.14164	19.63896 ± 0.54136	5.99036 ± 0.4028
Reduced Chi-Sqr	1.64E-05					
R-Square (COD)	0.99838					
Adj. R-Square	0.99817					

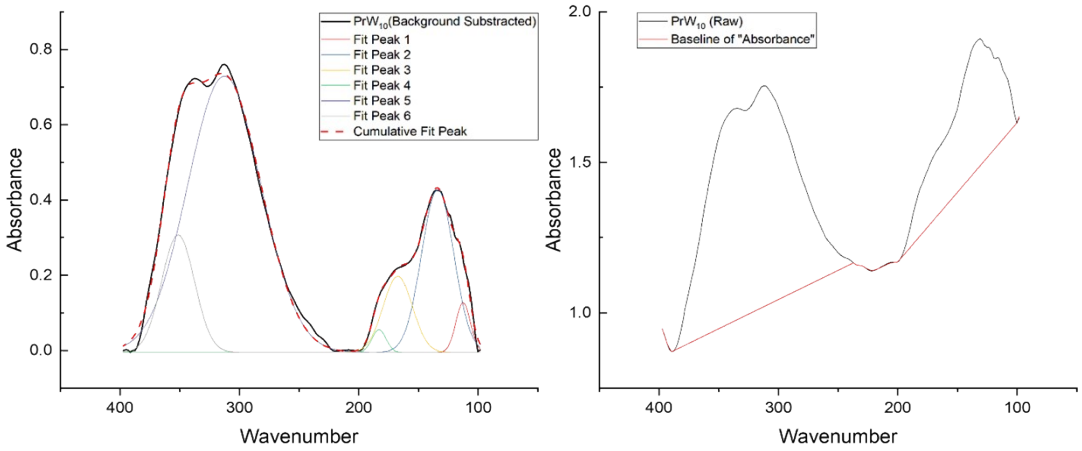

Figure S13. (**Left**) Background subtracted FIR spectrum of complex **3** (PrW_{10}) fit to Gaussian functions. (**Right**) Raw FIR spectrum for complex **3** and baseline used for background subtraction.

Table S5. Peak fitting parameters for FIR spectrum of complex **3**.

Model	Gauss					
Equation	y=y0 + (A/(w*sqrt(pi/2)))*exp(-2*((x-xc)/w)^2)					
Plot	Peak1 (Absorbance)	Peak2 (Absorbance)	Peak3 (Absorbance)	Peak4 (Absorbance)	Peak5 (Absorbance)	Peak6 (Absorbance)
y0	-0.0051 ± 0.00407	-0.0051 ± 0.00407	-0.0051 ± 0.00407	-0.0051 ± 0.00407	-0.0051 ± 0.00407	-0.0051 ± 0.00407
xc	112.63727 ± 0.64668	133.93395 ± 0.75763	167.36581 ± 2.80262	183.10611 ± 1.39164	312.64138 ± 0.85687	351.44096 ± 0.33357
w	12.21461 ± 2.28844	27.04648 ± 3.55909	24.53185 ± 5.56952	11.72703 ± 5.01449	61.47865 ± 1.3651	27.5978 ± 1.27906
A	2.01955 ± 0.96703	14.64679 ± 2.10448	6.21613 ± 2.02878	0.88837 ± 1.0223	56.55994 ± 1.79103	10.7953 ± 1.22373
Reduced Chi-Sqr	1.97E-04					
R-Square (COD)	0.99724					
Adj. R-Square	0.99687					

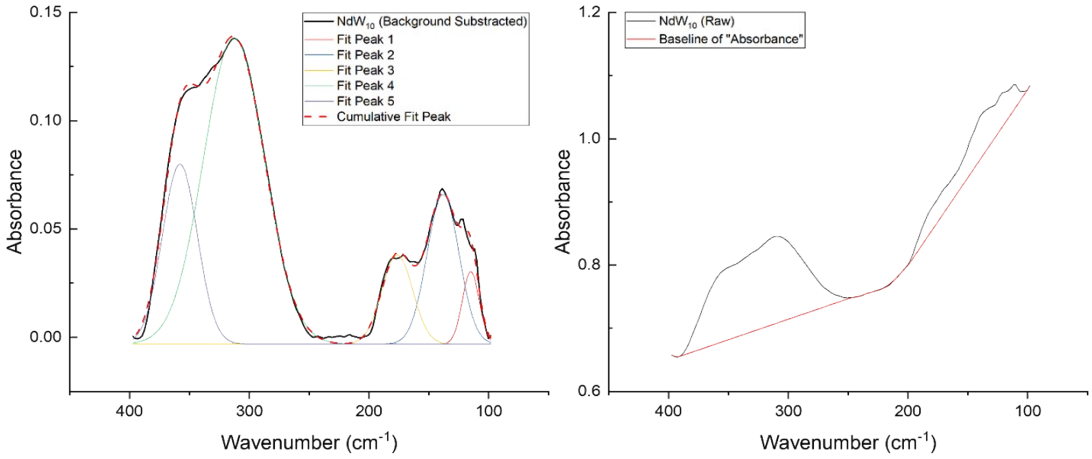

Figure S14. (**Left**) Background subtracted FIR spectrum of complex **4** (NdW_{10}) fit to Gaussian functions. (**Right**) Raw FIR spectrum for complex **4** and baseline used for background subtraction.

Table S6. Peak fitting parameters for FIR spectrum of complex **4**.

Model	Gauss				
Equation	y=y0 + (A/(w*sqrt(pi/2)))*exp(-2*((x-xc)/w)^2)				
Plot	Peak1 (Absorbance)	Peak2 (Absorbance)	Peak3 (Absorbance)	Peak4 (Absorbance)	Peak5 (Absorbance)
y0	-0.00313 ± 4.89231E-4	-0.00313 ± 4.89231E-4	-0.00313 ± 4.89231E-4	-0.00313 ± 4.89231E-4	-0.00313 ± 4.89231E-4
xc	115.02762 ± 0.56828	138.16236 ± 0.55437	176.37358 ± 0.80743	312.77532 ± 0.38157	357.98769 ± 0.32613
w	14.05863 ± 1.15648	26.72646 ± 1.97711	25.77504 ± 1.3446	50.96735 ± 0.66997	29.25358 ± 0.54115
A	0.58904 ± 0.11468	2.31367 ± 0.17189	1.32884 ± 0.08831	9.03162 ± 0.14064	3.04304 ± 0.11015
Reduced Chi-Sqr	5.12E-06				
R-Square (COD)	0.99782				
Adj. R-Square	0.99759				

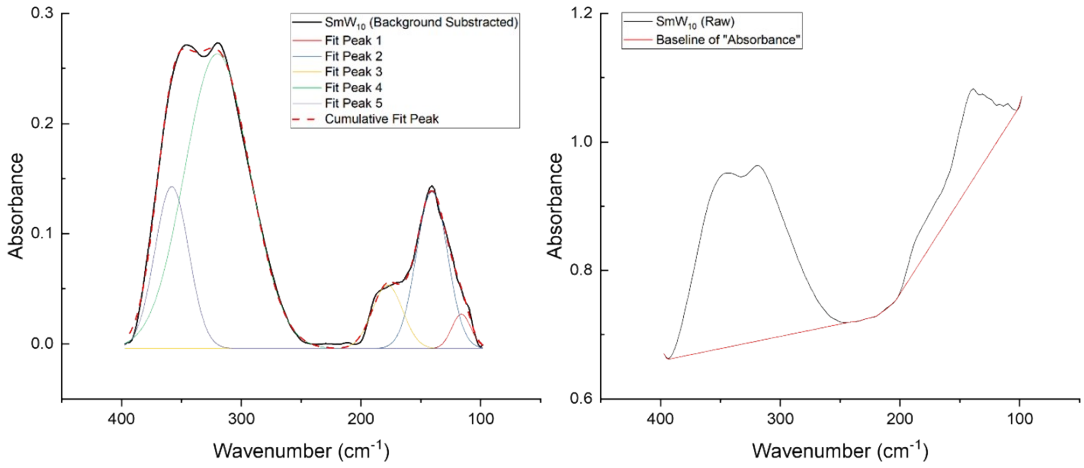

Figure S15. (**Left**) Background subtracted FIR spectrum of complex **5** (SmW_{10}) fit to Gaussian functions. (**Right**) Raw FIR spectrum for complex **5** and baseline used for background subtraction.

Table S7. Peak fitting parameters for FIR spectrum of complex **5**.

Model	Gauss				
Equation	y=y0 + (A/(w*sqrt(pi/2)))*exp(-2*((x-xc)/w)^2)				
Plot	Peak1 (Absorbance)	Peak2 (Absorbance)	Peak3 (Absorbance)	Peak4 (Absorbance)	Peak5 (Absorbance)
y0	-0.00426 ± 8.54812E-4	-0.00426 ± 8.54812E-4	-0.00426 ± 8.54812E-4	-0.00426 ± 8.54812E-4	-0.00426 ± 8.54812E-4
xc	116.22436 ± 1.39676	140.72246 ± 0.44826	177.89623 ± 0.95092	320.09039 ± 0.63736	358.09169 ± 0.28033
w	15.90813 ± 2.1656	26.03707 ± 1.55338	25.36484 ± 1.59339	54.46696 ± 0.91398	28.30262 ± 0.70443
A	0.62254 ± 0.19731	4.64274 ± 0.28435	1.82831 ± 0.14778	18.27035 ± 0.43004	5.21411 ± 0.34913
Reduced Chi-Sqr	1.37E-05				
R-Square (COD)	0.99863				
Adj. R-Square	0.99849				

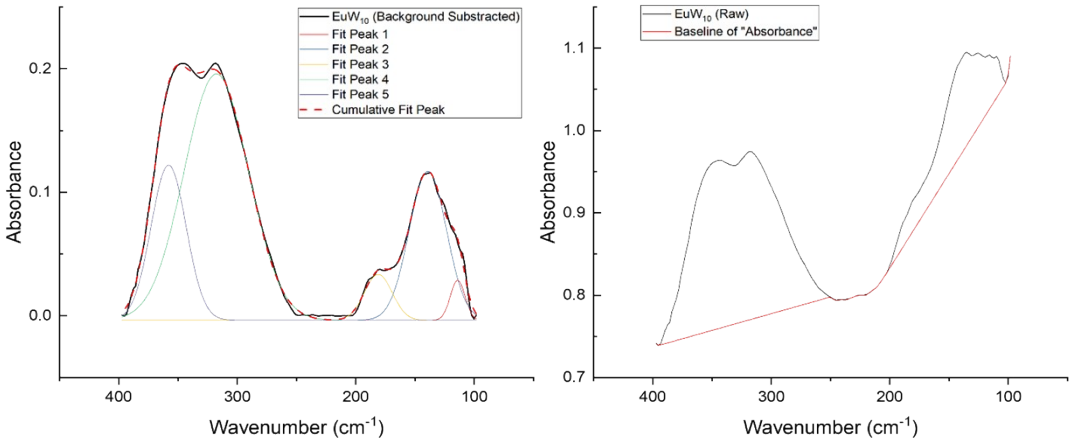

Figure S16. (**Left**) Background subtracted FIR spectrum of complex **6** (EuW_{10}) fit to Gaussian functions. (**Right**) Raw FIR spectrum for complex **6** and baseline used for background subtraction.

Table S8. Peak fitting parameters for FIR spectrum of complex **6**.

Model	Gauss				
Equation	y=y0 + (A/(w*sqrt(pi/2)))*exp(-2*((x-xc)/w)^2)				
Plot	Peak1 (Absorbance)	Peak2 (Absorbance)	Peak3 (Absorbance)	Peak4 (Absorbance)	Peak5 (Absorbance)
y0	-0.00371 ± 6.40253E-4	-0.00371 ± 6.40253E-4	-0.00371 ± 6.40253E-4	-0.00371 ± 6.40253E-4	-0.00371 ± 6.40253E-4
xc	114.04848 ± 0.4117	139.17813 ± 0.32718	181.01946 ± 0.77641	317.65023 ± 0.58243	357.96983 ± 0.28352
w	12.41008 ± 1.27069	31.46092 ± 1.18916	23.43034 ± 1.37347	54.36737 ± 0.8599	29.56028 ± 0.57944
A	0.504 ± 0.10143	4.75696 ± 0.16315	1.0918 ± 0.08244	13.58813 ± 0.29225	4.65387 ± 0.23946
Reduced Chi-Sqr	7.91E-06				
R-Square (COD)	0.99861				
Adj. R-Square	0.99846				

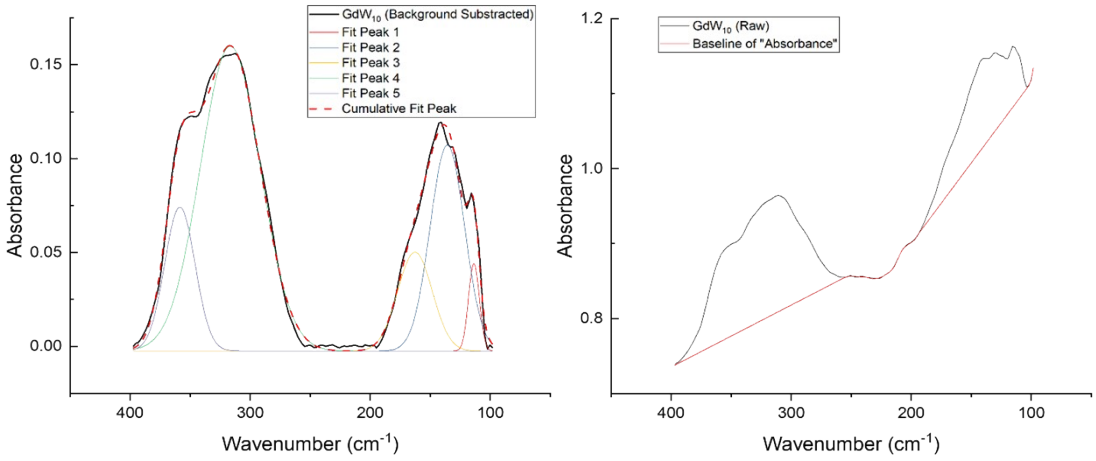

Figure S17. (**Left**) Background subtracted FIR spectrum of complex **7** (GdW_{10}) fit to Gaussian functions. (**Right**) Raw FIR spectrum for complex **7** and baseline used for background subtraction.

Table S9. Peak fitting parameters for FIR spectrum of complex **7**.

Model	Gauss				
Equation	y=y0 + (A/(w*sqrt(pi/2)))*exp(-2*((x-xc)/w)^2)				
Plot	Peak1 (Absorbance)	Peak2 (Absorbance)	Peak3 (Absorbance)	Peak4 (Absorbance)	Peak5 (Absorbance)
y0	-0.00249 ± 5.70065E-4	-0.00249 ± 5.70065E-4	-0.00249 ± 5.70065E-4	-0.00249 ± 5.70065E-4	-0.00249 ± 5.70065E-4
xc	113.65861 ± 0.23796	135.7411 ± 1.96707	162.71632 ± 4.31788	316.56981 ± 0.42085	358.5971 ± 0.36933
w	9.01536 ± 0.77988	28.65306 ± 2.58527	28.80401 ± 3.46352	49.89736 ± 0.75635	25.28882 ± 0.73178
A	0.52627 ± 0.08026	3.93905 ± 0.72087	1.90201 ± 0.66725	10.1528 ± 0.17404	2.42981 ± 0.13531
Reduced Chi-Sqr	9.77E-06				
R-Square (COD)	0.99704				
Adj. R-Square	0.99672				

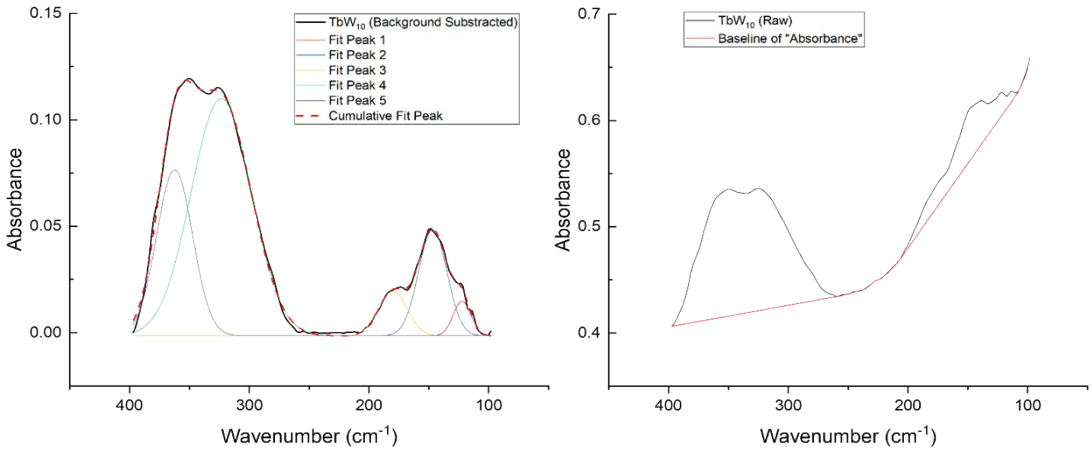

Figure S18. (**Left**) Background subtracted FIR spectrum of complex **8** (TbW_{10}) fit to Gaussian functions. (**Right**) Raw FIR spectrum for complex **8** and baseline used for background subtraction.

Table S10. Peak fitting parameters for FIR spectrum of complex **8**.

Model	Gauss				
Equation	y=y0 + (A/(w*sqrt(pi/2)))*exp(-2*((x-xc)/w)^2)				
Plot	Peak1 (Absorbance)	Peak2 (Absorbance)	Peak3 (Absorbance)	Peak4 (Absorbance)	Peak5 (Absorbance)
y0	-0.00146 ± 3.28384E-4	-0.00146 ± 3.28384E-4	-0.00146 ± 3.28384E-4	-0.00146 ± 3.28384E-4	-0.00146 ± 3.28384E-4
xc	122.30456 ± 1.01282	146.77592 ± 0.42215	180.02558 ± 1.21431	323.52819 ± 0.63728	362.39681 ± 0.3443
w	14.74442 ± 1.58728	23.75945 ± 1.65697	23.78321 ± 1.94549	50.16757 ± 0.86906	30.08413 ± 0.56683
A	0.30054 ± 0.06209	1.48346 ± 0.10407	0.6241 ± 0.06576	7.00648 ± 0.17108	2.93772 ± 0.15106
Reduced Chi-Sqr	2.83E-06				
R-Square (COD)	0.99853				
Adj. R-Square	0.99837				

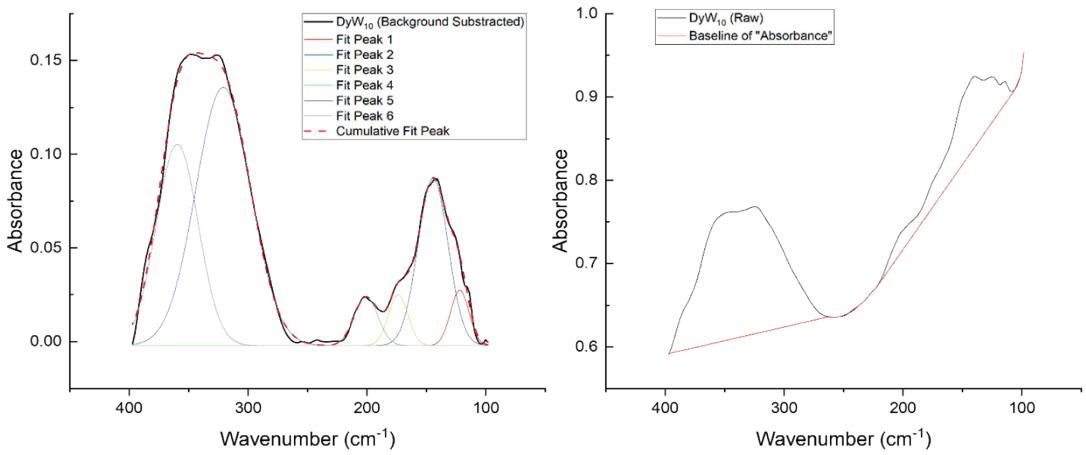

Figure S19. (**Left**) Background subtracted FIR spectrum of complex **9** (DyW_{10}) fit to Gaussian functions. (**Right**) Raw FIR spectrum for complex **9** and baseline used for background subtraction.

Table S11. Peak fitting parameters for FIR spectrum of complex **9**.

Model	Gauss					
Equation	y=y0 + (A/(w*sqrt(pi/2)))*exp(-2*((x-xc)/w)^2)					
Plot	Peak1 (Absorbance)	Peak2 (Absorbance)	Peak3 (Absorbance)	Peak4 (Absorbance)	Peak5 (Absorbance)	Peak6 (Absorbance)
y0	-0.00213 ± 6.46906E-4	-0.00213 ± 6.46906E-4	-0.00213 ± 6.46906E-4	-0.00213 ± 6.46906E-4	-0.00213 ± 6.46906E-4	-0.00213 ± 6.46906E-4
xc	121.9704 ± 1.56489	144.44177 ± 0.84121	173.75754 ± 1.32494	200.81162 ± 0.98586	320.93881 ± 1.20959	359.61223 ± 0.91668
w	15.56715 ± 2.21373	25.38535 ± 3.11543	16.60195 ± 2.89743	19.91491 ± 1.9612	46.2854 ± 1.37878	35.24128 ± 0.93525
A	0.57633 ± 0.2486	2.83554 ± 0.36035	0.56137 ± 0.15867	0.64874 ± 0.0679	7.9902 ± 0.41627	4.74341 ± 0.38777
Reduced Chi-Sqr	7.99E-06					
R-Square (COD)	0.99747					
Adj. R-Square	0.99713					

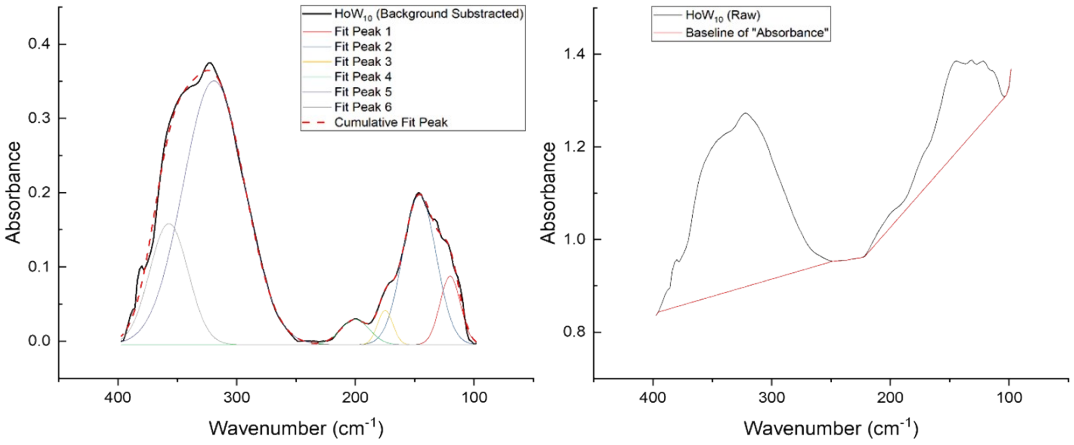

Figure S20. (**Left**) Background subtracted FIR spectrum of complex **10** (HoW_{10}) fit to Gaussian functions. (**Right**) Raw FIR spectrum for complex **10** and baseline used for background subtraction.

Table S12. Peak fitting parameters for FIR spectrum of complex **10**.

Model	Gauss					
Equation	y=y0 + (A/(w*sqrt(pi/2)))*exp(-2*((x-xc)/w)^2)					
Plot	Peak1(Absorbance)	Peak2(Absorbance)	Peak3(Absorbance)	Peak4(Absorbance)	Peak5 (Absorbance)	Peak6 (Absorbance)
y0	-0.00486 ± 0.00219	-0.00486 ± 0.00219	-0.00486 ± 0.00219	-0.00486 ± 0.00219	-0.00486 ± 0.00219	-0.00486 ± 0.00219
xc	120.1907 ± 1.12981	146.09711 ± 0.82763	174.88177 ± 1.10613	200.25038 ± 1.95197	319.21037 ± 1.24183	357.17141 ± 0.93971
w	17.1425 ± 1.67873	28.12845 ± 2.6777	12.93385 ± 2.55664	24.27551 ± 4.45292	51.90942 ± 1.60047	32.40071 ± 1.43206
A	1.9829 ± 0.4969	7.11147 ± 0.6675	0.75003 ± 0.26413	1.03766 ± 0.20632	23.12623 ± 1.12426	6.63026 ± 0.96227
Reduced Chi-Sqr	5.36E-05					
R-Square (COD)	0.9968					
Adj. R-Square	0.99638					

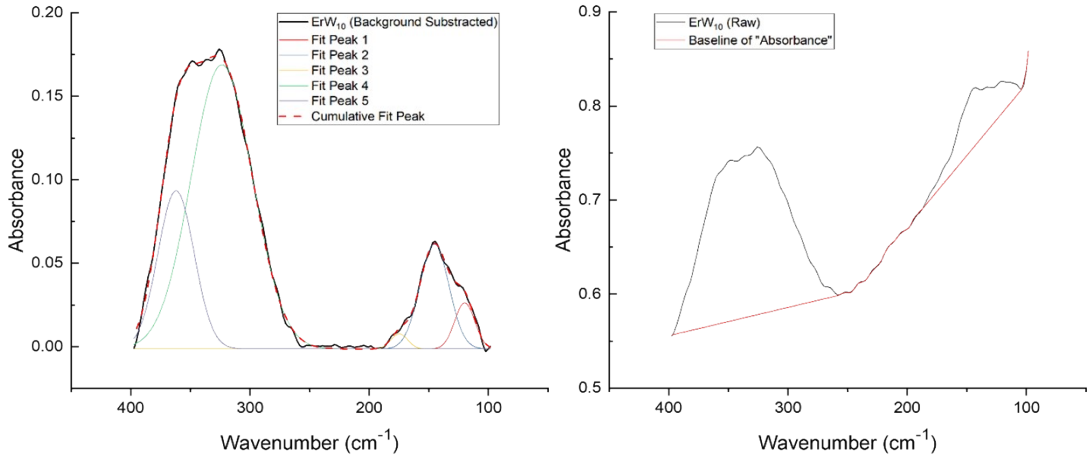

Figure S21. (**Left**) Background subtracted FIR spectrum of complex **11** (ErW_{10}) fit to Gaussian functions. (**Right**) Raw FIR spectrum for complex **11** and baseline used for background subtraction.

Table S13. Peak fitting parameters for FIR spectrum of complex **11**.

Model	Gauss				
Equation	y=y0 + (A/(w*sqrt(pi/2)))*exp(-2*((x-xc)/w)^2)				
Plot	Peak1(Absorbance)	Peak2(Absorbance)	Peak3(Absorbance)	Peak4(Absorbance)	Peak5 (Absorbance)
y0	-0.00143 ± 3.85681E-4	-0.00143 ± 3.85681E-4	-0.00143 ± 3.85681E-4	-0.00143 ± 3.85681E-4	-0.00143 ± 3.85681E-4
xc	119.92196 ± 1.0649	145.31788 ± 0.57166	174.70373 ± 1.66646	323.68575 ± 0.61227	362.05903 ± 0.37225
w	16.81096 ± 1.46261	24.44798 ± 1.67994	14.06775 ± 3.01482	51.34786 ± 0.79733	30.38759 ± 0.65606
A	0.58104 ± 0.1003	1.9242 ± 0.12777	0.15817 ± 0.04691	10.95733 ± 0.2471	3.60895 ± 0.2225
Reduced Chi-Sqr	4.92E-06				
R-Square (COD)	0.99885				
Adj. R-Square	0.99873				

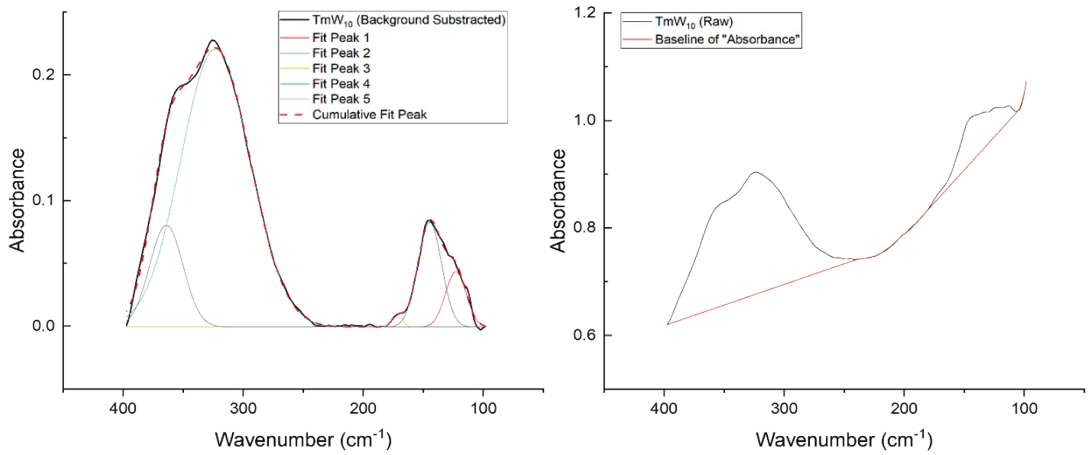

Figure S22. (**Left**) Background subtracted FIR spectrum of complex **12** (TmW_{10}) fit to Gaussian functions. (**Right**) Raw FIR spectrum for complex **12** and baseline used for background subtraction.

Table S14. Peak fitting parameters for FIR spectrum of complex **12**.

Model	Gauss				
Equation	y=y0 + (A/(w*sqrt(pi/2)))*exp(-2*((x-xc)/w)^2)				
Plot	Peak1 (Absorbance)	Peak2 (Absorbance)	Peak3 (Absorbance)	Peak4 (Absorbance)	Peak5 (Absorbance)
y0	-7.00596E-4 ± 4.83621E-4	-7.00596E-4 ± 4.83621E-4	-7.00596E-4 ± 4.83621E-4	-7.00596E-4 ± 4.83621E-4	-7.00596E-4 ± 4.83621E-4
xc	122.87894 ± 1.14593	144.56468 ± 0.68456	171.55142 ± 1.19836	323.08478 ± 0.46932	364.01294 ± 0.31328
w	17.27628 ± 1.41865	19.71013 ± 1.07762	8.94121 ± 2.48318	57.63121 ± 0.70642	27.7819 ± 0.85496
A	0.95152 ± 0.13912	2.05338 ± 0.14397	0.09353 ± 0.02657	15.98602 ± 0.25211	2.82232 ± 0.20598
Reduced Chi-Sqr	7.92E-06				
R-Square (COD)	0.99879				
Adj. R-Square	0.99866				

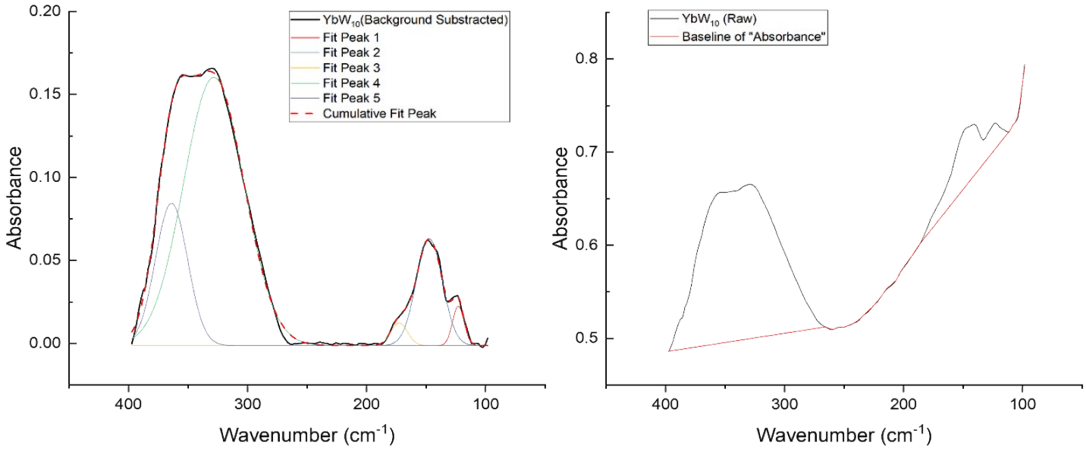

Figure S23. (**Left**) Background subtracted FIR spectrum of complex **13** (YbW_{10}) fit to Gaussian functions. (**Right**) Raw FIR spectrum for complex **13** and baseline used for background subtraction.

Table S15. Peak fitting parameters for FIR spectrum of complex **13**.

Model	Gauss				
Equation	y=y0 + (A/(w*sqrt(pi/2)))*exp(-2*((x-xc)/w)^2)				
Plot	Peak1 (Absorbance)	Peak2 (Absorbance)	Peak3 (Absorbance)	Peak4 (Absorbance)	Peak5 (Absorbance)
y0	-0.00134 ± 3.49829E-4	-0.00134 ± 3.49829E-4	-0.00134 ± 3.49829E-4	-0.00134 ± 3.49829E-4	-0.00134 ± 3.49829E-4
xc	122.9998 ± 0.40101	147.31932 ± 0.29823	172.65704 ± 1.21181	328.40213 ± 0.63809	363.94635 ± 0.29856
w	9.63044 ± 0.82639	21.90544 ± 0.99567	13.95031 ± 2.08204	50.77549 ± 0.84054	27.03132 ± 0.73279
A	0.28605 ± 0.03117	1.76656 ± 0.06742	0.23795 ± 0.04904	10.28396 ± 0.24083	2.90389 ± 0.21352
Reduced Chi-Sqr	5.19E-06				
R-Square (COD)	0.99866				
Adj. R-Square	0.99851				

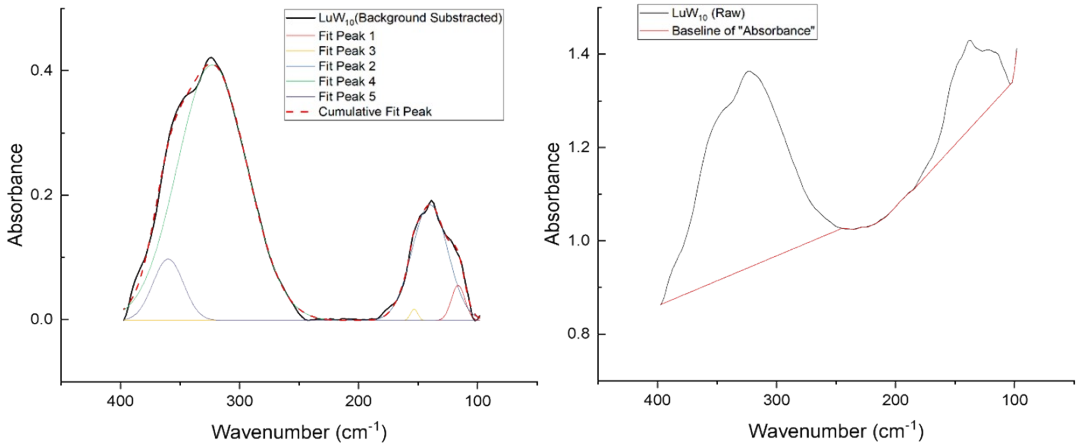

Figure S24. (**Left**) Background subtracted FIR spectrum of complex **14** (LuW_{10}) fit to Gaussian functions. (**Right**) Raw FIR spectrum for complex **14** and baseline used for background subtraction.

Table S16. Peak fitting parameters for FIR spectrum of complex **14**.

Model	Gauss				
Equation	y=y0 + (A/(w*sqrt(pi/2)))*exp(-2*((x-xc)/w)^2)				
Plot	Peak1 (Absorbance)	Peak2 (Absorbance)	Peak3 (Absorbance)	Peak4 (Absorbance)	Peak5 (Absorbance)
y0	-0.00155 ± 0.0011	-0.00155 ± 0.0011	-0.00155 ± 0.0011	-0.00155 ± 0.0011	-0.00155 ± 0.0011
xc	116.3922 ± 0.48106	140.09621 ± 0.57959	153.39291 ± 0.94903	323.06292 ± 0.58978	360.0016 ± 0.42479
w	11.3516 ± 1.30668	30.03854 ± 0.90127	6.13594 ± 2.29172	58.64299 ± 0.84353	25.68943 ± 1.64303
A	0.80194 ± 0.15786	7.01015 ± 0.20642	0.14074 ± 0.06626	30.18441 ± 0.59716	3.17751 ± 0.46578
Reduced Chi-Sqr	3.87E-05				
R-Square (COD)	0.99816				
Adj. R-Square	0.99796				

Table S17. Observed peaks in the FIR spectra for complexes **1- 14**.

Complex name	Observed peaks rounded to the first decimal (cm^{-1})
1 (LaW_{10})	134.6, 168.2, 184.4, 319.8, 353.9
2 (CeW_{10})	117.0, 134.5, 165.0, 184.4, 311.0, 352.2
3 (PrW_{10})	112.6, 133.9, 167.4, 183.1, 312.6, 351.4
4 (NdW_{10})	115.0, 138.2, 176.4, 312.8, 358.0
5 (SmW_{10})	116.2, 140.7, 177.9, 320.1, 358.1
6 (EuW_{10})	114.0, 139.2, 181.0, 317.7, 358.0
7 (GdW_{10})	113.7, 135.7, 162.7, 316.6, 358.6
8 (TbW_{10})	122.3, 146.8, 190.0, 323.5, 362.4
9 (DyW_{10})	122.0, 144.4, 173.8, 200.8, 320.9, 359.6
10 (HoW_{10})	120.2, 146.1, 174.9, 200.3, 319.2, 357.2
11 (ErW_{10})	119.9, 145.3, 174.7, 323.7, 362.1
12 (TmW_{10})	122.9, 144.6, 171.6, 323.1, 364.0
13 (YbW_{10})	123.0, 147.3, 172.7, 328.4, 363.9
14 (LuW_{10})	116.4, 140.1, 153.4, 323.1, 360.0

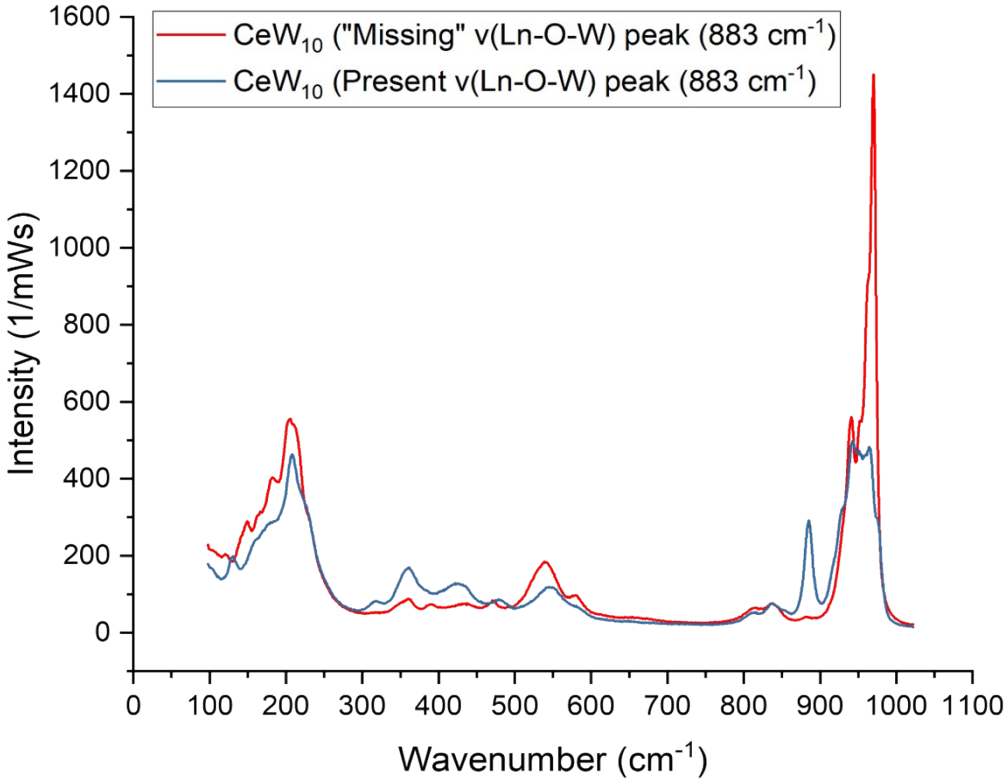

Figure S25. Raman spectra of two different crystals of **3** (CeW_{10}) that demonstrate fluctuations in peak intensities seen within spectra of different crystals of the same species. This fluctuation is especially pronounced for the peak centered around 888 cm^{-1} which has been assigned as the ν(Ln-O-W) mode. Intensity changes are generally indicative of Raman mode polarizability; however, there are not literature examples that suggest this mode is polarizable.[1]

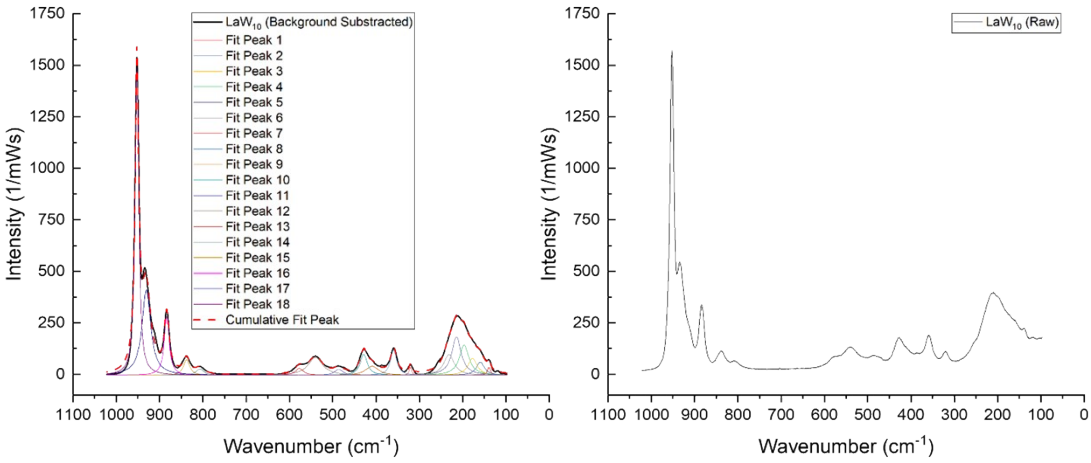

Figure S26. (**Left**) Background subtracted Raman spectrum of complex **1** (LaW_{10}) fit to Lorentzian functions. (**Right**) Raw Raman spectrum for complex **1**.

Table S18. Peak fitting parameters for Raman spectrum of complex **1**.

Model	Lorentz								
Equation	y = y0 + (2*A/pi)*(w/(4*(x-xc)^2 + w^2))								
Plot	Peak1 (Intensity)	Peak2 (Intensity)	Peak3 (Intensity)	Peak4 (Intensity)	Peak5 (Intensity)	Peak6 (Intensity)	Peak7 (Intensity)	Peak8 (Intensity)	Peak9 (Intensity)
y0	-4.44097 ± 0	-4.44097 ± 0	-4.44097 ± 0	-4.44097 ± 0	-4.44097 ± 0	-4.44097 ± 0	-4.44097 ± 0	-4.44097 ± 0	-4.44097 ± 0
xc	139.15724 ± 0.90544	158.91662 ± 2.81645	177.1049 ± 2.90142	196.42286 ± 2.17249	214.13305 ± 1.60011	231.46774 ± 3.31386	320.64152 ± 0.7151	359.3776 ± 0.37556	409.05642 ± 5.43423
w	8.60228 ± 3.67073	22.2198 ± 10.32624	25.34188 ± 19.65025	26.46136 ± 14.98734	26.06282 ± 11.53014	28.46782 ± 5.6696	6.64635 ± 2.09214	16.97664 ± 1.32747	36.21366 ± 11.68757
A	527.58229 ± 247.45669	2255.72602 ± 2015.93803	3256.78141 ± 4789.08222	6107.99196 ± 7068.68423	7608.7661 ± 6882.84616	4510.52803 ± 2976.28977	406.14257 ± 93.09556	3264.46689 ± 229.17489	2488.03969 ± 1290.98208
Plot	Peak10 (Intensity)	Peak11 (Intensity)	Peak12 (Intensity)	Peak13 (Intensity)	Peak14 (Intensity)	Peak15 (Intensity)	Peak16 (Intensity)	Peak17 (Intensity)	Peak18 (Intensity)
y0	-4.44097 ± 0	-4.44097 ± 0	-4.44097 ± 0	-4.44097 ± 0	-4.44097 ± 0	-4.44097 ± 0	-4.44097 ± 0	-4.44097 ± 0	-4.44097 ± 0
xc	428.4111 ± 0.8661	486.15513 ± 1.9471	540.01788 ± 1.07145	577.22867 ± 1.84535	806.94212 ± 1.78146	837.74219 ± 0.59947	883.72142 ± 0.1339	930.68305 ± 0.15613	952.48018 ± 0.023
w	19.41697 ± 3.4323	24.13489 ± 6.98988	39.66517 ± 4.3096	23.16324 ± 6.63377	22.18385 ± 5.70891	16.93034 ± 2.04008	13.45162 ± 0.42118	24.2968 ± 0.52192	9.94097 ± 0.08308
A	3107.72645 ± 966.70883	1087.94847 ± 284.95744	5388.10773 ± 573.04775	1192.41035 ± 370.76612	1054.46895 ± 224.33489	2017.28714 ± 206.16161	6003.48827 ± 144.06866	15817.25927 ± 297.76528	23311.11321 ± 188.10954
Reduced Chi-Sqr	167.97357								
R-Square (COD)	0.99459								
Adj. R-Square	0.99424								

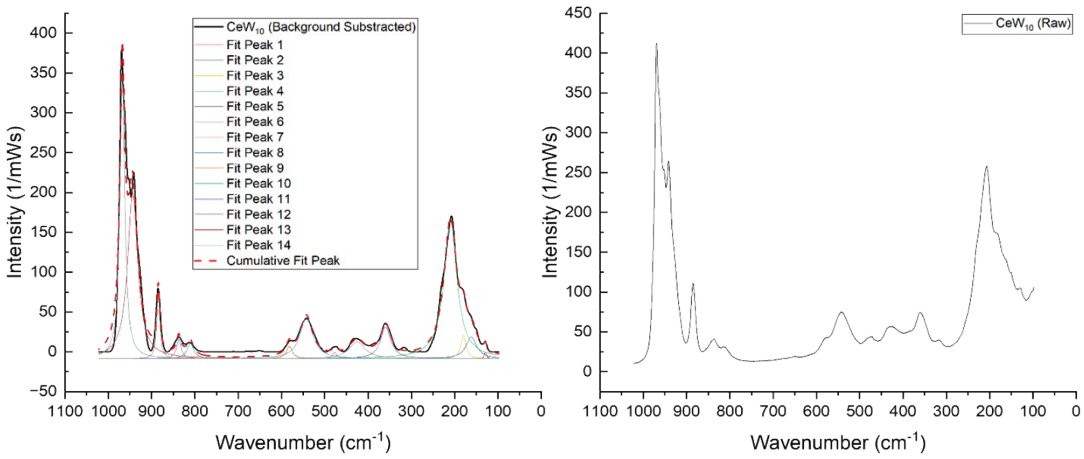

Figure S27. (**Left**) Background subtracted Raman spectrum of complex **2** (CeW_{10}) fit to Lorentzian functions. (**Right**) Raw Raman spectrum for complex **2**.

Table S19. Peak fitting parameters for Raman spectrum of complex **2**.

Model	Lorentz						
Equation	y = y0 + (2*A/pi)*(w/(4*(x-xc)^2 + w^2))						
Plot	Peak1 (Intensity)	Peak2 (Intensity)	Peak3 (Intensity)	Peak4 (Intensity)	Peak5 (Intensity)	Peak6 (Intensity)	Peak7 (Intensity)
y0	-8.55346 ± 0.6172	-8.55346 ± 0.6172	-8.55346 ± 0.6172	-8.55346 ± 0.6172	-8.55346 ± 0.6172	-8.55346 ± 0.6172	-8.55346 ± 0.6172
xc	128.72767 ± 2.16135	161.347 ± 3.76867	179.60768 ± 1.40311	209.56164 ± 0.36787	359.19543 ± 1.05638	425.13805 ± 2.61231	476.52888 ± 3.53264
w	5.43205 ± 7.14445	29.71914 ± 10.10783	14.00117 ± 6.15885	35.79716 ± 1.12508	28.24098 ± 3.49421	44.54835 ± 9.91003	12.65236 ± 11.42054
A	71.22089 ± 77.45904	1262.34581 ± 529.52242	644.77781 ± 387.32842	9711.06075 ± 291.85097	1752.05296 ± 181.09798	1467.27418 ± 269.11653	151.39527 ± 110.77511
Plot	Peak8 (Intensity)	Peak9 (Intensity)	Peak10 (Intensity)	Peak11 (Intensity)	Peak12 (Intensity)	Peak13 (Intensity)	Peak14 (Intensity)
y0	-8.55346 ± 0.6172	-8.55346 ± 0.6172	-8.55346 ± 0.6172	-8.55346 ± 0.6172	-8.55346 ± 0.6172	-8.55346 ± 0.6172	-8.55346 ± 0.6172
xc	542.55195 ± 0.86989	581.78554 ± 1.99147	810.49072 ± 1.71269	837.12121 ± 1.09978	884.57275 ± 0.25193	943.77607 ± 0.26422	967.55739 ± 0.08724
w	34.09285 ± 0	16.32541 ± 0	18.82615 ± 0	12.7444 ± 0	8.08721 ± 0.74639	28.04757 ± 0.81359	13.53983 ± 0.3172
A	2806.57498 ± 111.64957	392.8631 ± 74.21776	560.56509 ± 77.927	479.72222 ± 62.71792	1034.93814 ± 70.65604	9174.91526 ± 257.73164	7327.26229 ± 179.07014
Reduced Chi-Sqr	83.1653						
R-Square (COD)	0.97781						
Adj. R-Square	0.97682						

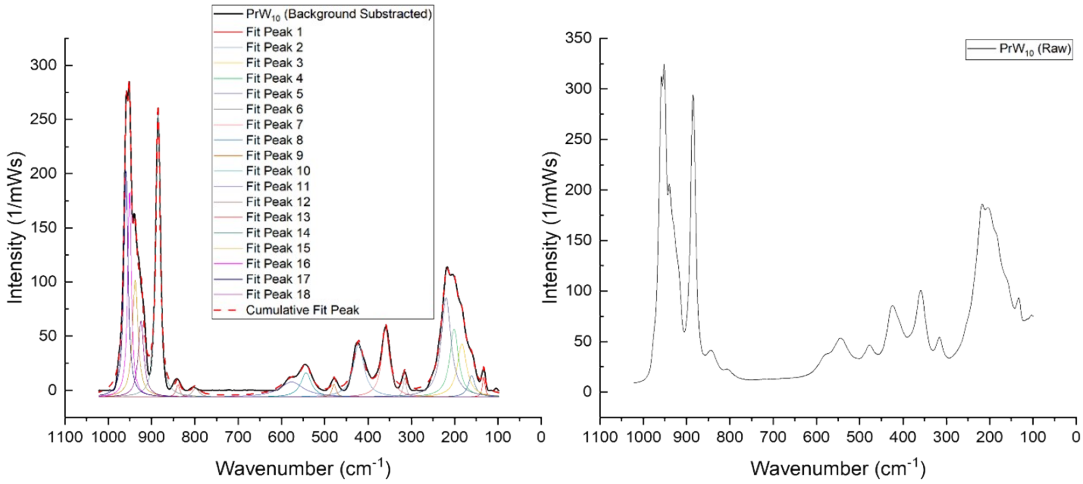

Figure S28. (**Left**) Background subtracted Raman spectrum of complex **3** (PrW_{10}) fit to Lorentzian functions. (**Right**) Raw Raman spectrum for complex **3**.

Table S20. Peak fitting parameters for Raman spectrum of complex **3**.

Model	Lorentz								
Equation	y = y0 + (2*A/pi)*(w/(4*(x-xc)^2 + w^2))								
Plot	Peak1 (Intensity)	Peak2 (Intensity)	Peak3 (Intensity)	Peak4 (Intensity)	Peak5 (Intensity)	Peak6 (Intensity)	Peak7 (Intensity)	Peak8 (Intensity)	Peak9 (Intensity)
y0	-6.13315 ± 0.30949	-6.13315 ± 0.30949	-6.13315 ± 0.30949	-6.13315 ± 0.30949	-6.13315 ± 0.30949	-6.13315 ± 0.30949	-6.13315 ± 0.30949	-6.13315 ± 0.30949	-6.13315 ± 0.30949
xc	132.65658 ± 0.5081	160.57111 ± 1.31367	183.02827 ± 1.54241	201.06143 ± 0.96284	219.54585 ± 0.74281	315.31067 ± 0.55977	359.33723 ± 0.25536	421.64325 ± 0.38188	478.51372 ± 0.92153
w	7.19654 ± 1.59907	18.59429 ± 4.948	25.88199 ± 6.55112	24.25583 ± 6.41885	26.7591 ± 1.44909	8.43506 ± 1.66657	21.63972 ± 0.81648	29.20224 ± 1.24331	10.84667 ± 2.78179
A	207.7142 ± 36.40934	575.75034 ± 233.09212	1996.3406 ± 912.45055	2387.02292 ± 1142.85807	3863.13013 ± 522.73052	233.48396 ± 34.21467	2121.10266 ± 61.85019	2221.18544 ± 73.8408	204.11032 ± 39.26909
Plot	Peak10 (Intensity)	Peak11 (Intensity)	Peak12 (Intensity)	Peak13 (Intensity)	Peak14 (Intensity)	Peak15 (Intensity)	Peak16 (Intensity)	Peak17 (Intensity)	Peak18 (Intensity)
y0	-6.13315 ± 0.30949	-6.13315 ± 0.30949	-6.13315 ± 0.30949	-6.13315 ± 0.30949	-6.13315 ± 0.30949	-6.13315 ± 0.30949	-6.13315 ± 0.30949	-6.13315 ± 0.30949	-6.13315 ± 0.30949
xc	543.15903 ± 1.08326	576.27918 ± 4.13816	798.42671 ± 1.82479	839.38277 ± 0.90287	885.0843 ± 0.04099	937.87606 ± 0.2367	951.08579 ± 0.12143	959.20744 ± 0.14161	924.53192 ± 0.40584
w	28.47215 ± 4.03939	65.54114 ± 0	19.18812 ± 0	10.12777 ± 2.69725	11.07876 ± 0.1255	14.9474 ± 1.3701	9.94549 ± 0.59544	11.18136 ± 0.29712	15.31284 ± 1.08122
A	1009.49661 ± 183.97148	1430.81422 ± 180.54781	236.69367 ± 35.0556	181.66716 ± 35.94961	4578.59697 ± 39.29689	2535.40016 ± 316.45758	2967.1853 ± 270.01727	3664.28302 ± 181.71676	1689.50647 ± 196.73666
Reduced Chi-Sqr	16.59829								
R-Square (COD)	0.99403								
Adj. R-Square	0.99366								

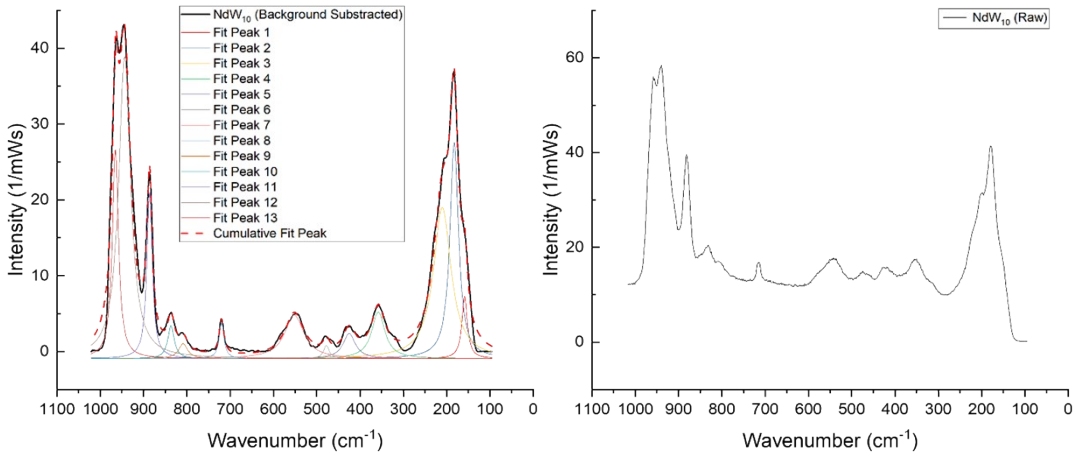

Figure S29. (**Left**) Background subtracted Raman spectrum of complex **4** (NdW_{10}) fit to Lorentzian functions. (**Right**) Raw Raman spectrum for complex **4**.

Table S21. Peak fitting parameters for Raman spectrum of complex **4**.

Model	Lorentz						
Equation	y = y0 + (2*A/pi)*(w/(4*(x-xc)^2 + w^2))						
Plot	Peak1 (Intensity)	Peak2 (Intensity)	Peak3 (Intensity)	Peak4 (Intensity)	Peak5 (Intensity)	Peak6 (Intensity)	Peak7 (Intensity)
y0	-0.91247 ± 0.042	-0.91247 ± 0.042	-0.91247 ± 0.042	-0.91247 ± 0.042	-0.91247 ± 0.042	-0.91247 ± 0.042	-0.91247 ± 0.042
xc	158.22159 ± 0.13764	182.32357 ± 0.06481	209.91086 ± 0.23978	357.77593 ± 0.27189	424.98358 ± 0.63326	477.83019 ± 0.62728	551.8646 ± 0.4143
w	15.19911 ± 0.4665	23.87127 ± 0.32844	49.24361 ± 0.5203	36.7959 ± 0.96932	34.24839 ± 2.10125	15.95868 ± 2.00263	52.90546 ± 1.46803
A	195.32326 ± 6.67199	1068.1673 ± 20.69703	1541.83531 ± 24.83975	353.51301 ± 8.33341	176.72614 ± 9.98382	42.45262 ± 4.66086	475.32889 ± 12.30822
Plot	Peak8 (Intensity)	Peak9 (Intensity)	Peak10 (Intensity)	Peak11 (Intensity)	Peak12 (Intensity)	Peak13 (Intensity)	
y0	-0.91247 ± 0.042	-0.91247 ± 0.042	-0.91247 ± 0.042	-0.91247 ± 0.042	-0.91247 ± 0.042	-0.91247 ± 0.042	
xc	719.91293 ± 0.17402	808.83191 ± 0.75853	836.79723 ± 0.25663	886.34283 ± 0.04137	943.88869 ± 0.07773	965.20651 ± 0.04992	
w	13.17334 ± 0.55452	24.72573 ± 2.76829	17.60192 ± 0.86959	14.75484 ± 0.12728	33.06819 ± 0.19211	17.00212 ± 0.1828	
A	96.82962 ± 3.32828	75.84663 ± 8.00664	119.85697 ± 5.88933	507.24263 ± 3.69056	2066.36838 ± 15.45656	735.85251 ± 11.04901	
Reduced Chi-Sqr	0.12505						
R-Square (COD)	0.99902						
Adj. R-Square	0.99899						

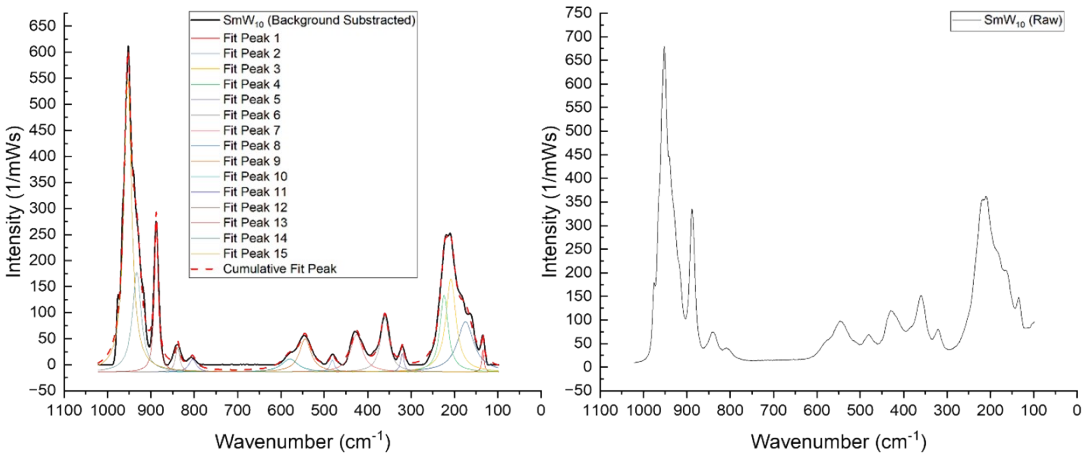

Figure S30. (**Left**) Background subtracted Raman spectrum of complex **5** (SmW_{10}) fit to Lorentzian functions. (**Right**) Raw Raman spectrum for complex **5**.

Table S22. Peak fitting parameters for Raman spectrum of complex **5**.

Model	Lorentz							
Equation	y = y0 + (2*A/pi)*(w/(4*(x-xc)^2 + w^2))							
Plot	Peak1 (Intensity)	Peak2 (Intensity)	Peak3 (Intensity)	Peak4 (Intensity)	Peak5 (Intensity)	Peak6 (Intensity)	Peak7 (Intensity)	Peak8 (Intensity)
y0	-13.79663 ± 0.76681	-13.79663 ± 0.76681	-13.79663 ± 0.76681	-13.79663 ± 0.76681	-13.79663 ± 0.76681	-13.79663 ± 0.76681	-13.79663 ± 0.76681	-13.79663 ± 0.76681
xc	134.00419 ± 0.49918	174.25849 ± 1.70217	207.90455 ± 1.30403	223.62324 ± 1.09715	320.02186 ± 0.7642	360.44298 ± 0.42154	425.59196 ± 0.69825	481.52103 ± 1.341
w	5.72887 ± 1.67707	45.76764 ± 4.5009	28.02555 ± 4.42401	22.73975 ± 2.67608	9.49252 ± 2.32467	23.83083 ± 1.39163	32.1992 ± 2.33333	12.55676 ± 4.0963
A	383.05717 ± 94.07888	6941.65437 ± 1040.21171	7868.66869 ± 2328.63241	5266.44999 ± 1591.79972	526.41124 ± 97.47249	3858.58163 ± 176.02167	3647.86028 ± 207.98227	449.97155 ± 111.26042
Plot	Peak9 (Intensity)	Peak10 (Intensity)	Peak11 (Intensity)	Peak12 (Intensity)	Peak13 (Intensity)	Peak14 (Intensity)	Peak15 (Intensity)	
y0	-13.79663 ± 0.76681	-13.79663 ± 0.76681	-13.79663 ± 0.76681	-13.79663 ± 0.76681	-13.79663 ± 0.76681	-13.79663 ± 0.76681	-13.79663 ± 0.76681	
xc	544.2887 ± 0.91513	579.45719 ± 2.95947	804.05604 ± 1.58428	838.51521 ± 0.60545	887.58566 ± 0.09511	932.54182 ± 0.39862	953.32337 ± 0.11197	
w	31.98048 ± 0	44.52225 ± 0	20.72059 ± 0	11.72595 ± 0	10.11706 ± 0.29396	24.47152 ± 1.15604	20.82246 ± 0.33509	
A	3194.81318 ± 167.13228	1754.23858 ± 192.98359	789.20564 ± 94.13166	871.56642 ± 67.54177	4427.03706 ± 99.05513	7364.16196 ± 434.1419	18463.3915 ± 395.14759	
Reduced Chi-Sqr	109.80477							
R-Square (COD)	0.98916							
Adj. R-Square	0.98863							

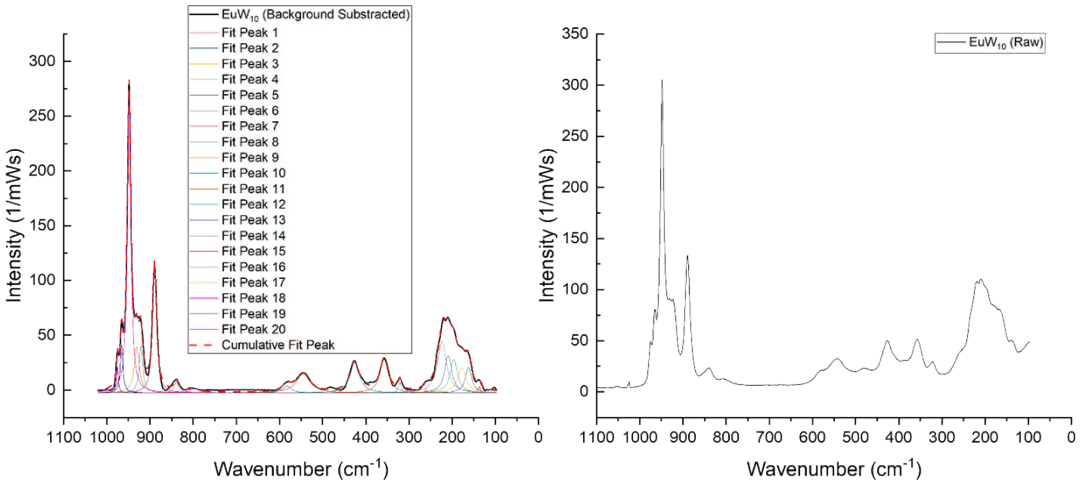

Figure S31. (**Left**) Background subtracted Raman spectrum of complex **6** (EuW_{10}) fit to Lorentzian functions. (**Right**) Raw Raman spectrum for complex **6**.

Table S23. Peak fitting parameters for Raman spectrum of complex **6**.

Model	Lorentz									
Equation	y = y0 + (2*A/pi)*(w/(4*(x-xc)^2 + w^2))									
Plot	Peak1 (Intensity)	Peak2 (Intensity)	Peak3 (Intensity)	Peak4 (Intensity)	Peak5 (Intensity)	Peak6 (Intensity)	Peak7 (Intensity)	Peak8 (Intensity)	Peak9 (Intensity)	Peak10 (Intensity)
y0	-2.52683 ± 0.14072	-2.52683 ± 0.14072	-2.52683 ± 0.14072	-2.52683 ± 0.14072	-2.52683 ± 0.14072	-2.52683 ± 0.14072	-2.52683 ± 0.14072	-2.52683 ± 0.14072	-2.52683 ± 0.14072	-2.52683 ± 0.14072
xc	136.61183 ± 0.73754	162.31996 ± 0.84784	177.51798 ± 1.22385	195.86656 ± 1.3314	209.11304 ± 1.05015	223.3791 ± 0.92806	260.84929 ± 1.14289	321.12088 ± 0.47215	357.63562 ± 0.2526	425.79264 ± 0.28609
w	6.65705 ± 2.39836	17.40553 ± 2.816	23.19336 ± 8.53615	20.41627 ± 7.08987	19.82037 ± 6.83001	24.40104 ± 1.49028	5.53803 ± 3.54357	8.15313 ± 1.4342	22.7188 ± 0.81487	25.22724 ± 0.88991
A	59.29344 ± 17.63172	636.2522 ± 221.91115	826.53119 ± 514.5439	973.80657 ± 694.24993	1052.37696 ± 736.93689	1805.88285 ± 338.30652	28.44883 ± 14.11466	122.53544 ± 16.28791	1078.64992 ± 29.65796	1093.95059 ± 29.79114
Plot	Peak11 (Intensity)	Peak12 (Intensity)	Peak13 (Intensity)	Peak14 (Intensity)	Peak15 (Intensity)	Peak16 (Intensity)	Peak17 (Intensity)	Peak18 (Intensity)	Peak19 (Intensity)	Peak20 (Intensity)
y0	-2.52683 ± 0.14072	-2.52683 ± 0.14072	-2.52683 ± 0.14072	-2.52683 ± 0.14072	-2.52683 ± 0.14072	-2.52683 ± 0.14072	-2.52683 ± 0.14072	-2.52683 ± 0.14072	-2.52683 ± 0.14072	-2.52683 ± 0.14072
xc	545.43993 ± 0.63987	582.73841 ± 1.30487	796.72954 ± 2.33203	839.34071 ± 0.49237	889.30137 ± 0.04237	920.90189 ± 0.21728	930.64708 ± 0.34947	948.42238 ± 0.01944	965.86079 ± 0.10423	975.62603 ± 0.14437
w	38.02573 ± 2.15506	23.23998 ± 0	27.37242 ± 0	11.68462 ± 1.49179	10.68922 ± 0.12942	9.99667 ± 0.69475	14.10453 ± 1.1652	9.61491 ± 0.07637	7.40089 ± 0.38068	4.93255 ± 0.47973
A	1034.5242 ± 50.67772	228.61892 ± 24.40241	149.07574 ± 20.19175	192.32128 ± 18.41828	1951.57874 ± 17.89472	674.40618 ± 77.81334	933.46296 ± 105.47454	4156.04801 ± 33.401	504.553 ± 22.24967	188.79426 ± 15.85178
Reduced Chi-Sqr	3.58779									
R-Square (COD)	0.99665									
Adj. R-Square	0.99642									

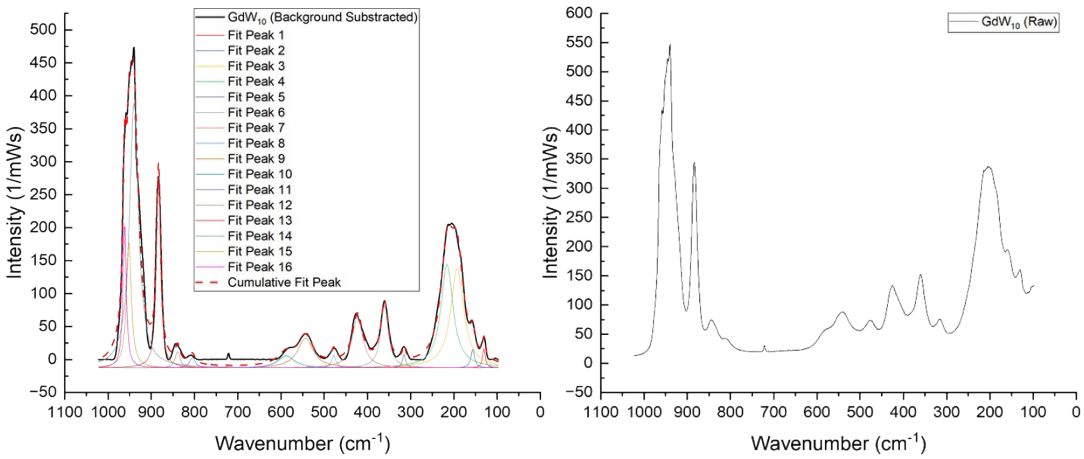

Figure S32. (**Left**) Background subtracted Raman spectrum of complex **7** (GdW_{10}) fit to Lorentzian functions. (**Right**) Raw Raman spectrum for complex **7**.

Table S24. Peak fitting parameters for Raman spectrum of complex **7**.

Model	Lorentz							
Equation	y = y0 + (2*A/pi)*(w/(4*(x-xc)^2 + w^2))							
Plot	Peak1 (Intensity)	Peak2 (Intensity)	Peak3 (Intensity)	Peak4 (Intensity)	Peak5 (Intensity)	Peak6 (Intensity)	Peak7 (Intensity)	Peak8 (Intensity)
y0	-12.62297 ± 0.86491	-12.62297 ± 0.86491	-12.62297 ± 0.86491	-12.62297 ± 0.86491	-12.62297 ± 0.86491	-12.62297 ± 0.86491	-12.62297 ± 0.86491	-12.62297 ± 0.86491
xc	130.45262 ± 0.88895	156.26011 ± 1.0588	192.30316 ± 1.26284	215.90714 ± 1.05595	315.3342 ± 1.31249	360.49808 ± 0.43674	423.10466 ± 0.64309	478.04667 ± 1.59749
w	7.88471 ± 2.71149	10.07125 ± 3.92622	36.39697 ± 3.50848	33.84296 ± 2.35806	8.93426 ± 3.909	20.71288 ± 1.38839	29.79798 ± 2.11351	12.05742 ± 4.99748
A	355.88525 ± 93.60914	442.85319 ± 163.21948	8586.33284 ± 1419.36031	8322.08126 ± 1257.5369	285.36207 ± 92.64009	3047.88769 ± 157.8477	3581.7536 ± 198.548	364.35498 ± 117.08066
Plot	Peak9 (Intensity)	Peak10 (Intensity)	Peak11 (Intensity)	Peak12 (Intensity)	Peak13 (Intensity)	Peak14 (Intensity)	Peak15 (Intensity)	Peak16 (Intensity)
y0	-12.62297 ± 0.86491	-12.62297 ± 0.86491	-12.62297 ± 0.86491	-12.62297 ± 0.86491	-12.62297 ± 0.86491	-12.62297 ± 0.86491	-12.62297 ± 0.86491	-12.62297 ± 0.86491
xc	543.47435 ± 1.66882	587.92677 ± 4.40144	804.77165 ± 2.20429	839.18297 ± 1.25963	883.30679 ± 0.0976	940.16952 ± 0.49338	951.91484 ± 0.3877	961.7652 ± 0.22629
w	42.94573 ± 5.85775	46.34339 ± 0	15.78434 ± 0	13.37497 ± 3.8811	11.06548 ± 0.29888	24.61605 ± 0.6441	13.41294 ± 2.56009	9.07133 ± 0.74558
A	3039.71476 ± 403.26916	1318.00234 ± 258.619	386.92806 ± 83.44296	521.86639 ± 114.14627	5041.44633 ± 103.43263	15520.63048 ± 1060.18016	3993.26545 ± 1248.21143	3087.43205 ± 423.12238
Reduced Chi-Sqr	114.72288							
R-Square (COD)	0.98642							
Adj. R-Square	0.98568							

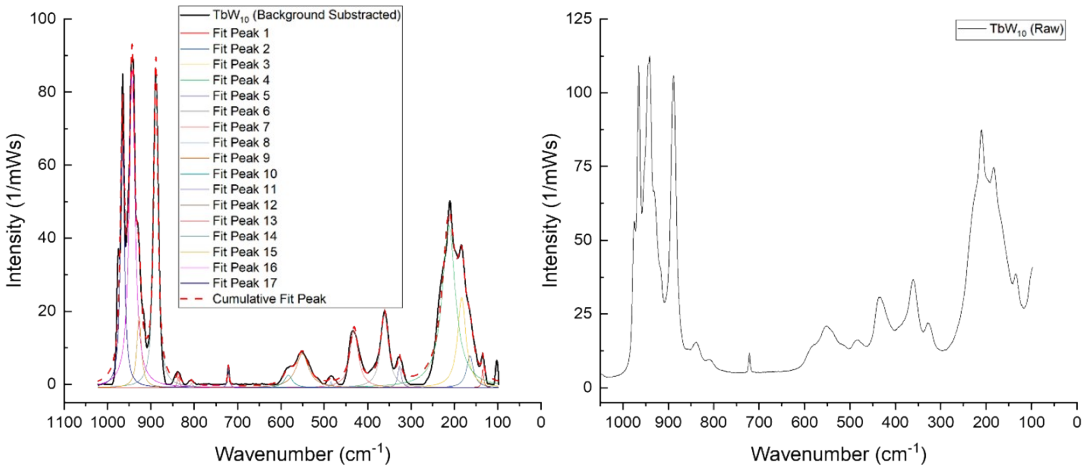

Figure S33. (**Left**) Background subtracted Raman spectrum of complex **8** (TbW_{10}) fit to Lorentzian functions. (**Right**) Raw Raman spectrum for complex **8**.

Table S25. Peak fitting parameters for Raman spectrum of complex **8**.

Model	Lorentz								
Equation	y = y0 + (2*A/pi)*(w/(4*(x-xc)^2 + w^2))								
Plot	Peak1 (Intensity)	Peak2 (Intensity)	Peak3 (Intensity)	Peak4 (Intensity)	Peak5 (Intensity)	Peak6 (Intensity)	Peak7 (Intensity)	Peak8 (Intensity)	Peak9 (Intensity)
y0	-0.94331 ± 0	-0.94331 ± 0	-0.94331 ± 0	-0.94331 ± 0	-0.94331 ± 0	-0.94331 ± 0	-0.94331 ± 0	-0.94331 ± 0	-0.94331 ± 0
xc	134.36866 ± 0.85004	163.86361 ± 1.80798	182.88278 ± 0.736	212.61083 ± 0.51382	326.5303 ± 0.99399	361.00161 ± 0.45447	431.31034 ± 0.59557	484.55942 ± 2.62685	550.81478 ± 1.74414
w	4.88353 ± 2.57163	18.84902 ± 5.64137	22.7707 ± 3.53204	36.38905 ± 1.26325	9.21112 ± 3.03028	21.09244 ± 1.43682	23.3402 ± 1.79274	5.65293 ± 7.65649	34.52318 ± 5.27793
A	39.26389 ± 15.54266	258.26664 ± 112.04602	883.11427 ± 182.2413	2537.60648 ± 113.91388	85.96864 ± 21.33573	659.8311 ± 33.33057	572.66574 ± 31.92864	15.32858 ± 15.07313	505.36019 ± 77.60135
Plot	Peak10 (Intensity)	Peak11 (Intensity)	Peak12 (Intensity)	Peak13 (Intensity)	Peak14 (Intensity)	Peak15 (Intensity)	Peak16 (Intensity)	Peak17 (Intensity)	
y0	-0.94331 ± 0	-0.94331 ± 0	-0.94331 ± 0	-0.94331 ± 0	-0.94331 ± 0	-0.94331 ± 0	-0.94331 ± 0	-0.94331 ± 0	
xc	582.97816 ± 3.26201	721.44674 ± 0.70735	806.43705 ± 4.22005	836.82412 ± 1.49766	888.53059 ± 0.07102	927.30868 ± 0.44799	943.34038 ± 0.12077	965.72414 ± 0.0905	
w	22.58543 ± 11.19487	4.70112 ± 2.00436	7.54766 ± 12.07794	5.76545 ± 4.29342	11.45973 ± 0.20905	12.53741 ± 1.51151	15.96491 ± 0.48443	10.49092 ± 0.30388	
A	120.7757 ± 64.34171	42.22655 ± 12.73218	14.3005 ± 16.24657	26.82281 ± 14.21857	1582.40483 ± 20.85967	382.20437 ± 51.76799	2177.88523 ± 68.42718	1145.45459 ± 29.19604	
Reduced Chi-Sqr	5.40776								
R-Square (COD)	0.98372								
Adj. R-Square	0.98275								

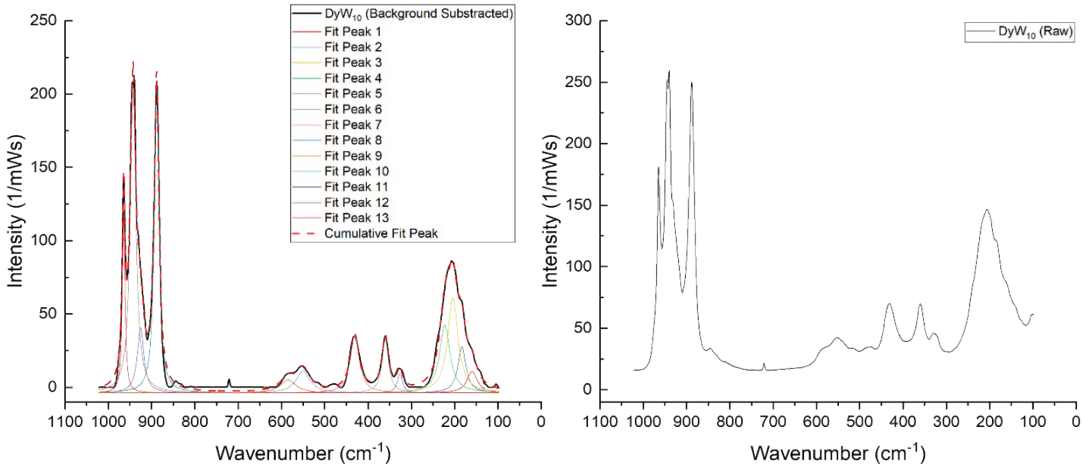

Figure S34. (**Left**) Background subtracted Raman spectrum of complex **9** (DyW_{10}) fit to Lorentzian functions. (**Right**) Raw Raman spectrum for complex **9**.

Table S26. Peak fitting parameters for Raman spectrum of complex **9**.

Model	Lorentz						
Equation	y = y0 + (2*A/pi)*(w/(4*(x-xc)^2 + w^2))						
Plot	Peak1 (Intensity)	Peak2 (Intensity)	Peak3 (Intensity)	Peak4 (Intensity)	Peak5 (Intensity)	Peak6 (Intensity)	Peak7 (Intensity)
y0	-3.8213 ± 0.20131	-3.8213 ± 0.20131	-3.8213 ± 0.20131	-3.8213 ± 0.20131	-3.8213 ± 0.20131	-3.8213 ± 0.20131	-3.8213 ± 0.20131
xc	159.44421 ± 2.14938	183.1203 ± 1.13396	204.02762 ± 0.89636	222.55568 ± 1.60906	326.62788 ± 0.82848	360.03715 ± 0.33334	430.72425 ± 0.35187
w	28.03719 ± 5.22539	22.26128 ± 5.50615	28.55785 ± 5.95515	29.20812 ± 3.189	14.4475 ± 2.62756	18.00083 ± 1.07171	24.81114 ± 1.0726
A	650.51273 ± 175.55093	1102.08441 ± 479.02076	2909.63597 ± 1064.29383	2111.20196 ± 669.6457	293.61803 ± 41.68224	1020.29745 ± 47.05772	1511.32926 ± 49.55328
Plot	Peak8 (Intensity)	Peak9 (Intensity)	Peak10 (Intensity)	Peak11 (Intensity)	Peak12 (Intensity)	Peak13 (Intensity)	
y0	-3.8213 ± 0.20131	-3.8213 ± 0.20131	-3.8213 ± 0.20131	-3.8213 ± 0.20131	-3.8213 ± 0.20131	-3.8213 ± 0.20131	
xc	550.11207 ± 1.48106	584.53307 ± 2.71951	888.41791 ± 0.04462	925.49493 ± 0.4012	942.89256 ± 0.07214	964.64988 ± 0.05791	
w	38.73845 ± 0	43.10164 ± 0	12.66885 ± 0.14024	18.09119 ± 1.27504	15.64452 ± 0.2728	7.21588 ± 0.1894	
A	910.02582 ± 65.02037	601.78193 ± 67.64933	4218.93562 ± 36.38183	1269.93896 ± 103.07191	5164.85575 ± 102.15237	1400.17142 ± 30.3482	
Reduced Chi-Sqr	10.98503						
R-Square (COD)	0.99299						
Adj. R-Square	0.99268						

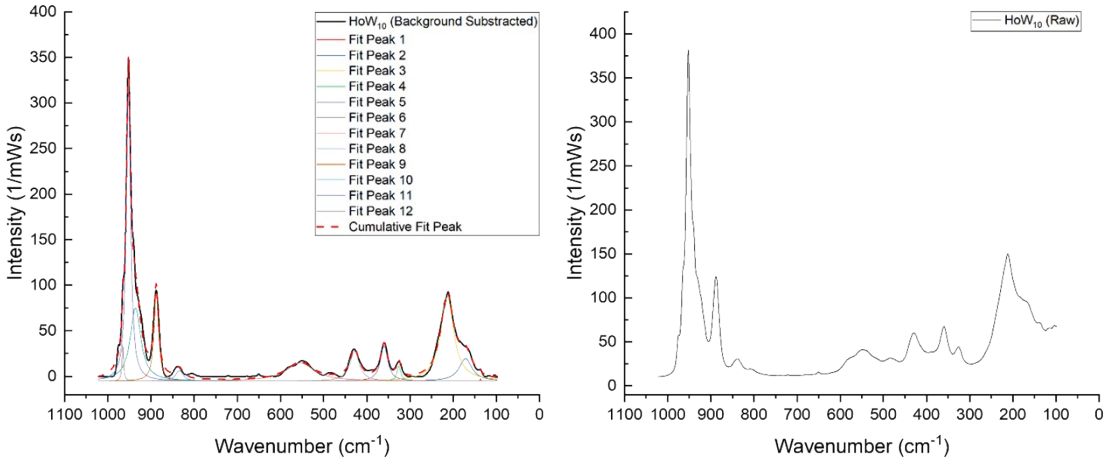

Figure S35. (**Left**) Background subtracted Raman spectrum of complex **10** (HoW_{10}) fit to Lorentzian functions. (**Right**) Raw Raman spectrum for complex **10**.

Table S27. Peak fitting parameters for Raman spectrum of complex **10**.

Model	Lorentz					
Equation	y = y0 + (2*A/pi)*(w/(4*(x-xc)^2 + w^2))					
Plot	Peak1 (Intensity)	Peak2 (Intensity)	Peak3 (Intensity)	Peak4 (Intensity)	Peak5 (Intensity)	Peak6 (Intensity)
y0	-5.15579 ± 0.31037	-5.15579 ± 0.31037	-5.15579 ± 0.31037	-5.15579 ± 0.31037	-5.15579 ± 0.31037	-5.15579 ± 0.31037
xc	136.50065 ± 1.48541	171.17673 ± 0.9212	213.57506 ± 0.25333	325.60043 ± 0.58834	359.89863 ± 0.34907	428.36284 ± 0.45074
w	2.41564 ± 5.91118	35.58838 ± 3.27865	36.34657 ± 0.82169	10.97035 ± 1.834	20.41994 ± 1.13341	25.8764 ± 1.40946
A	10.55151 ± 16.9029	1382.94991 ± 127.76801	5270.99351 ± 123.53303	283.05813 ± 36.584	1227.26424 ± 52.75593	1322.92483 ± 55.68471
Plot	Peak7 (Intensity)	Peak8 (Intensity)	Peak9 (Intensity)	Peak10 (Intensity)	Peak11 (Intensity)	Peak12 (Intensity)
y0	-5.15579 ± 0.31037	-5.15579 ± 0.31037	-5.15579 ± 0.31037	-5.15579 ± 0.31037	-5.15579 ± 0.31037	-5.15579 ± 0.31037
xc	554.48895 ± 1.27341	834.40936 ± 1.10812	887.82357 ± 0.10066	935.85083 ± 0.46362	952.20406 ± 0.03912	965.3809 ± 0.15269
w	78.30547 ± 4.66433	21.08813 ± 3.47656	12.21955 ± 0.32111	29.53394 ± 1.06407	11.85647 ± 0.18906	4.47384 ± 0.51427
A	2456.27221 ± 134.04934	379.87744 ± 49.01913	1850.42543 ± 38.59096	3729.45239 ± 176.79462	5935.3627 ± 123.7291	274.56501 ± 27.34255
Reduced Chi-Sqr	12.03751					
R-Square (COD)	0.99358					
Adj. R-Square	0.9933					

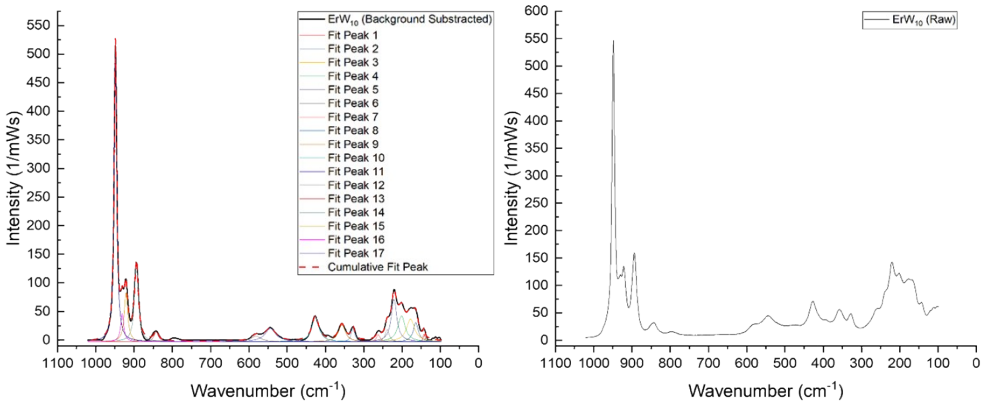

Figure S36. (**Left**) Background subtracted Raman spectrum of complex **11** (ErW_{10}) fit to Lorentzian functions. (**Right**) Raw Raman spectrum for complex **11**.

Table S28. Peak fitting parameters for Raman spectrum of complex **11**.

Model	Lorentz								
Equation	y = y0 + (2*A/pi)*(w/(4*(x-xc)^2 + w^2))								
Plot	Peak1 (Intensity)	Peak2 (Intensity)	Peak3 (Intensity)	Peak4 (Intensity)	Peak5 (Intensity)	Peak6 (Intensity)	Peak7 (Intensity)	Peak8 (Intensity)	Peak9 (Intensity)
y0	-2.57295 ± 0.16242	-2.57295 ± 0.16242	-2.57295 ± 0.16242	-2.57295 ± 0.16242	-2.57295 ± 0.16242	-2.57295 ± 0.16242	-2.57295 ± 0.16242	-2.57295 ± 0.16242	-2.57295 ± 0.16242
xc	142.34617 ± 0.39463	163.95516 ± 0.64392	177.6406 ± 1.14645	201.12081 ± 0.47555	220.66066 ± 0.20774	238.70978 ± 0.43627	261.67537 ± 0.60601	327.95741 ± 0.30933	356.98812 ± 0.34629
w	5.67228 ± 1.32403	15.68309 ± 2.49927	24.98159 ± 4.73377	22.5443 ± 2.80578	17.28984 ± 1.03846	12.34456 ± 1.68776	11.22567 ± 1.94589	10.63907 ± 0.99556	21.27942 ± 1.14121
A	114.82462 ± 22.96463	823.49636 ± 274.76954	1551.4863 ± 484.89149	1597.0937 ± 295.10426	1996.4662 ± 161.68754	421.86429 ± 63.51898	211.60668 ± 29.48396	373.40241 ± 28.15245	976.81488 ± 41.2265
Plot	Peak10 (Intensity)	Peak11 (Intensity)	Peak12 (Intensity)	Peak13 (Intensity)	Peak14 (Intensity)	Peak15 (Intensity)	Peak16 (Intensity)	Peak17 (Intensity)	
y0	-2.57295 ± 0.16242	-2.57295 ± 0.16242	-2.57295 ± 0.16242	-2.57295 ± 0.16242	-2.57295 ± 0.16242	-2.57295 ± 0.16242	-2.57295 ± 0.16242	-2.57295 ± 0.16242	
xc	426.24457 ± 0.21912	544.02418 ± 0.68629	581.38374 ± 1.52594	842.39011 ± 0.42801	893.88167 ± 0.05015	921.19791 ± 0.13122	931.01681 ± 0.20005	948.66463 ± 0.01099	
w	21.49291 ± 0.66808	33.0597 ± 2.19893	30.53211 ± 4.99974	13.45215 ± 1.28347	11.70831 ± 0.15776	10.73949 ± 0.39355	9.63341 ± 0.69689	7.95211 ± 0.03544	
A	1472.18248 ± 34.70302	1176.76634 ± 78.69389	455.27207 ± 76.2062	358.41829 ± 25.60835	2518.83077 ± 26.13016	1442.99705 ± 65.12958	742.47665 ± 65.06589	6518.7246 ± 23.51159	
Reduced Chi-Sqr	6.20764								
R-Square (COD)	0.99757								
Adj. R-Square	0.99742								

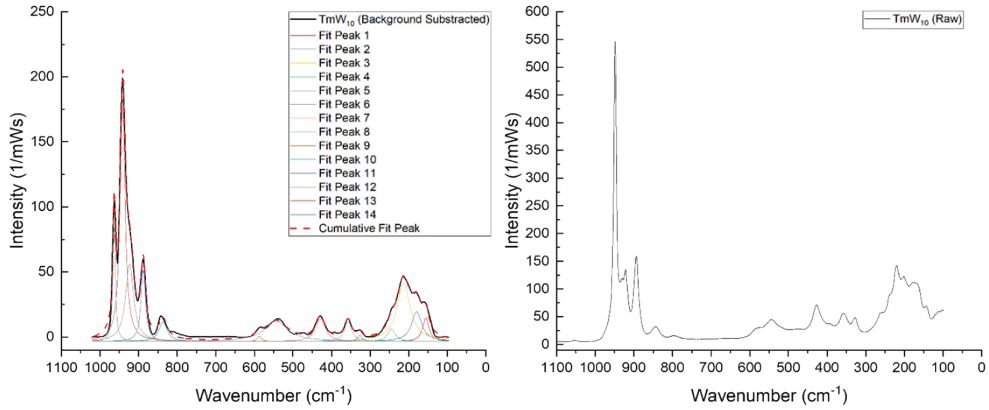

Figure S37. (**Left**) Background subtracted Raman spectrum of complex **12** (TmW_{10}) fit to Lorentzian functions. (**Right**) Raw Raman spectrum for complex **12**.

Table S29. Peak fitting parameters for Raman spectrum of complex **12**.

Model	Lorentz						
Equation	y = y0 + (2*A/pi)*(w/(4*(x-xc)^2 + w^2))						
Plot	Peak1 (Intensity)	Peak2 (Intensity)	Peak3 (Intensity)	Peak4 (Intensity)	Peak5 (Intensity)	Peak6 (Intensity)	Peak7 (Intensity)
y0	-3.32657 ± 0.28031	-3.32657 ± 0.28031	-3.32657 ± 0.28031	-3.32657 ± 0.28031	-3.32657 ± 0.28031	-3.32657 ± 0.28031	-3.32657 ± 0.28031
xc	155.53057 ± 1.05966	179.2298 ± 1.39368	213.28231 ± 0.87187	244.53931 ± 2.03363	326.90104 ± 1.9559	357.12303 ± 0.89931	428.82853 ± 0.82127
w	19.34995 ± 3.93527	31.59093 ± 8.41462	41.01969 ± 5.16222	23.43297 ± 8.48999	12.20829 ± 6.4301	22.46785 ± 3.03268	28.96437 ± 2.63865
A	544.2663 ± 168.28691	1126.71866 ± 433.92799	2873.31266 ± 498.46763	346.98584 ± 188.45811	92.61116 ± 40.34892	522.77159 ± 57.03721	788.4039 ± 56.64486
Plot	Peak8 (Intensity)	Peak9 (Intensity)	Peak10 (Intensity)	Peak11 (Intensity)	Peak12 (Intensity)	Peak13 (Intensity)	Peak14 (Intensity)
y0	-3.32657 ± 0.28031	-3.32657 ± 0.28031	-3.32657 ± 0.28031	-3.32657 ± 0.28031	-3.32657 ± 0.28031	-3.32657 ± 0.28031	-3.32657 ± 0.28031
xc	543.63258 ± 2.0473	587.13701 ± 2.52912	836.72544 ± 0.8463	888.05465 ± 0.17854	923.4078 ± 0.45452	941.54361 ± 0.08245	963.44761 ± 0.08072
w	73.50244 ± 6.89525	13.46822 ± 9.7723	24.60006 ± 2.71977	13.57051 ± 0.6161	24.85823 ± 1.40848	15.4876 ± 0.32658	7.6697 ± 0.26408
A	1788.50777 ± 166.12602	80.77858 ± 57.23207	581.13261 ± 51.1563	1165.85891 ± 46.28604	2328.73638 ± 162.61203	4530.05136 ± 126.80038	1071.75593 ± 30.48672
Reduced Chi-Sqr	6.22488						
R-Square (COD)	0.99315						
Adj. R-Square	0.99259						

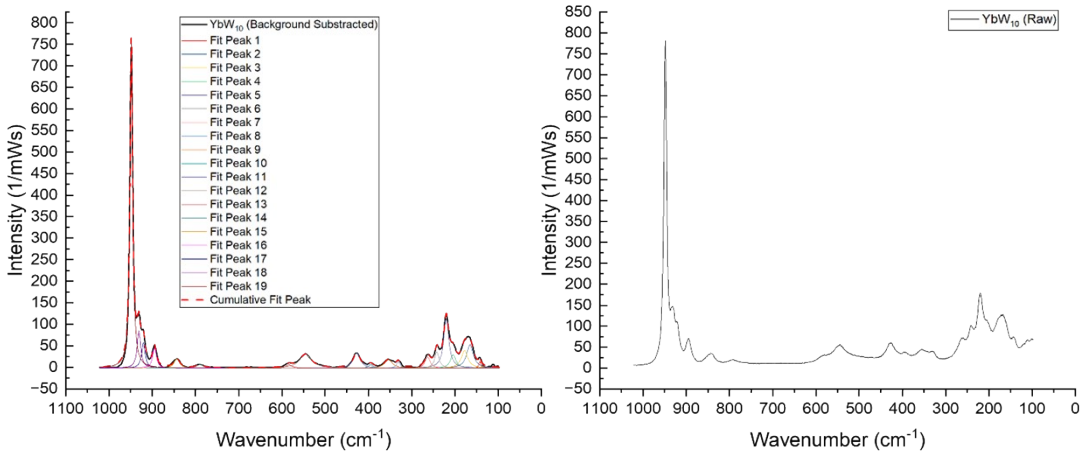

Figure S38. (**Left**) Background subtracted Raman spectrum of complex **13** (YbW_{10}) fit to Lorentzian functions. (**Right**) Raw Raman spectrum for complex **13**.

Table S30. Peak fitting parameters for Raman spectrum of complex **13**.

Model	Lorentz									
Equation	y = y0 + (2*A/pi)*(w/(4*(x-xc)^2 + w^2))									
Plot	Peak1 (Intensity)	Peak2 (Intensity)	Peak3 (Intensity)	Peak4 (Intensity)	Peak5 (Intensity)	Peak6 (Intensity)	Peak7 (Intensity)	Peak8 (Intensity)	Peak9 (Intensity)	Peak10 (Intensity)
y0	-1.57594 ± 0	-1.57594 ± 0	-1.57594 ± 0	-1.57594 ± 0	-1.57594 ± 0	-1.57594 ± 0	-1.57594 ± 0	-1.57594 ± 0	-1.57594 ± 0	-1.57594 ± 0
xc	142.06612 ± 0.45755	165.1466 ± 0.7484	177.58063 ± 0.97463	203.83679 ± 0.52617	219.87538 ± 0.13602	241.62165 ± 0.29625	262.80605 ± 0.4375	330.98736 ± 0.71067	353.29041 ± 0.84347	394.64074 ± 1.36194
w	5.44794 ± 1.52575	18.28082 ± 1.80867	18.16372 ± 2.87665	15.09187 ± 2.2679	14.04623 ± 0.54651	12.16892 ± 1.15315	13.40715 ± 1.41081	10.35215 ± 2.47853	21.88668 ± 2.96962	13.44784 ± 4.5724
A	126.90263 ± 29.76482	1564.60582 ± 301.32906	1168.77217 ± 326.02538	744.73837 ± 129.3076	2521.17813 ± 110.45707	724.10415 ± 63.12785	546.88467 ± 47.74276	222.4029 ± 49.28459	650.39004 ± 75.60801	165.30121 ± 45.38872
Plot	Peak11 (Intensity)	Peak12 (Intensity)	Peak13 (Intensity)	Peak14 (Intensity)	Peak15 (Intensity)	Peak16 (Intensity)	Peak17 (Intensity)	Peak18 (Intensity)	Peak19 (Intensity)	
y0	-1.57594 ± 0	-1.57594 ± 0	-1.57594 ± 0	-1.57594 ± 0	-1.57594 ± 0	-1.57594 ± 0	-1.57594 ± 0	-1.57594 ± 0	-1.57594 ± 0	
xc	427.09809 ± 0.3614	545.71885 ± 0.56393	583.48875 ± 1.69091	789.81053 ± 1.6419	843.343 ± 0.49196	894.88349 ± 0.18168	920.71926 ± 0.21137	931.00772 ± 0.14268	948.58158 ± 0.00997	
w	18.73297 ± 1.13582	32.26173 ± 1.80386	17.94324 ± 5.66779	20.29093 ± 4.83127	14.71944 ± 1.46234	9.98882 ± 0.55476	9.66076 ± 0.67968	9.77226 ± 0.50813	7.49652 ± 0.03174	
A	1024.37714 ± 47.25217	1618.84248 ± 74.49974	206.69985 ± 56.87218	238.40736 ± 40.78158	488.91766 ± 35.22682	742.67209 ± 30.63028	892.6115 ± 71.35549	1333.44753 ± 76.39619	8935.75016 ± 30.18851	
Reduced Chi-Sqr	11.58636									
R-Square (COD)	0.99746									
Adj. R-Square	0.99729									

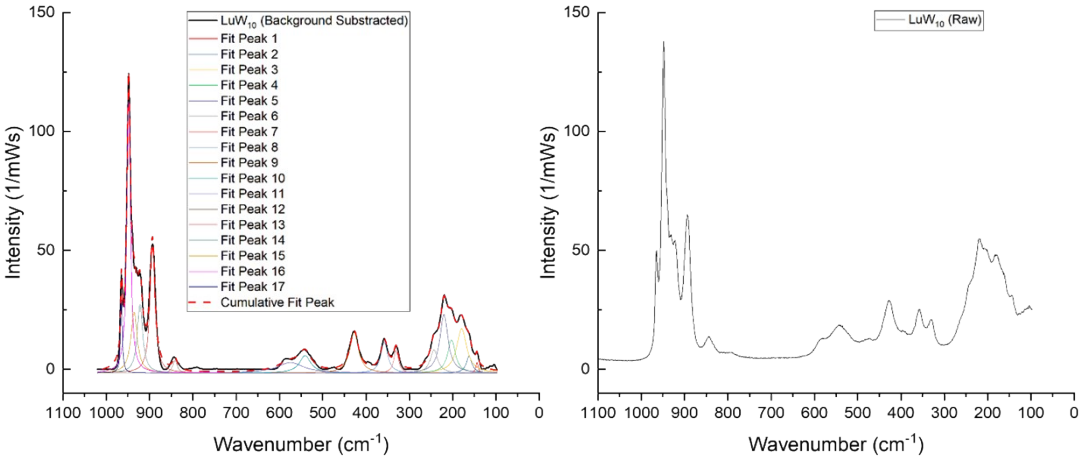

Figure S39. (**Left**) Background subtracted Raman spectrum of complex **14** (LuW_{10}) fit to Lorentzian functions. (**Right**) Raw Raman spectrum for complex **14**.

Table S31. Peak fitting parameters for Raman spectrum of complex **14**.

Model	Lorentz								
Equation	y = y0 + (2*A/pi)*(w/(4*(x-xc)^2 + w^2))								
Plot	Peak1 (Intensity)	Peak2 (Intensity)	Peak3 (Intensity)	Peak4 (Intensity)	Peak5 (Intensity)	Peak6 (Intensity)	Peak7 (Intensity)	Peak8 (Intensity)	Peak9 (Intensity)
y0	-1.5271 ± 0.10874	-1.5271 ± 0.10874	-1.5271 ± 0.10874	-1.5271 ± 0.10874	-1.5271 ± 0.10874	-1.5271 ± 0.10874	-1.5271 ± 0.10874	-1.5271 ± 0.10874	-1.5271 ± 0.10874
xc	143.53553 ± 0.6021	161.9763 ± 1.01224	179.02571 ± 0.84521	202.58103 ± 0.89919	219.96742 ± 0.55658	242.95444 ± 0.77109	330.53956 ± 0.39705	357.69378 ± 0.35548	427.44238 ± 0.27839
w	6.5617 ± 2.08449	15.46924 ± 4.64417	27.83429 ± 4.37326	21.44611 ± 4.85814	22.52026 ± 2.48354	20.46131 ± 2.4236	13.04824 ± 1.30329	18.83612 ± 1.17766	23.83136 ± 0.85881
A	45.24377 ± 12.927	170.45183 ± 86.66066	816.30862 ± 187.48321	469.22536 ± 178.87641	874.78223 ± 152.19054	314.98535 ± 52.67001	190.16536 ± 15.75302	378.72798 ± 19.26669	637.47057 ± 17.66765
Plot	Peak10 (Intensity)	Peak11 (Intensity)	Peak12 (Intensity)	Peak13 (Intensity)	Peak14 (Intensity)	Peak15 (Intensity)	Peak16 (Intensity)	Peak17 (Intensity)	
y0	-1.5271 ± 0.10874	-1.5271 ± 0.10874	-1.5271 ± 0.10874	-1.5271 ± 0.10874	-1.5271 ± 0.10874	-1.5271 ± 0.10874	-1.5271 ± 0.10874	-1.5271 ± 0.10874	
xc	540.79735 ± 1.15483	574.53346 ± 6.73794	841.38369 ± 0.61531	893.42023 ± 0.06636	922.15657 ± 0.28663	936.04982 ± 0.35765	948.45836 ± 0.04044	965.07238 ± 0.06625	
w	31.57012 ± 5.27392	72.81944 ± 11.43938	12.24784 ± 1.86149	13.48841 ± 0.21752	14.96935 ± 0.90919	17.58372 ± 2.26592	9.77441 ± 0.17318	4.87237 ± 0.21228	
A	361.43949 ± 99.87321	501.88078 ± 141.96962	101.83494 ± 11.73204	1131.50174 ± 14.99203	677.30642 ± 71.61584	708.15771 ± 125.69339	1752.08256 ± 49.17821	237.10942 ± 8.40695	
Reduced Chi-Sqr	1.37166								
R-Square (COD)	0.99461								
Adj. R-Square	0.99428								

Table S32. Observed peaks in the Raman spectra of complexes **1-14**.

Complex name	Observed peaks rounded to the first decimal (cm^{-1})
1 (LaW_{10})	139.2, 158.9, 177.1, 196.4, 214.1, 231.5, 320.6, 359.4, 409.1, 428.4, 486.2, 540, 577.2, 806. 9, 837.7, 930.7, 952.5
2 (CeW_{10})	128.7, 161.3, 179.6, 209.5, 359.2, 425.1, 476.5, 542.5, 581.8, 810.5, 837.1, 884.6, 943.8, 967.6
3 (PrW_{10})	132.7, 160.6, 183, 201, 219.5, 315.3, 359.3, 421.6, 478.5, 543.2, 576.3, 798.4, 839.8, 885.1, 924.6,937.9, 951.1, 959.2
4 (NdW_{10})	158.2, 182.3, 209.9, 357.8, 425.0, 477.8, 551.8, 719.9, 808.8, 836.8, 886.3, 943.9, 965.2
5 (SmW_{10})	134.0, 174.3, 207.9, 223.6, 320.0, 360.4, 425.6, 481.5, 544.3, 579.5, 804.1, 838.5, 887.6, 932.5, 953.3
6 (EuW_{10})	136.6, 162.3, 177.5, 195.9, 209.1, 223.4, 260.8, 321.1, 357.6, 425.8, 545.4, 587.7, 796.7, 839.4, 889.3, 921.0, 930.6, 948.4, 965.9, 976.6
7 (GdW_{10})	130.5, 156.3, 192.3, 215.9, 315.3, 360.5, 423.1, 478.0, 543.5, 587.9, 804.8, 839.2, 883.3, 940.2, 951.9, 961.8
8 (TbW_{10})	134.4, 163.9, 182.9, 212.6, 326.5, 361.0, 432.3, 484.6, 550.8, 583.0, 721.4, 806.4, 836.8, 888.5, 927.3, 943.3, 965.7
9 (DyW_{10})	159.4, 183.1, 204.0, 222.6, 326.6, 360.0, 430.7, 550.1, 584.5, 888.4, 925.5, 942.5, 942.9, 964.6
10 (HoW_{10})	136.5, 171.2, 213.6, 325.6, 359.9, 428.4, 554.5, 834.4, 997.9, 935.9, 952.2, 965.4
11 (ErW_{10})	142.3, 164.0, 177.6, 201.1, 220.7, 238.7, 261.7, 328.0, 357.0, 426.2, 544.0, 581.4, 842.4, 893.9, 921.2, 931.0, 948.7
12 (TmW_{10})	155.5, 179.2, 213.3, 244.5, 326.9, 357.1, 428.8, 543.6, 587.1, 836.7, 888.1, 923.4, 941.5, 963.4
13 (YbW_{10})	142.1, 165.1, 177.6, 203.8, 219.9, 241.6, 262.8, 331.0, 353.3, 394.6, 427.1, 545.7, 583.5, 789.8, 843.3, 894.9, 920.7, 931.0, 948.6
14 (LuW_{10})	143.5, 162.0, 179.0, 202.6, 220.0, 243.0, 330.5, 357.7, 427.4, 540.8, 574.5, 841.4, 893.4, 922.2, 936.0, 948.5, 965.1

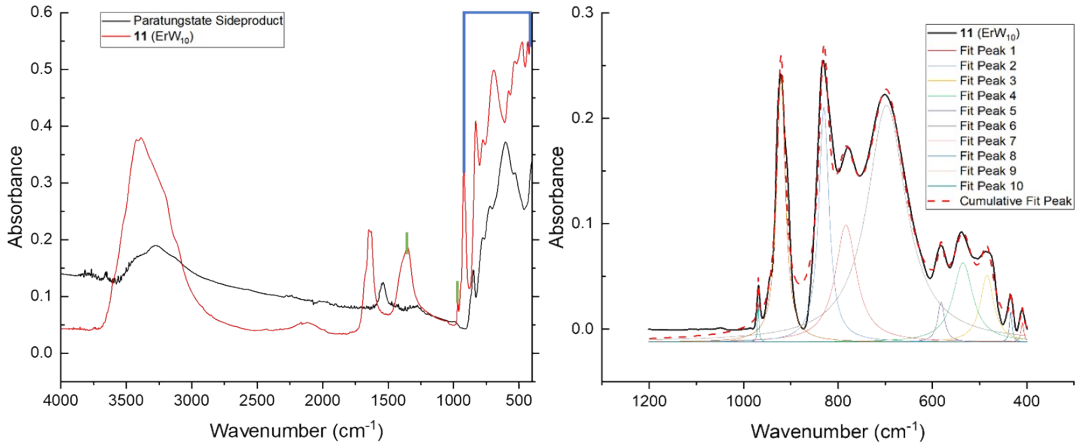

Figure S40. (**Left**) MIR spectrum of complex **11** (ErW_{10}) in red trace overlayed on MIR spectrum of sodium paratungstate ($Na_{10}H_2W_{12}O_{40}•XH_2O$) in black trace. Peaks highlighted with green lines are from $NaNO_3$ ($\nu_{as}(NO_3)$ at 1357 cm^{-1} and $\nu(NO_3)$ at 968 cm^{-1}), while peaks highlighted by blue lines are characteristic of complex **11**. (**Right**) Peak fitting conducted on background subtracted MIR spectra of complex **11** with a spectral window of 1200 – 400 cm^{-1}.

Table S33. Peak fitting parameters for MIR spectrum of complex **11**.

Model	Lorentz				
Equation	y = y0 + (2*A/pi)*(w/(4*(x-xc)^2 + w^2))				
Plot	Peak1(Absorbance)	Peak2(Absorbance)	Peak3(Absorbance)	Peak4(Absorbance)	Peak5(Absorbance)
y0	-0.01217 ± 0.00117	-0.01217 ± 0.00117	-0.01217 ± 0.00117	-0.01217 ± 0.00117	-0.01217 ± 0.00117
xc	409.49463 ± 1.83663	434.14856 ± 1.18035	484.42164 ± 1.50333	535.2119 ± 1.7141	581.73622 ± 1.5098
w	6.90019 ± 5.52321	6.48957 ± 3.49072	34.16717 ± 5.58469	50.66594 ± 8.1525	17.36906 ± 5.67881
A	0.20138 ± 0.11698	0.28889 ± 0.11714	3.39713 ± 0.60988	5.98339 ± 0.9645	1.03615 ± 0.33195
Plot	Peak6(Absorbance)	Peak7(Absorbance)	Peak8(Absorbance)	Peak9(Absorbance)	Peak10(Absorbance)
y0	-0.01217 ± 0.00117	-0.01217 ± 0.00117	-0.01217 ± 0.00117	-0.01217 ± 0.00117	-0.01217 ± 0.00117
xc	697.07477 ± 0.92848	783.26797 ± 1.24826	829.85105 ± 0.34842	920.72996 ± 0.24127	968.94064 ± 0.56284
w	99.42783 ± 3.24602	54.01111 ± 5.91018	26.09676 ± 1.30755	21.81061 ± 0.74384	3.25548 ± 2.55137
A	35.05256 ± 1.22548	9.42117 ± 1.15994	9.12435 ± 0.50266	8.63811 ± 0.22588	0.19416 ± 0.07955
Reduced Chi-Sqr	1.38E-04				
R-Square (COD)	0.97829				
Adj. R-Square	0.9766				

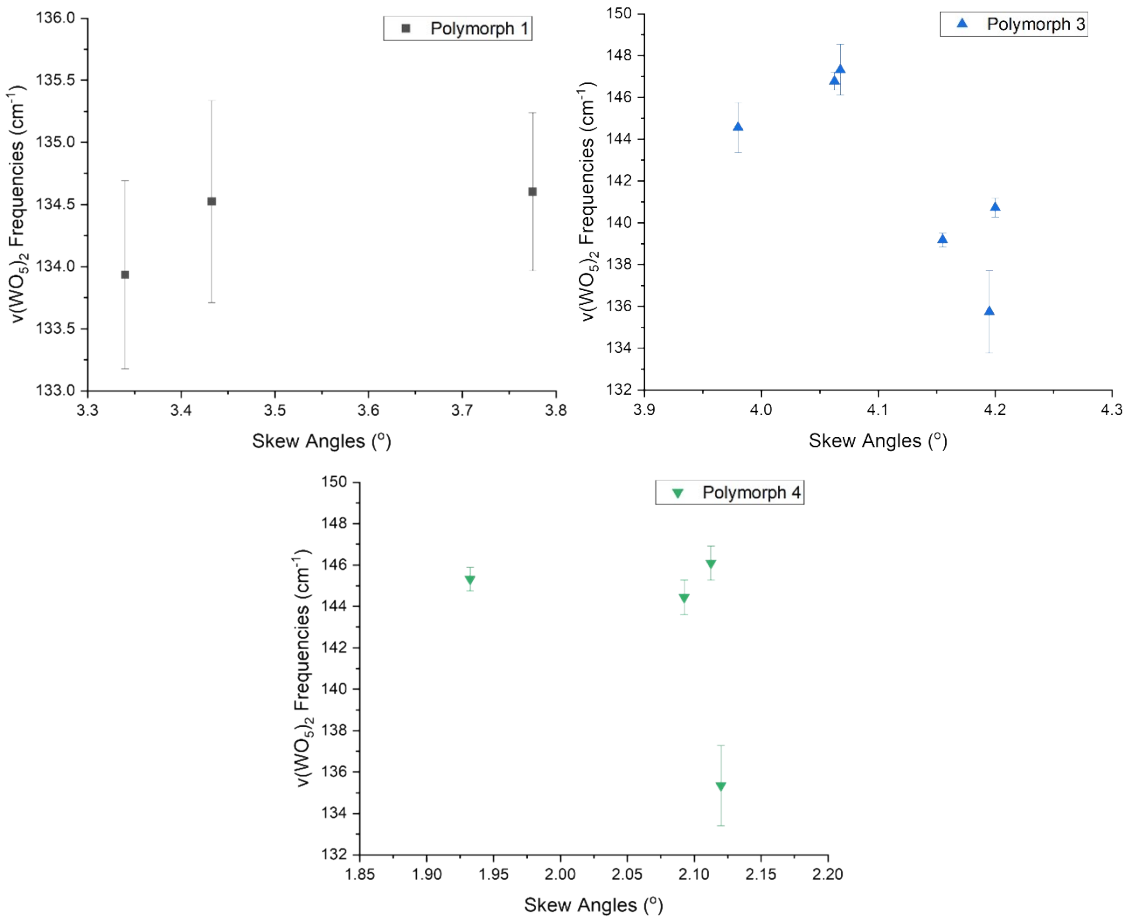

Figure S41. Plots of FIR $\nu(WO_5)_2$ frequencies vs. SAs for LnW_{10} polymorphs. The $\nu(WO_5)_2$ frequencies were obtained from the fitted FIR spectra of complexes **1-14**. Error bars represent uncertainties of the peak center obtained from the fitting regime.

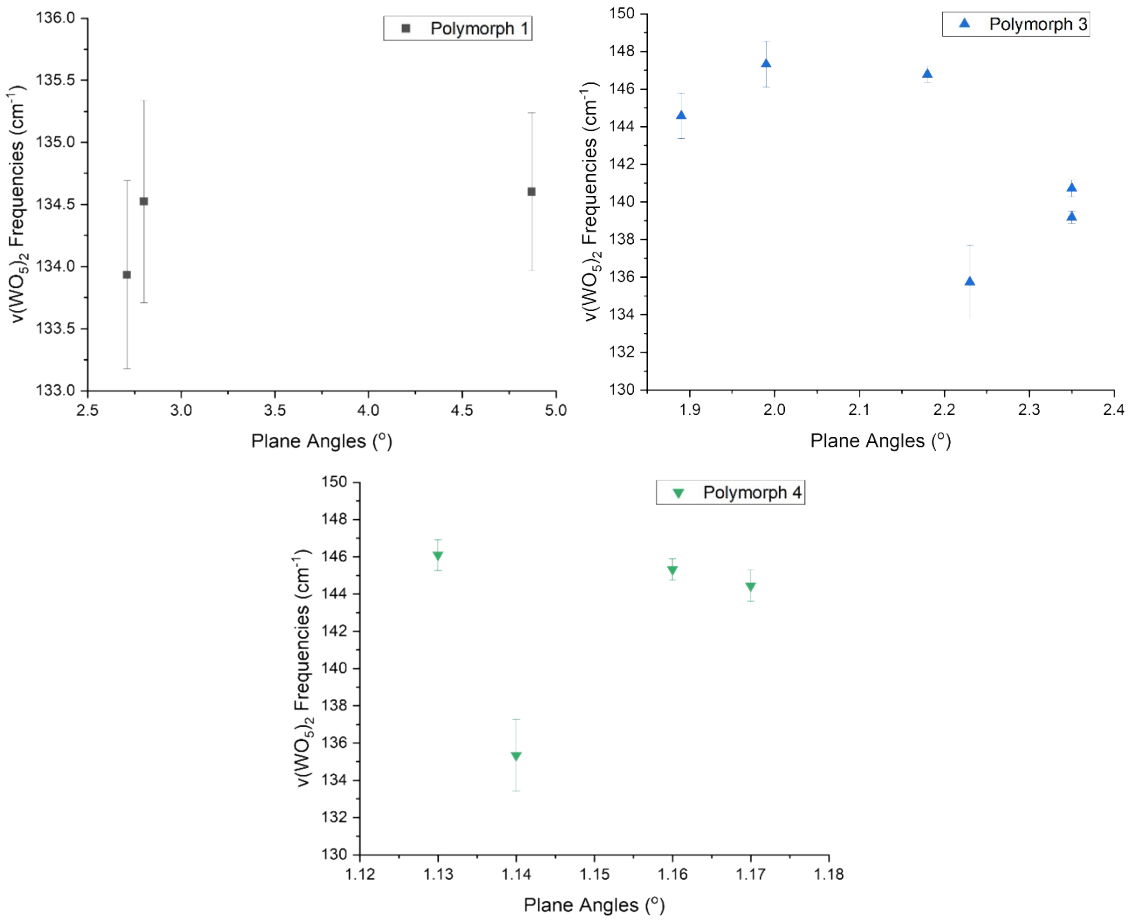

Figure S42. Plots of FIR $\nu(WO_5)_2$ frequencies vs. PAs for LnW_{10} polymorphs. The $\nu(WO_5)_2$ frequencies were obtained from the fitted FIR spectra of complexes **1-14**. Error bars represent uncertainties of the peak center obtained from the fitting regime.

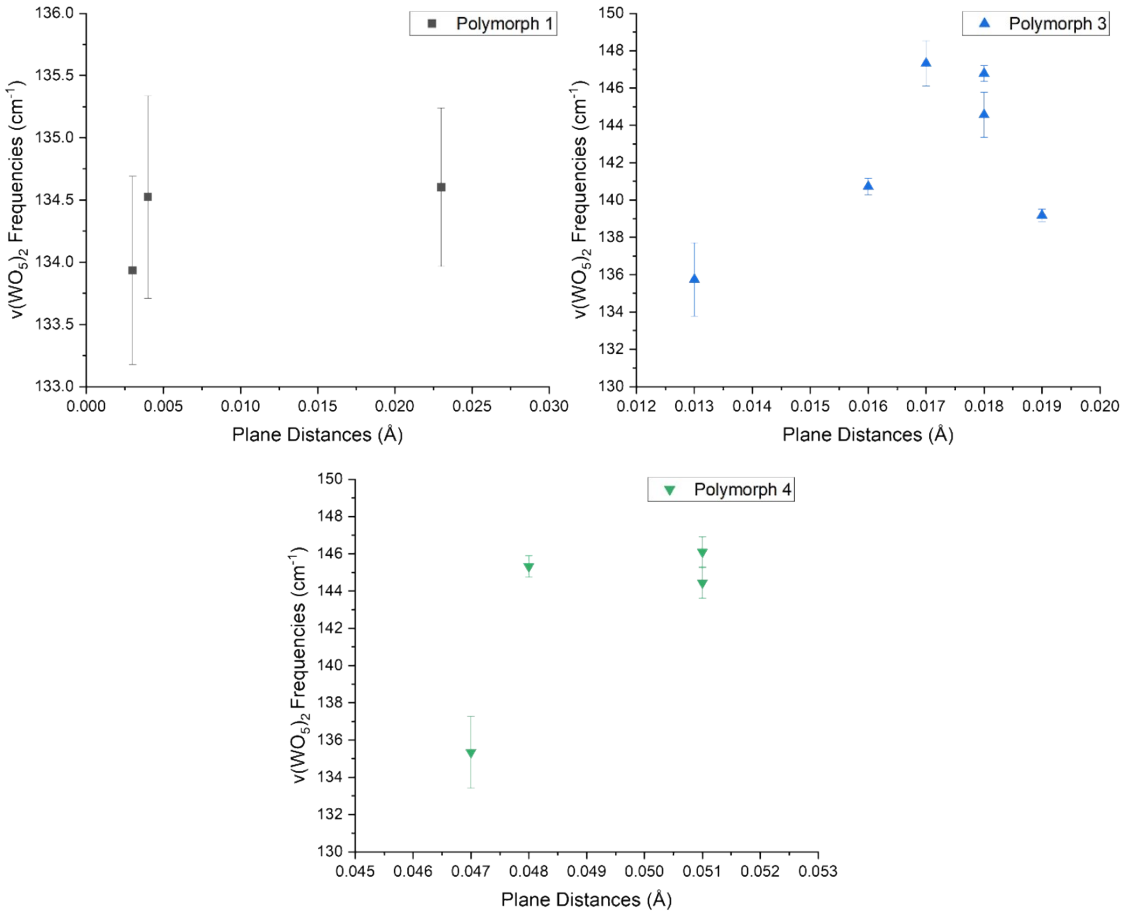

Figure S43. Plots of FIR $\nu(WO_5)_2$ frequencies vs. PDs for LnW_{10} polymorphs. The $\nu(WO_5)_2$ frequencies were obtained from the fitted FIR spectra of complexes **1-14**. Error bars represent uncertainties of the peak center obtained from the fitting regime.

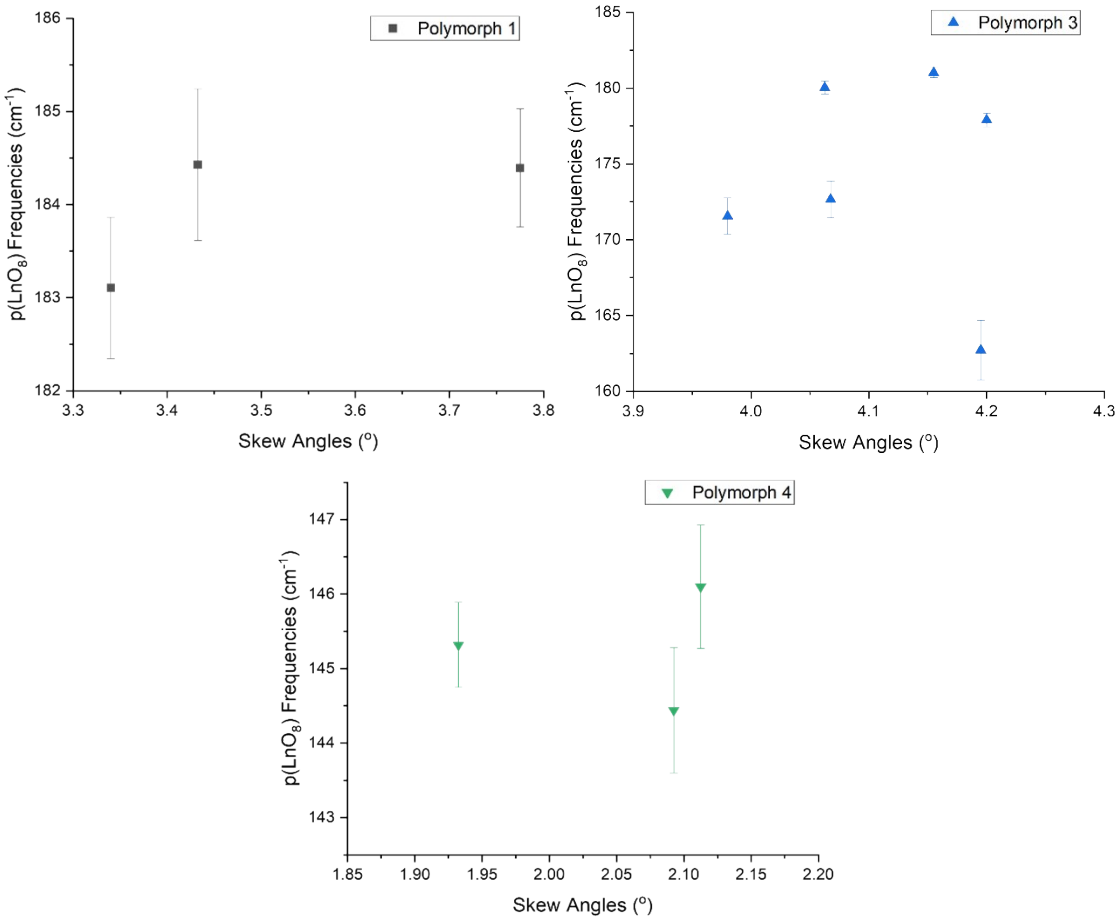

Figure S44. Plots of FIR $\rho(LnO_8)$ frequencies vs. SAs for LnW_{10} polymorphs. The $\rho(LnO_8)$ frequencies were obtained from the fitted FIR spectra of complexes **1-14**. Error bars represent uncertainties of the peak center obtained from the fitting regime.

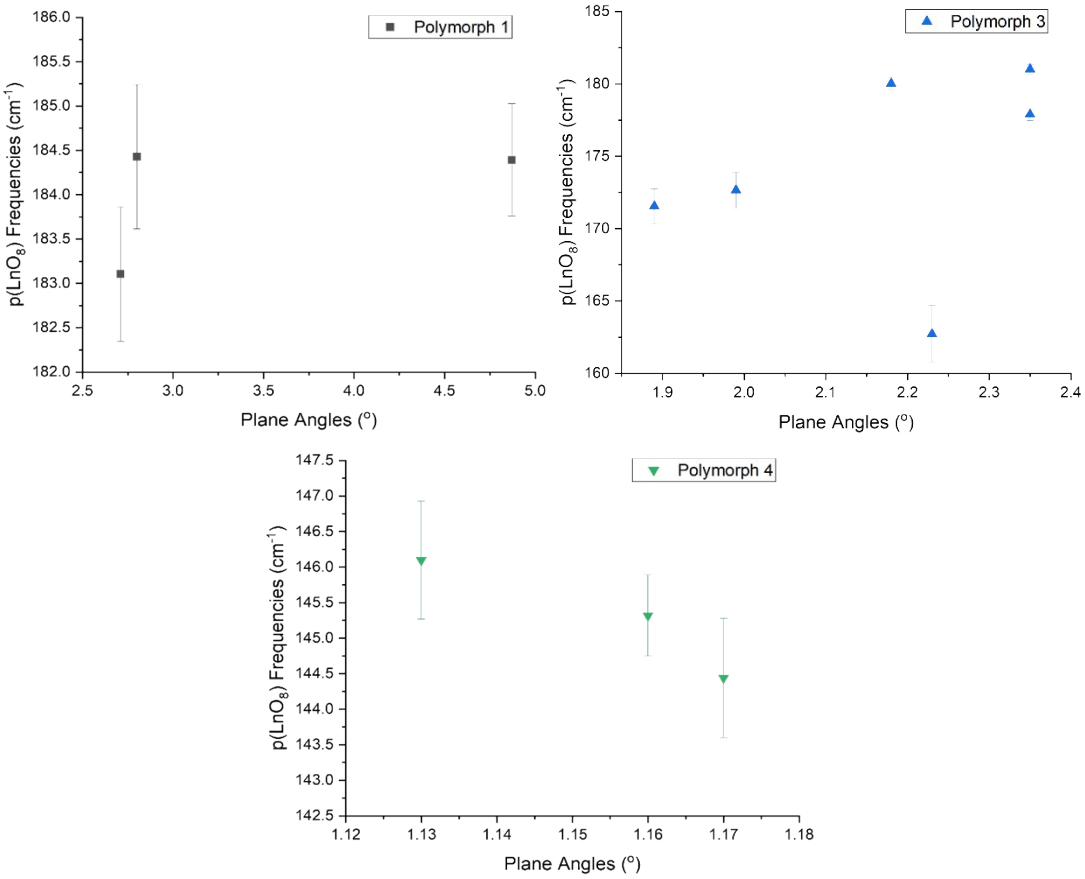

Figure S45. Plots of FIR $\rho(LnO_8)$ frequencies vs. PAs for LnW_{10} polymorphs. The $\rho(LnO_8)$ frequencies were obtained from the fitted FIR spectra of complexes **1-14**. Error bars represent uncertainties of the peak center obtained from the fitting regime.

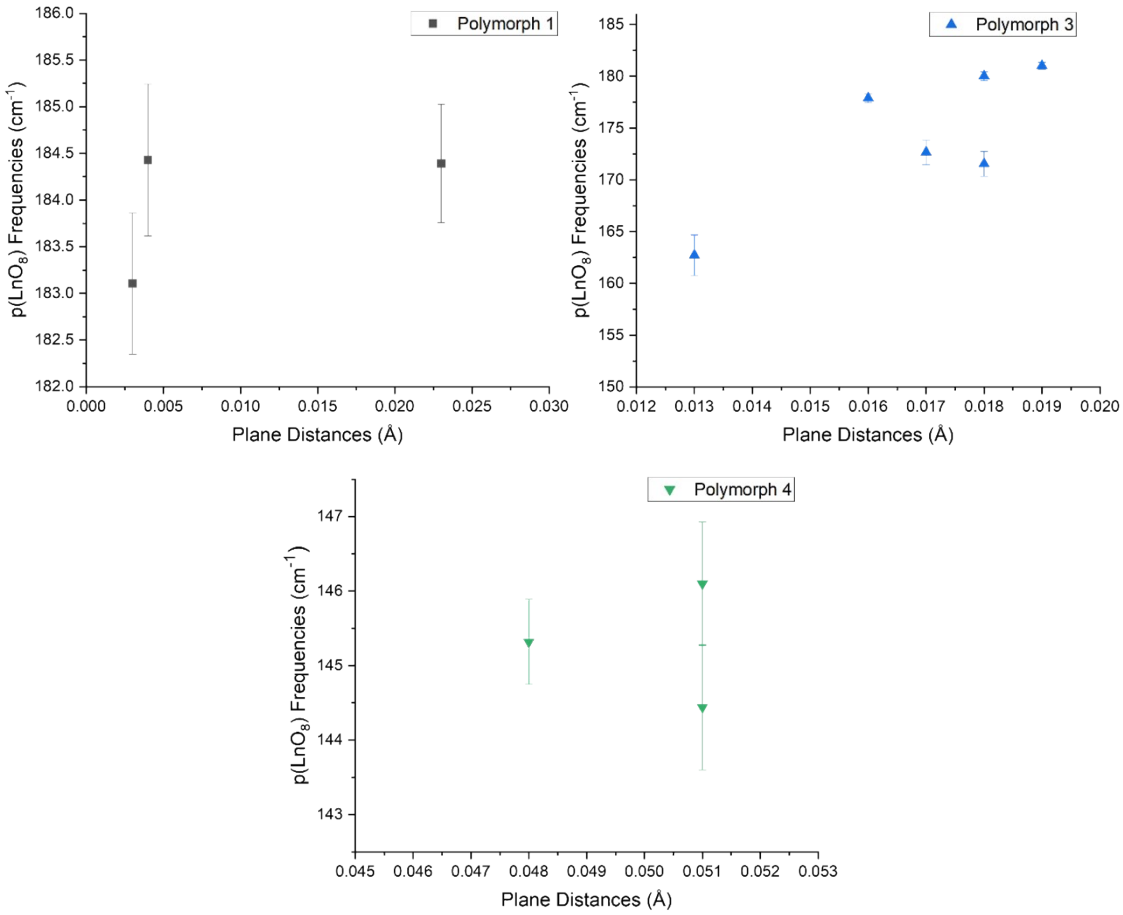

Figure S46. Plots of FIR $\rho(LnO_8)$ frequencies vs. PDs for LnW_{10} polymorphs. The $\rho(LnO_8)$ frequencies were obtained from the fitted FIR spectra of complexes **1-14**. Error bars represent uncertainties of the peak center obtained from the fitting regime.

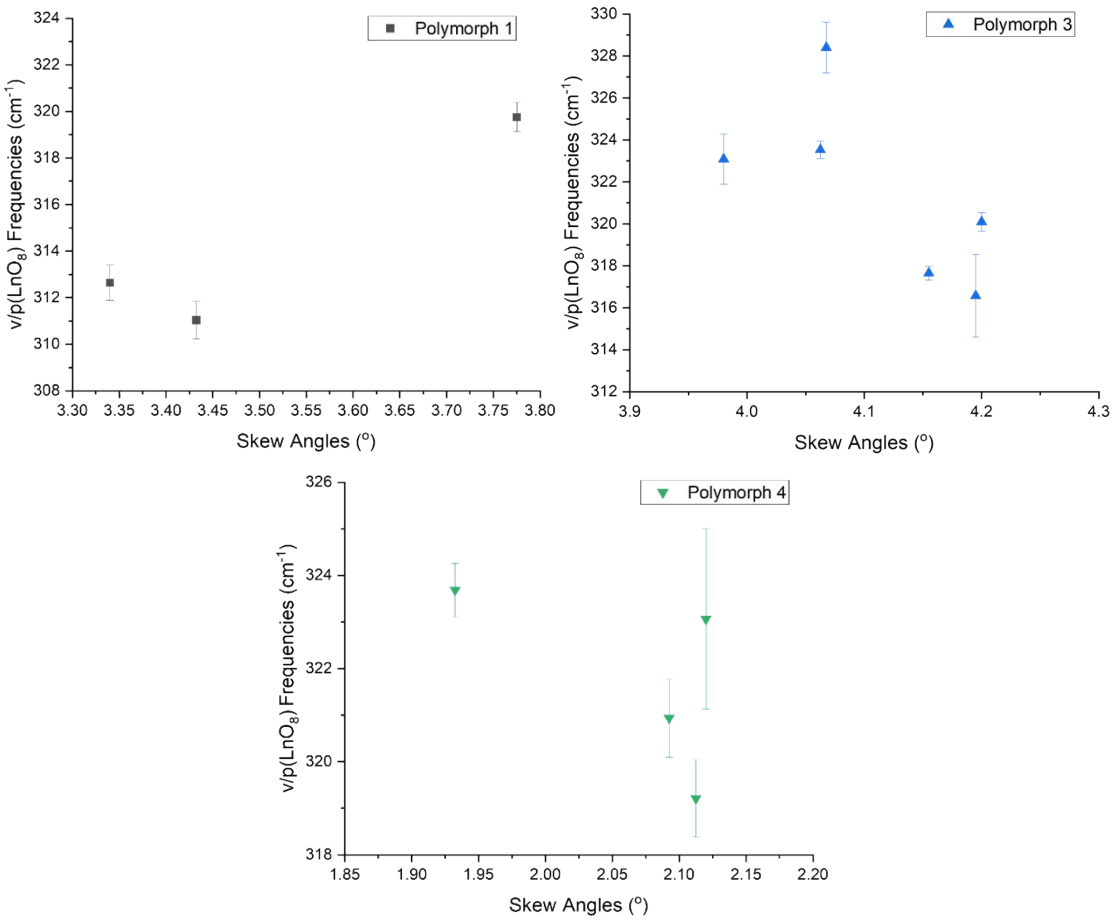

Figure S47. Plots of FIR ν/ρ(LnO_8) frequencies vs. SAs for LnW_{10} polymorphs. The ν/ρ(LnO_8) frequencies were obtained from the fitted FIR spectra of complexes **1-14**. Error bars represent uncertainties of the peak center obtained from the fitting regime.

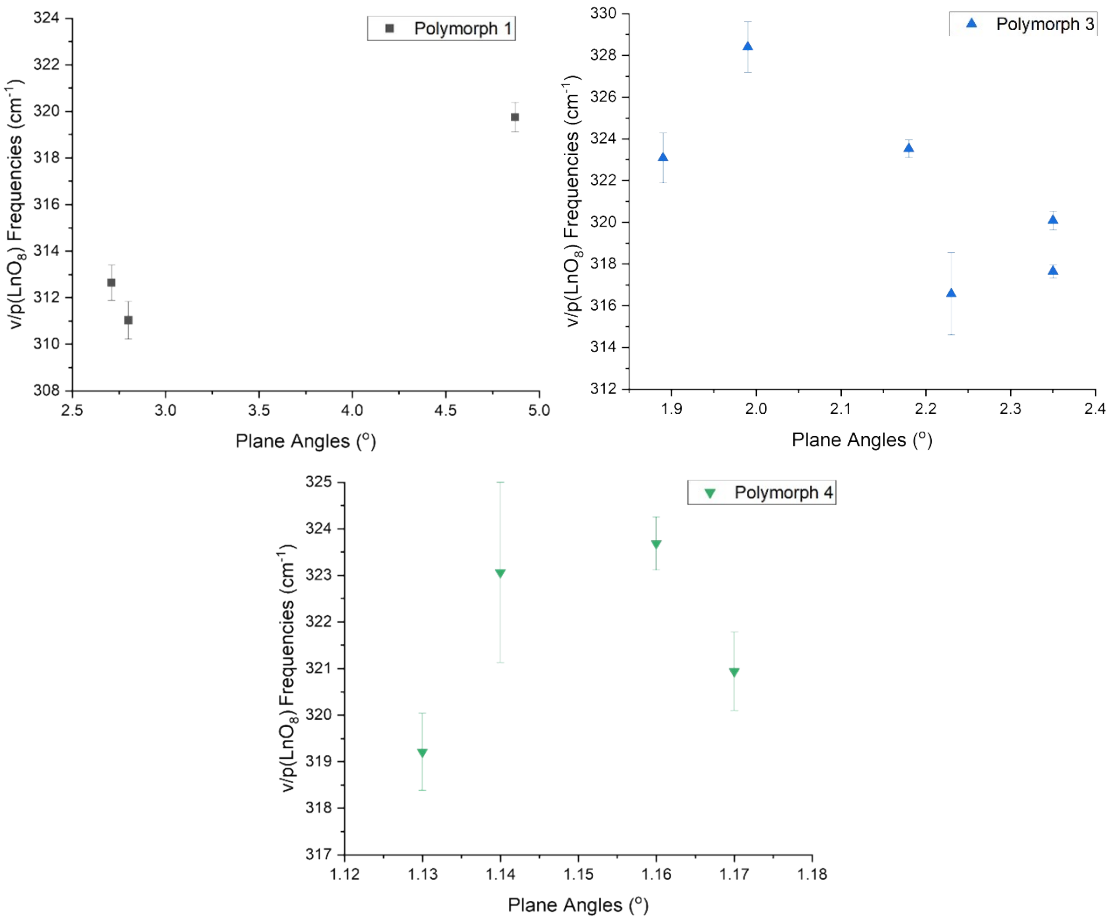

Figure S48. Plots of FIR ν/ρ(LnO_8) frequencies vs. PAs for LnW_{10} polymorphs. The ν/ρ(LnO_8) frequencies were obtained from the fitted FIR spectra of complexes **1-14**. Error bars represent uncertainties of the peak center obtained from the fitting regime.

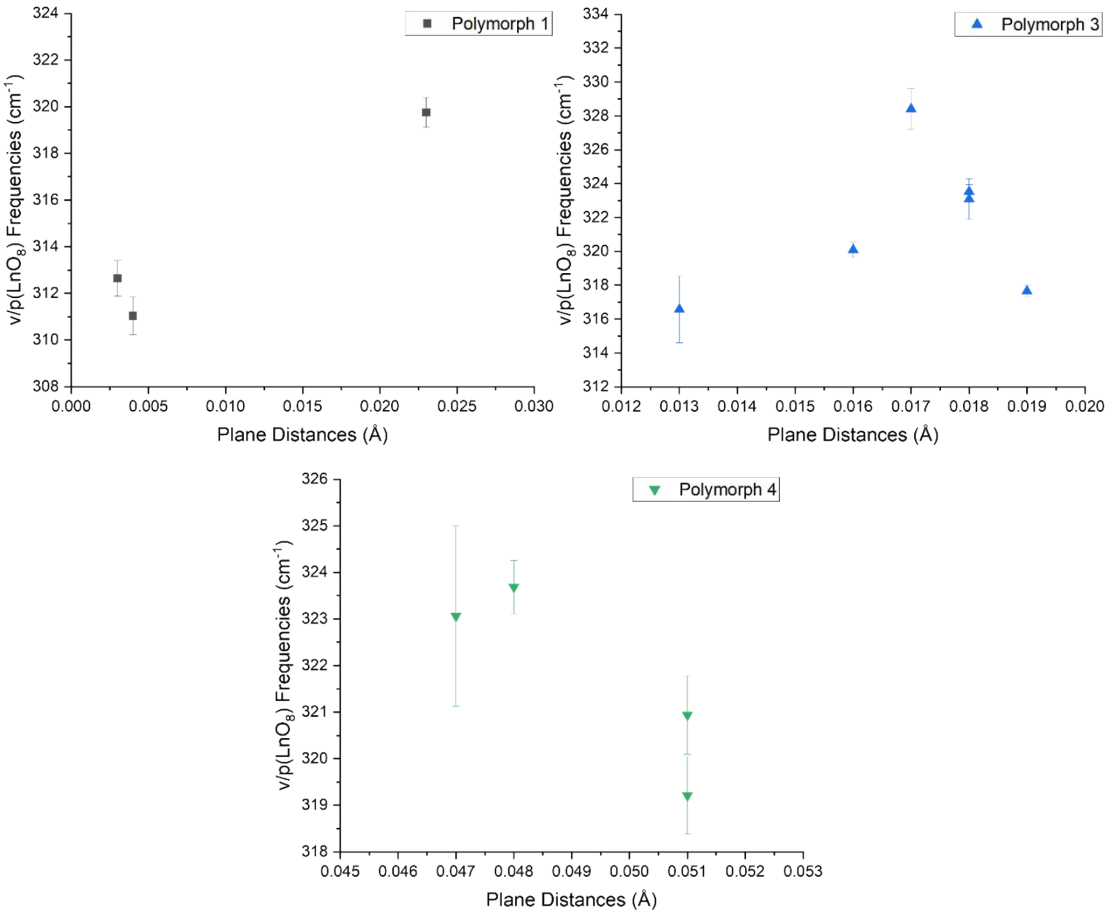

Figure S49. Plots of FIR ν/ρ(LnO_8) frequencies vs. PDs for LnW_{10} polymorphs. The ν/ρ(LnO_8) frequencies were obtained from the fitted FIR spectra of complexes **1-14**. Error bars represent uncertainties of the peak center obtained from the fitting regime.

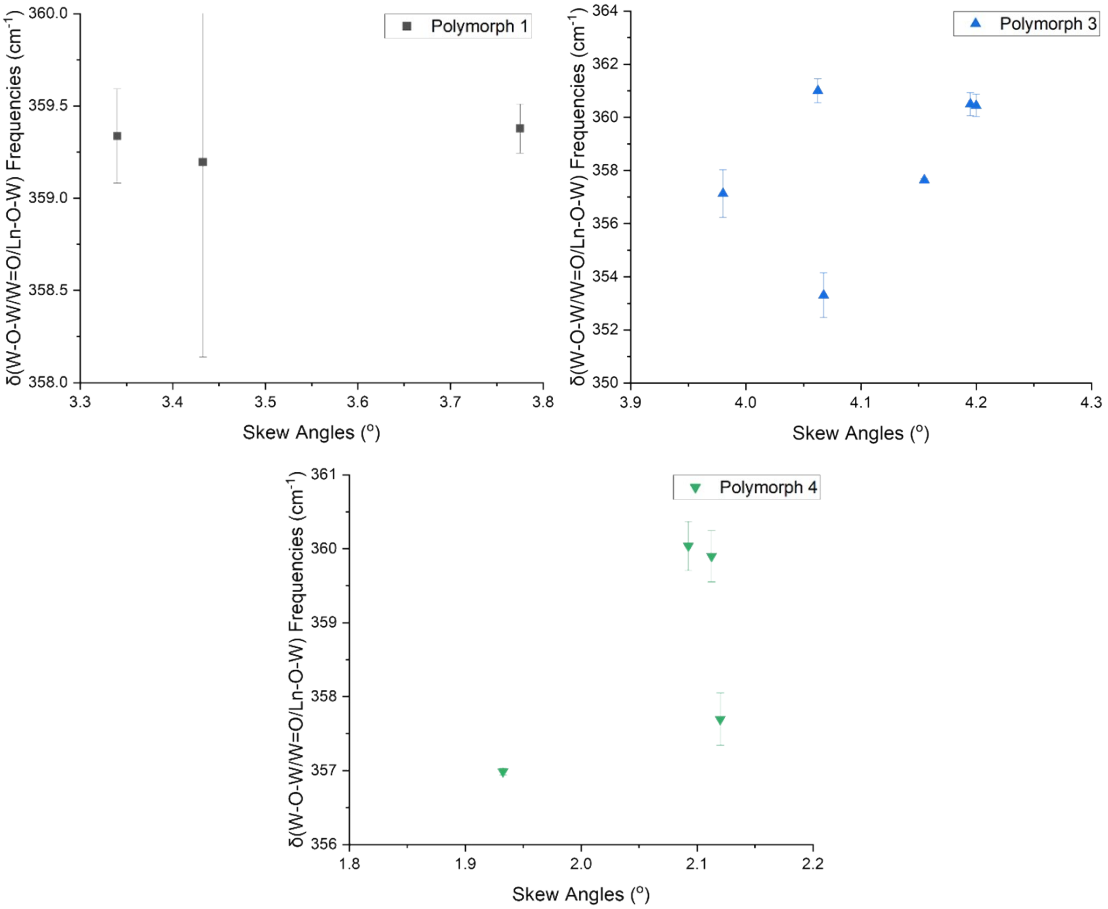

Figure S50. Plots of Raman δ(W-O-W/W=O/Ln-O-W) frequencies vs. SAs for LnW_{10} polymorphs. The δ(W-O-W/W=O/Ln-O-W) frequencies were obtained from the fitted Raman spectra of complexes **1-14**. Error bars represent uncertainties of the peak center obtained from the fitting regime.

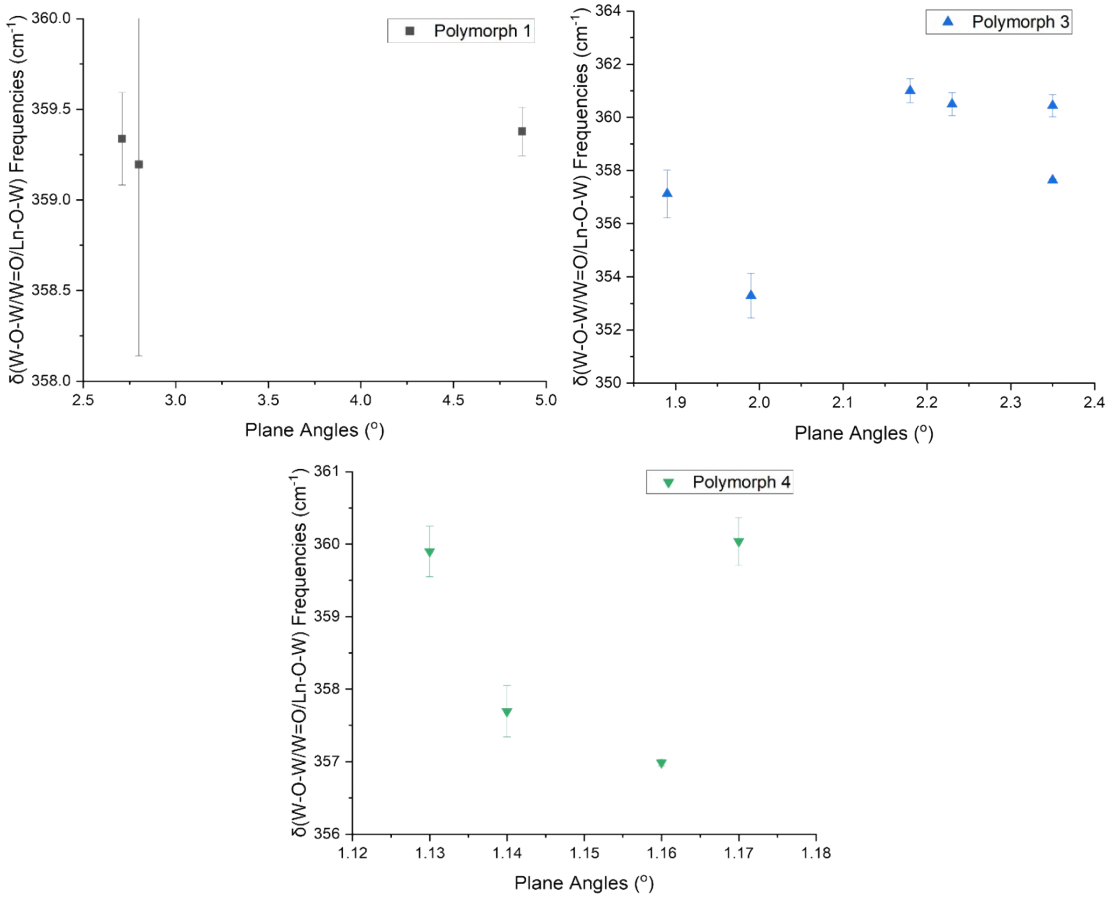

Figure S51. Plots of Raman δ(W-O-W/W=O/Ln-O-W) frequencies vs. PAs for LnW_{10} polymorphs. The δ(W-O-W/W=O/Ln-O-W) frequencies were obtained from the fitted Raman spectra of complexes **1-14**. Error bars represent uncertainties of the peak center obtained from the fitting regime.

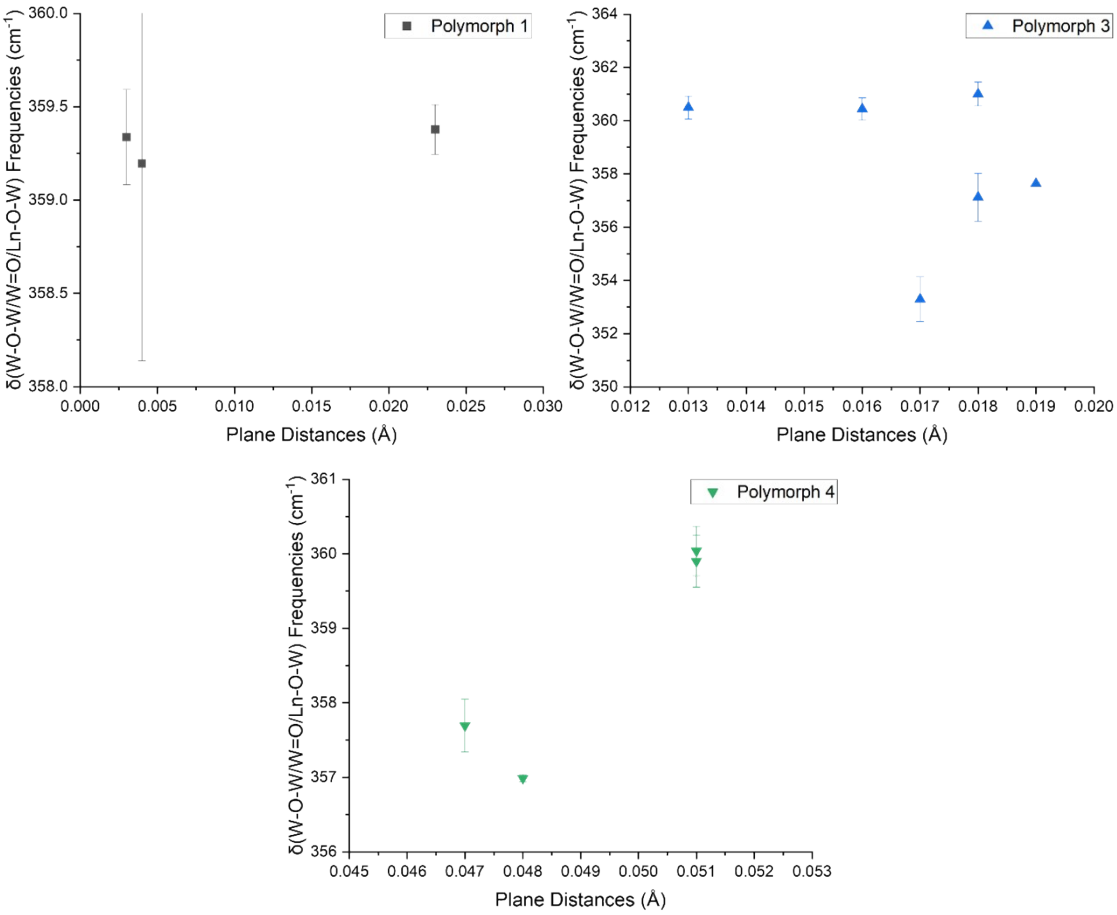

Figure S52. Plots of Raman δ(W-O-W/W=O/Ln-O-W) frequencies vs. PDs for LnW_{10} polymorphs. The δ(W-O-W/W=O/Ln-O-W) frequencies were obtained from the fitted Raman spectra of complexes **1-14**. Error bars represent uncertainties of the peak center obtained from the fitting regime.

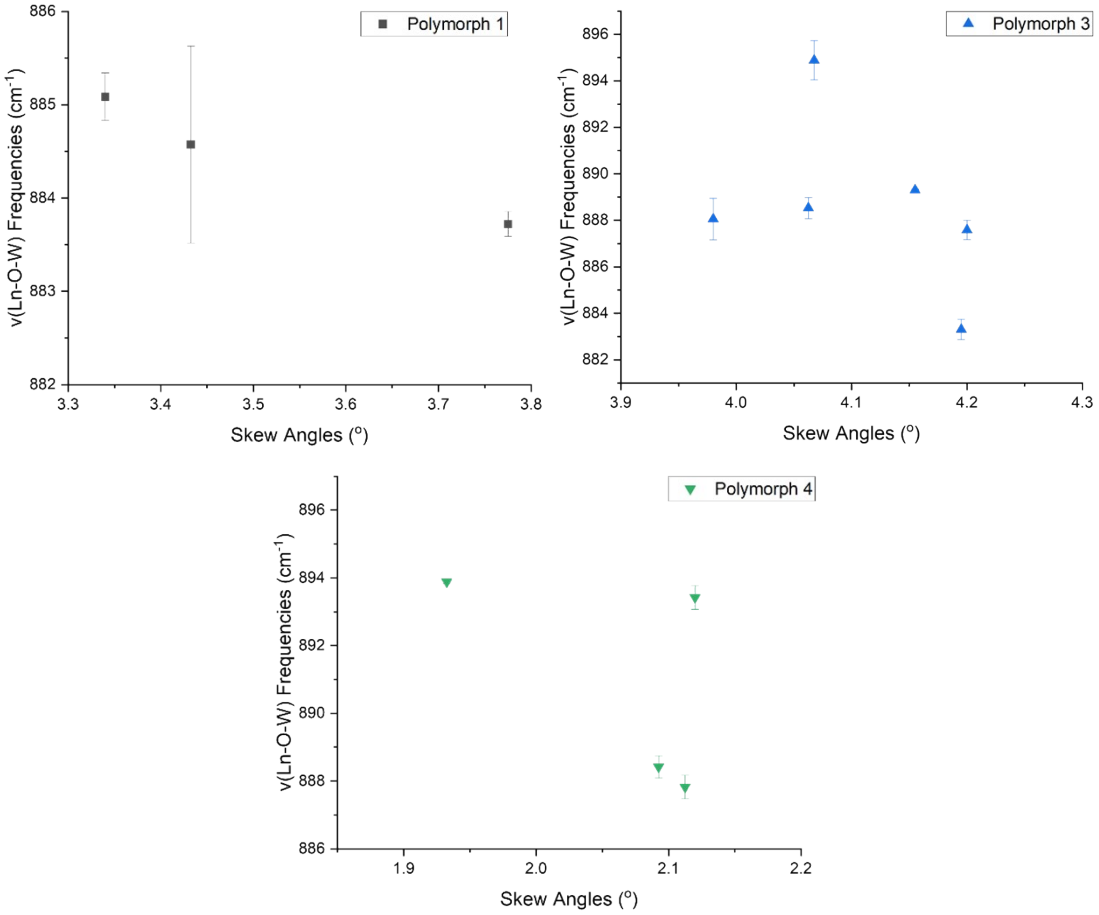

Figure S53. Plots of Raman ν(Ln-O-W) frequencies vs. SAs for LnW_{10} polymorphs. The ν(Ln-O-W) frequencies were obtained from the fitted Raman spectra of complexes **1-14**. Error bars represent uncertainties of the peak center obtained from the fitting regime.

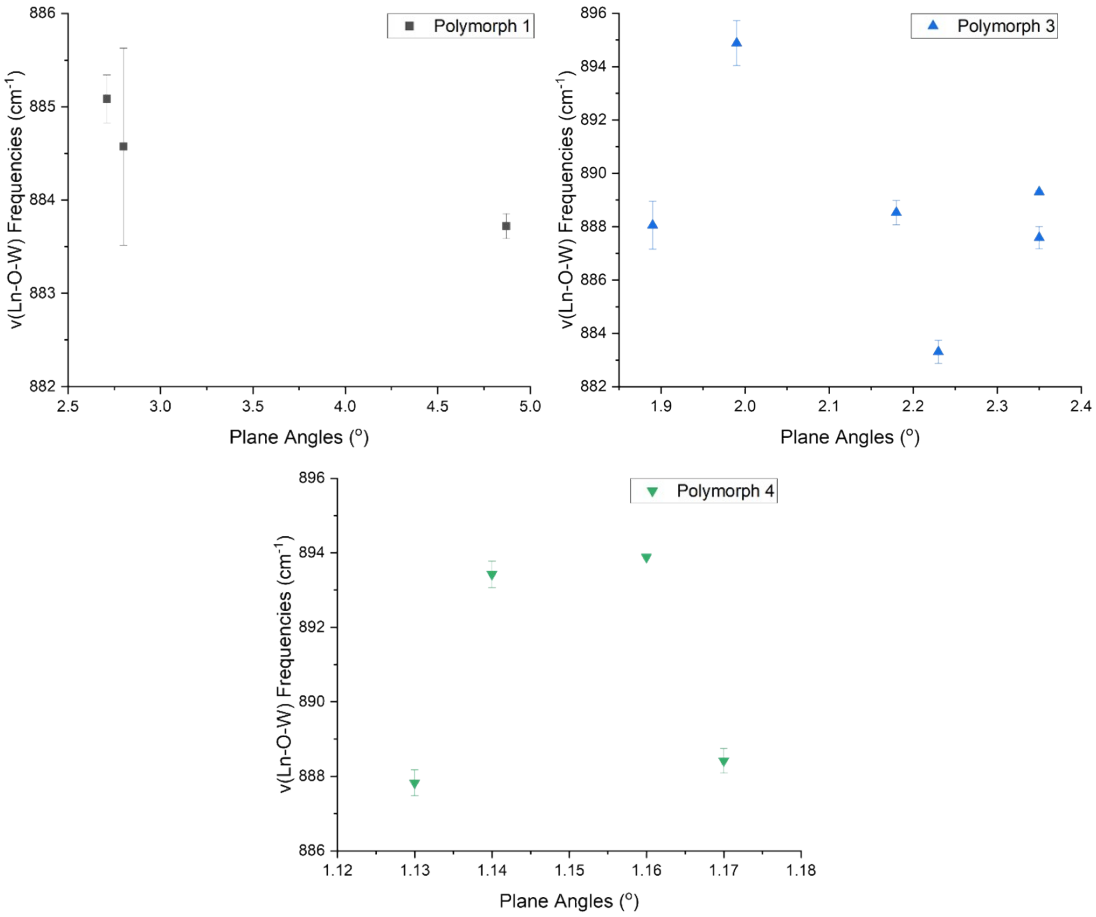

Figure S54. Plots of Raman ν(Ln-O-W) frequencies vs. PAs for LnW_{10} polymorphs. The ν(Ln-O-W) frequencies were obtained from the fitted Raman spectra of complexes **1-14**. Error bars represent uncertainties of the peak center obtained from the fitting regime.

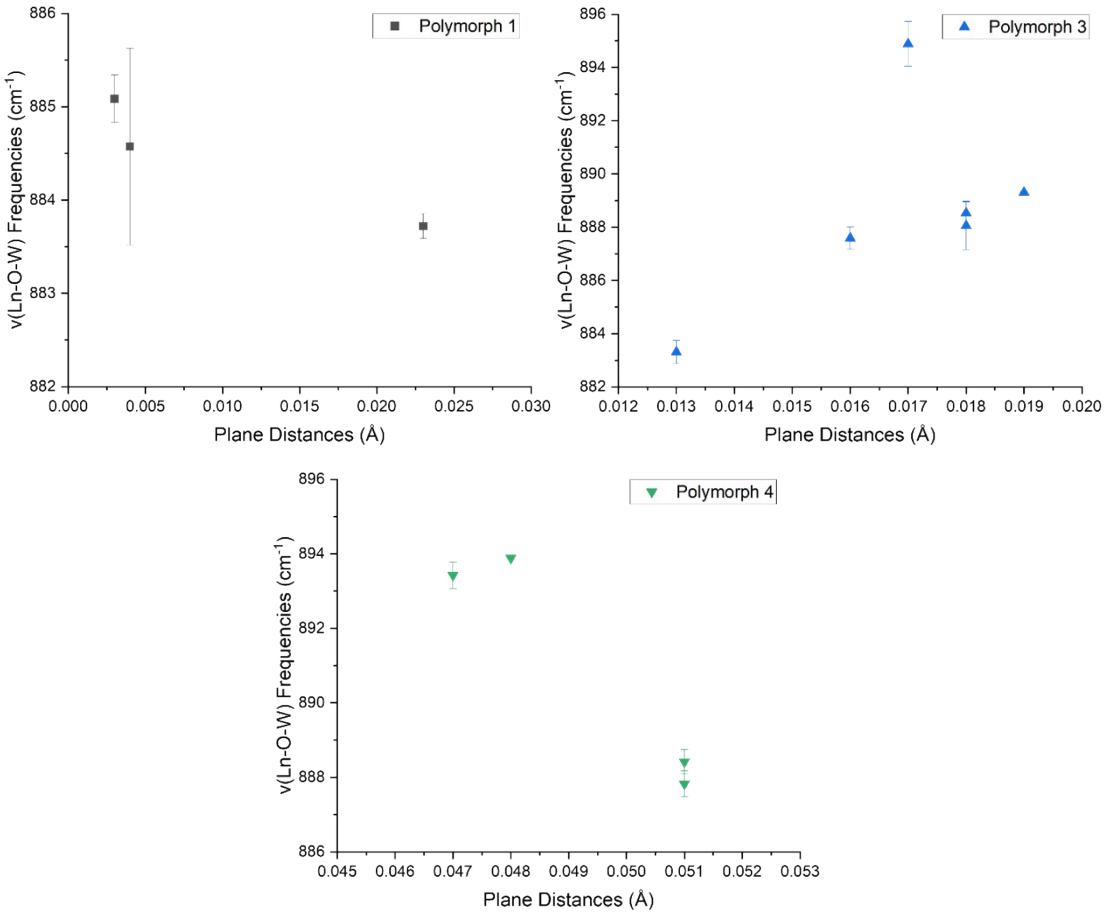

Figure S55. Plots of Raman ν(Ln-O-W) frequencies vs. PDs for LnW_{10} polymorphs. The ν(Ln-O-W) frequencies were obtained from the fitted Raman spectra of complexes **1-14**. Error bars represent uncertainties of the peak center obtained from the fitting regime.

Partial Least Squares (PLS) Analysis. PLS is a mix of both principal component and multiple regression analysis and is often used to identify factors that contribute to covariances between the independent and dependent variables.[2] Partial Least Square analysis was conducted with the OriginPro2023b software package[3] using the singular value decomposition (SVD) method in which:

$X = n \bullet m$

$Y = n \bullet r$

Where X is the matrix size for the independent variables and Y is the matrix size for the dependent variables and n, m, and r are the number of observations, number of independent variables, and number of dependent variables, respectively. The mean from each column in matrix X and Y are subtracted to produce X_0 and Y_0. In SVD, the weight (w) of the independent variables is extracted by normalizing the first left singular vector of $X_0^T Y_0$ which then is used to calculate:

$t = X_0 w$

$p = X_0^T t$

$q = Y_0^T t$

$u = Y_0 q$

where t, p, q, and u are the x scores, y scores, x loadings, and y loadings which can also be expressed by matrices, T, P, Q, and U. These parameters are then refined against the residual matrices, $\mathbf{k}$, until they converge, and $\mathbf{k}$ factors can be synthesized to construct the model.

The leave-one-out cross-validation (CV) method tests the performance of a model and is often used to prevent overfitting of a model by producing multiple models with one of the independent variables left out and looking into which combination of independent variables give the best model to predict the dependent variables.[2] In Origin2023b, this is done by finding the minimum root mean PRESS (predicted residual sum of squares) which can be found by using the following equation:

$$PRESS = \sum_{i=1}^{n} \sum_{j=1}^{r} \left(Y_{ij} - \hat{Y}_{ij}\right)^2$$

$$Root\ Mean\ PRESS = \sqrt{\frac{PRESS}{(n-1)r}}$$

Y_{ij} represents the predicted value of Y based on the leave-one-out cross-validation test. Prediction of dependent variables can then be done by calculating the coefficients of the fitted model which can be obtained from the following equation:

$$C = W(P^T W)^{-1} Q^T$$

where C and W are coefficient and weight matrices, respectively. The predicted dependent variables value can then be calculated by:

$$\hat{Y}_0 = C X_0$$

From PLS analysis, a variety of figures are generated; however, only the root mean PRESS plot, Y-variance accountability plot, variable influence on projection (VIP) plot, and diagnostic plots are presented here. The root mean PRESS plot shows the results of the CV test with the optimal number of factors having the lowest root mean PRESS value. The Y-variance accountability plots show how each factor accounts for the

variance in the dependent (*Y*) variable. In Origin2023b the variance explained for *Y* variables is calculated using the following equation:

$$\frac{\sum_{j=1}^{k} Q_{lj}^{2}}{\sum_{i=1}^{n} Y_{0il}^{2}}$$

The VIP plots show the significance of each independent variable related to the dependent variable with a VIP value above 0.8 indicating statistical significance. Four diagnostic plots are generated by the PLS analysis which include: the actual versus predicted dependent variable value plots that show the quality of the model generated based on the independent variables inputted, the residual versus observed and predicted dependent variable plots that provide information regarding the distribution of the dependent variable dataset where a normal distribution exhibits random scattering of the data around the fitted line with a constant bandwidth, and the normal percentile plot which also provides information about data distribution with a normal distribution of data represented by the residual against percentiles forming a linear line.

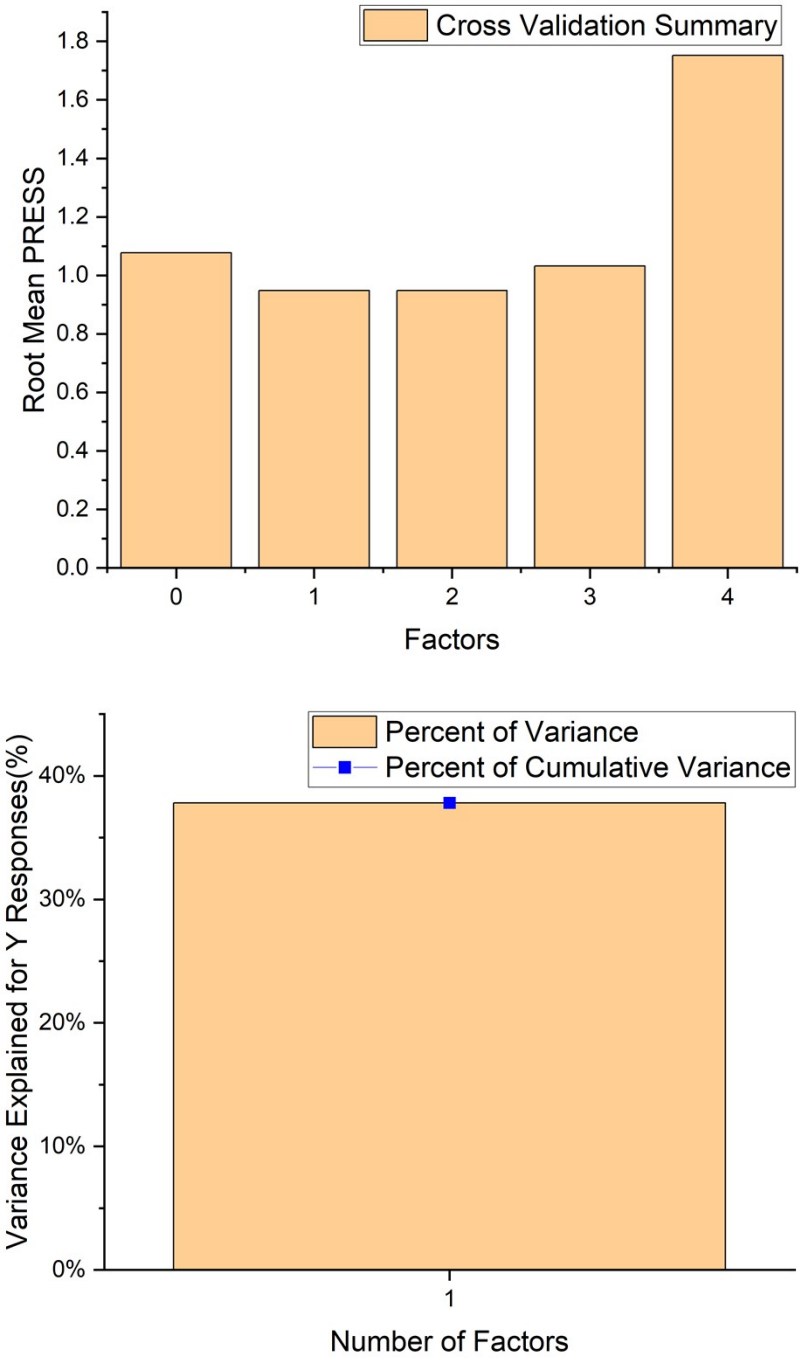

Figure S56. (Top) Root mean PRESS and (**Bottom**) Y-variance accountability plots for SAs, PAs, PDs, and ionic radii as independent variables with the $\nu(WO_5)_2$ frequencies as the dependent variable. The $\nu(WO_5)_2$ frequencies were obtained from the fitted FIR spectra of complexes **1-14**.

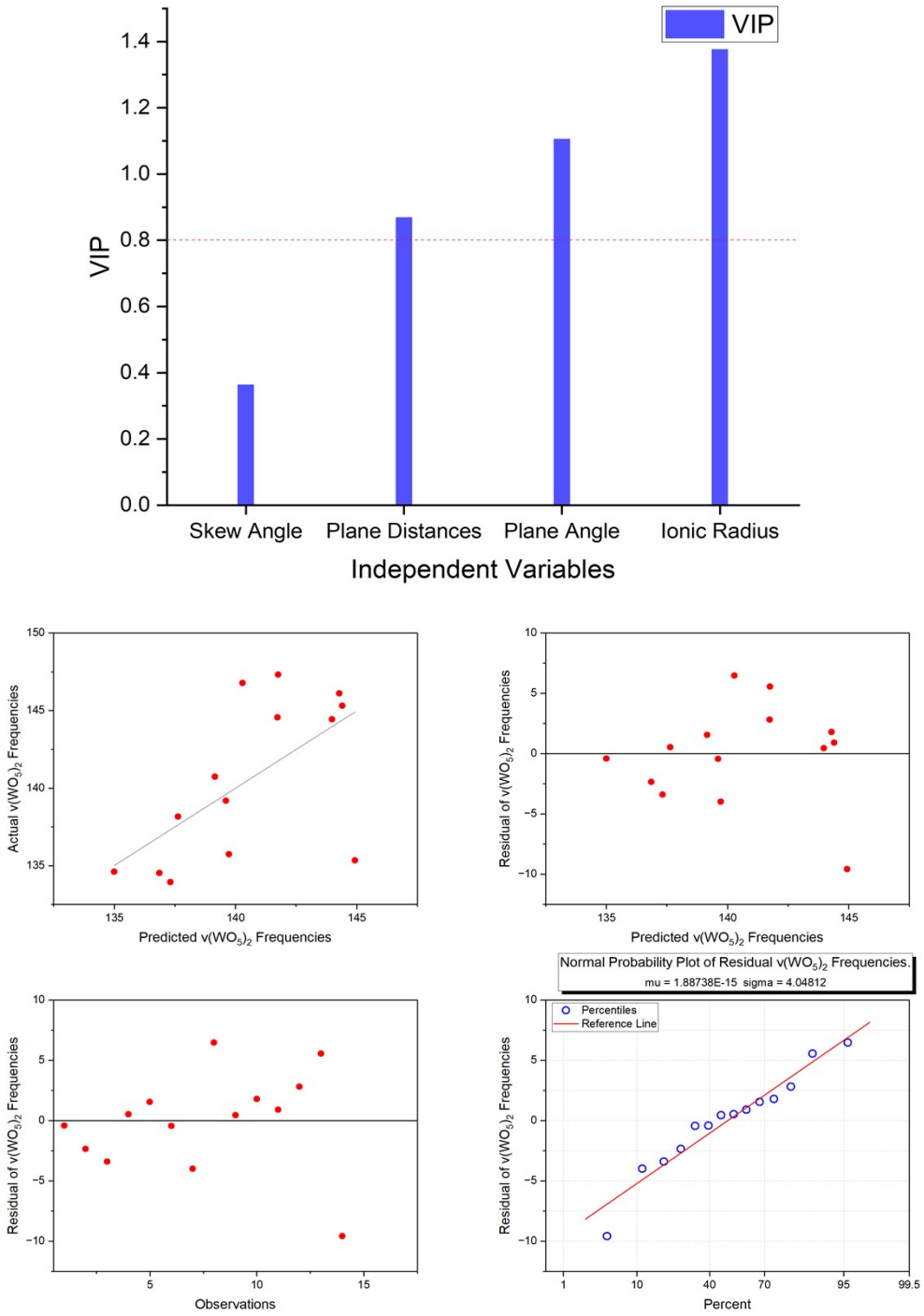

Figure S57. (**Top**) VIP plot and (**Bottom**) diagnostic plots for SAs, PAs, PDs, and ionic radii as independent variables with $\nu(WO_5)_2$ frequencies as the dependent variable. The $\nu(WO_5)_2$ frequencies were obtained from the fitted FIR spectra of complexes **1-14**.

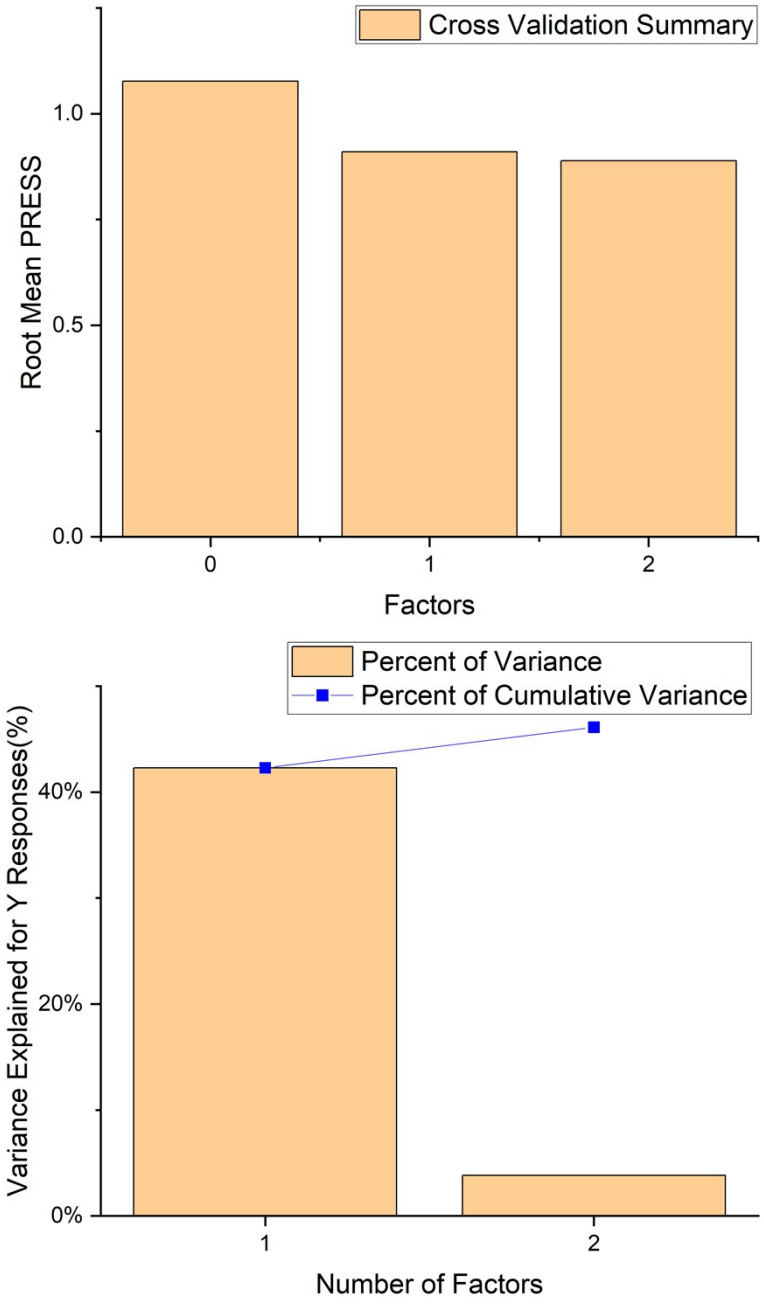

Figure S58. (Top) Root mean PRESS and (**Bottom**) Y-variance accountability plots for PAs and ionic radii as the independent variables and $\nu(WO_5)_2$ frequencies as the dependent variable. The $\nu(WO_5)_2$ frequencies were obtained from the fitted FIR spectra of complexes **1-14**.

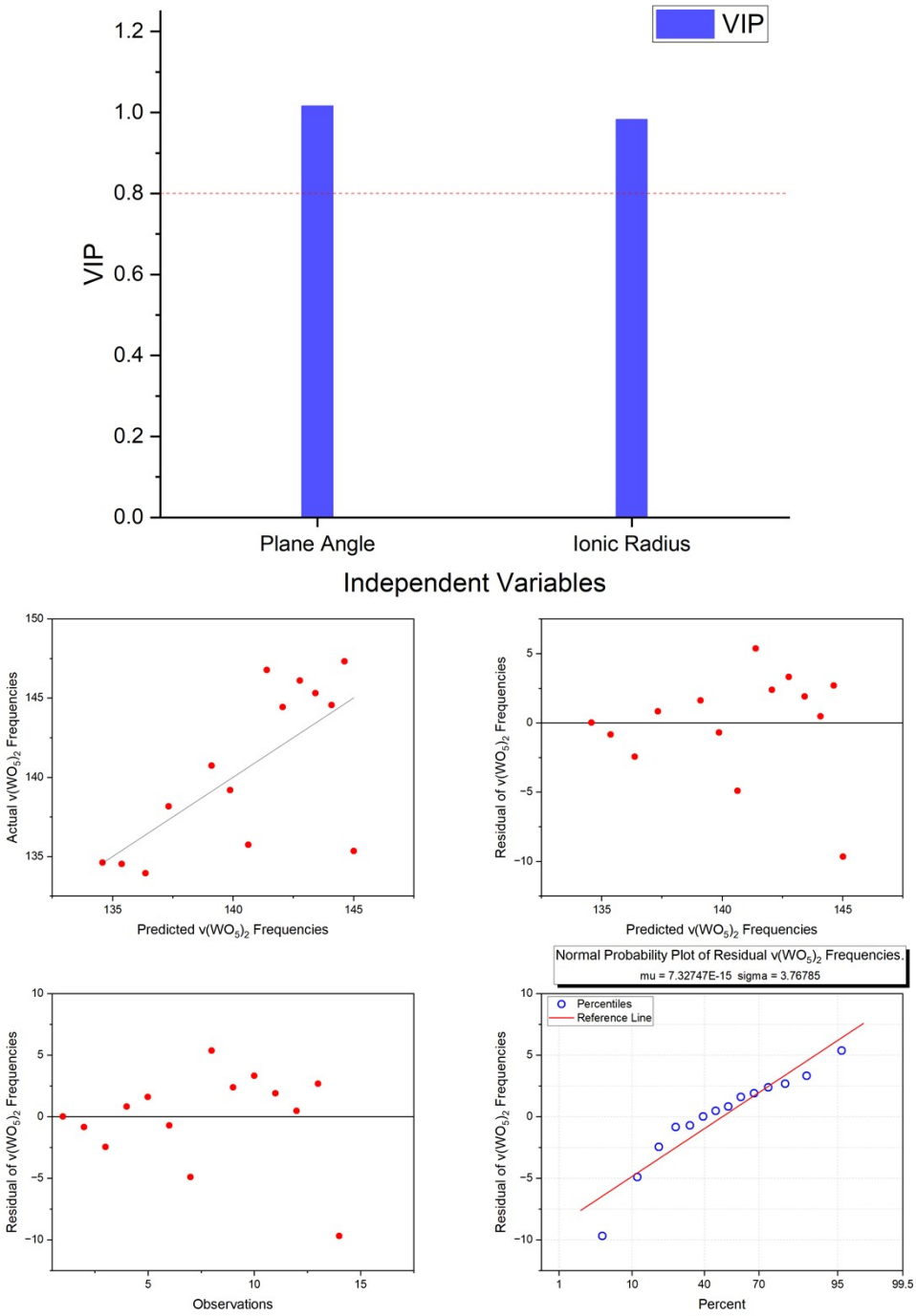

Figure S59. (**Top**) VIP plot and (**Bottom**) diagnostic plots for PAs and ionic radii as independent variables with $\nu(WO_5)_2$ frequencies as the dependent variable. The $\nu(WO_5)_2$ frequencies were obtained from the fitted FIR spectra of complexes **1-14**.

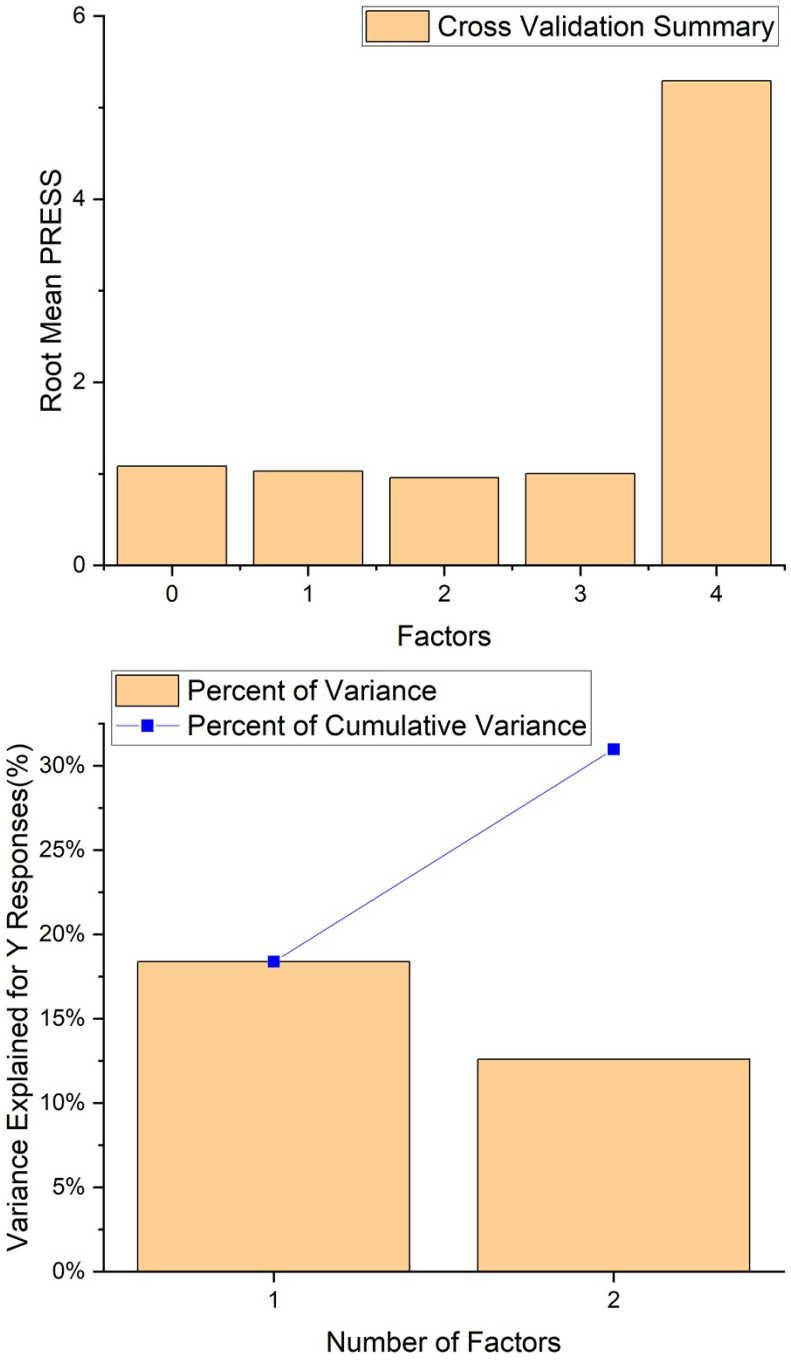

Figure S60. (**Top**) Root mean PRESS and (**Bottom**) Y-variance accountability plots for SAs, PAs, PDs, and ionic radii as independent variables with $\rho(LnO_8)$ frequencies as the dependent variable. The $\rho(LnO_8)$ frequencies were obtained from the fitted FIR spectra of complexes **1-14**.

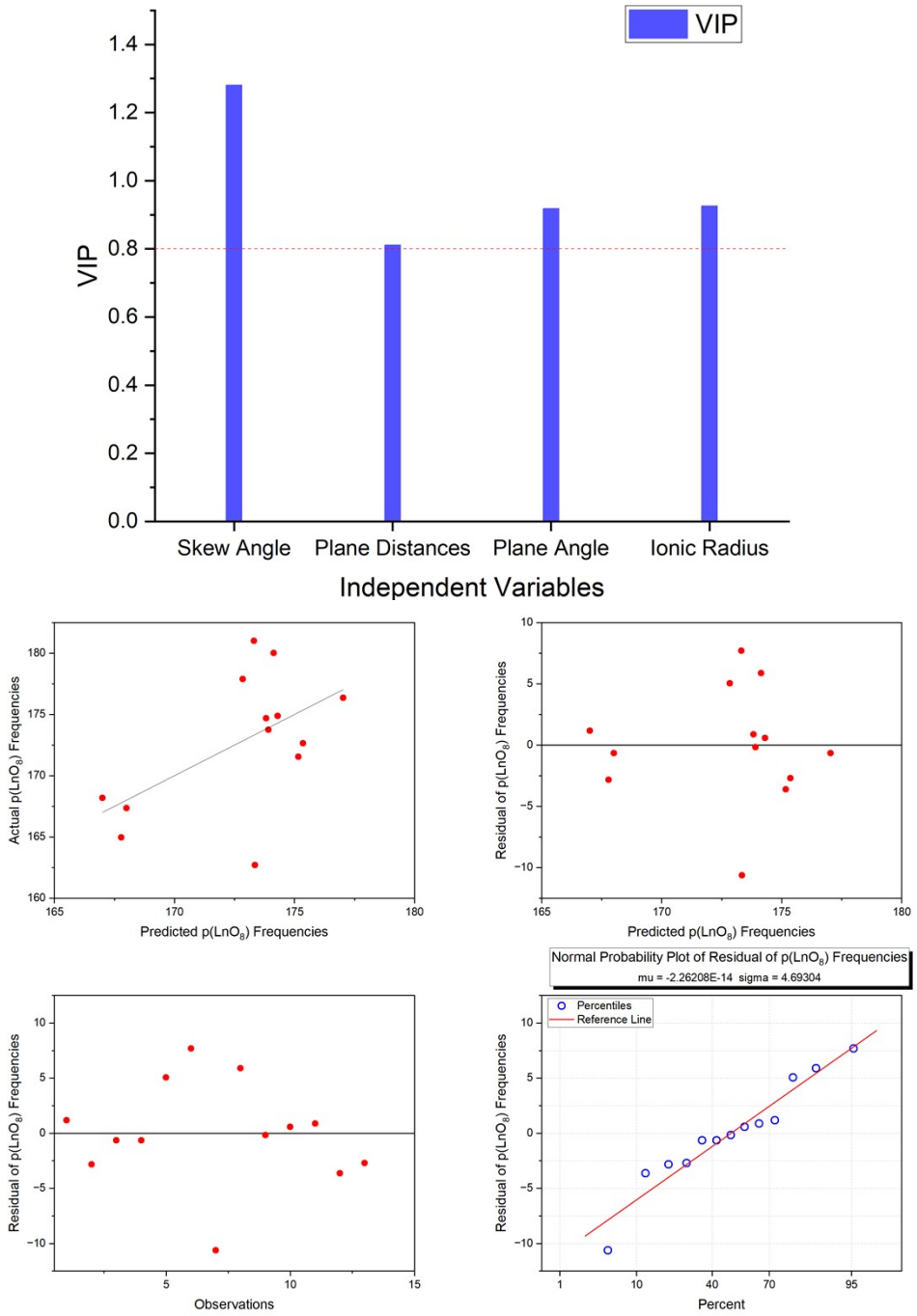

Figure S61. (**Top**) VIP plot and (**Bottom**) diagnostic plots for SAs, PAs, PDs, and ionic radii as independent variables and $\rho(LnO_8)$ frequencies as the dependent variable. The $\rho(LnO_8)$ frequencies were obtained from the fitted FIR spectra of complexes **1-14**.

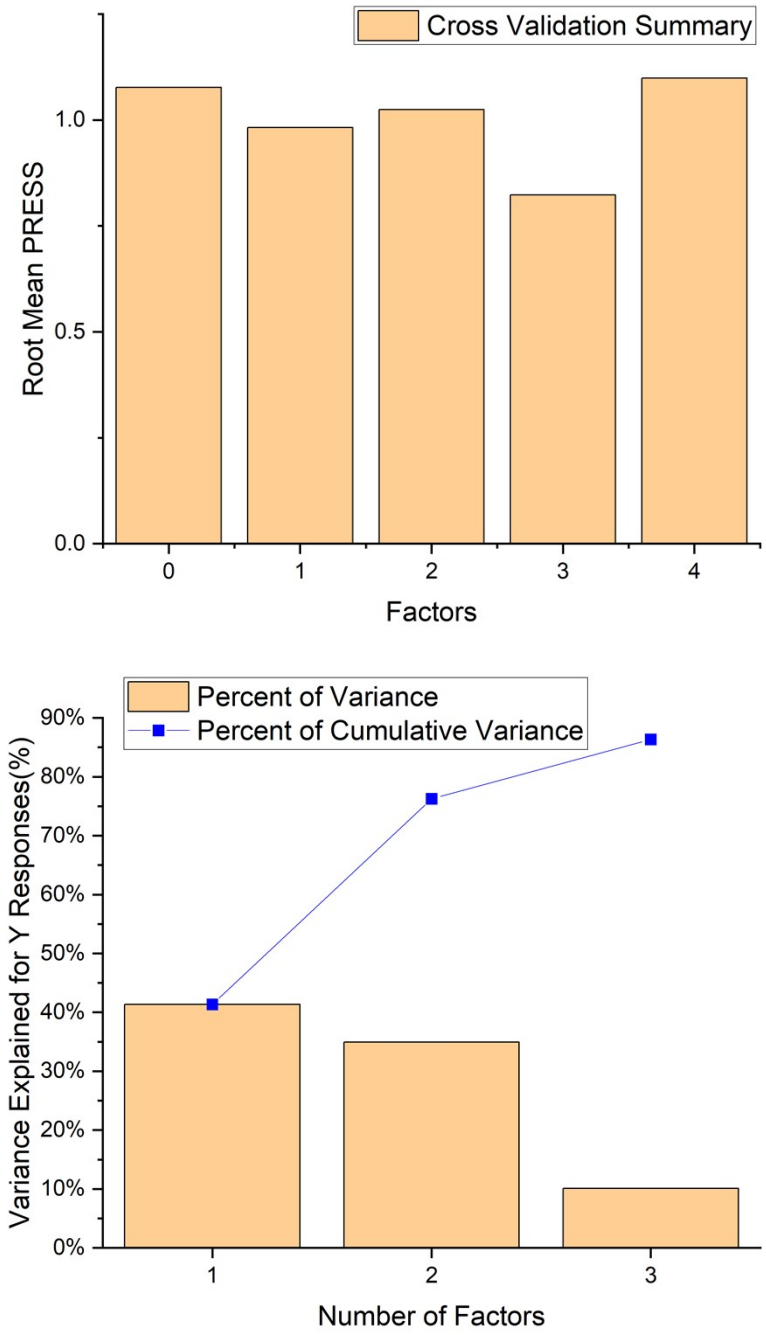

Figure S62. (**Top**) Root mean PRESS and (**Bottom**) Y-variance accountability plots for SAs, PAs, PDs, and ionic radii as independent variables with ν/ρ(LnO_8) frequencies as the dependent variable. The ν/ρ(LnO_8) frequencies were obtained from the fitted FIR spectra of complexes **1-14**.

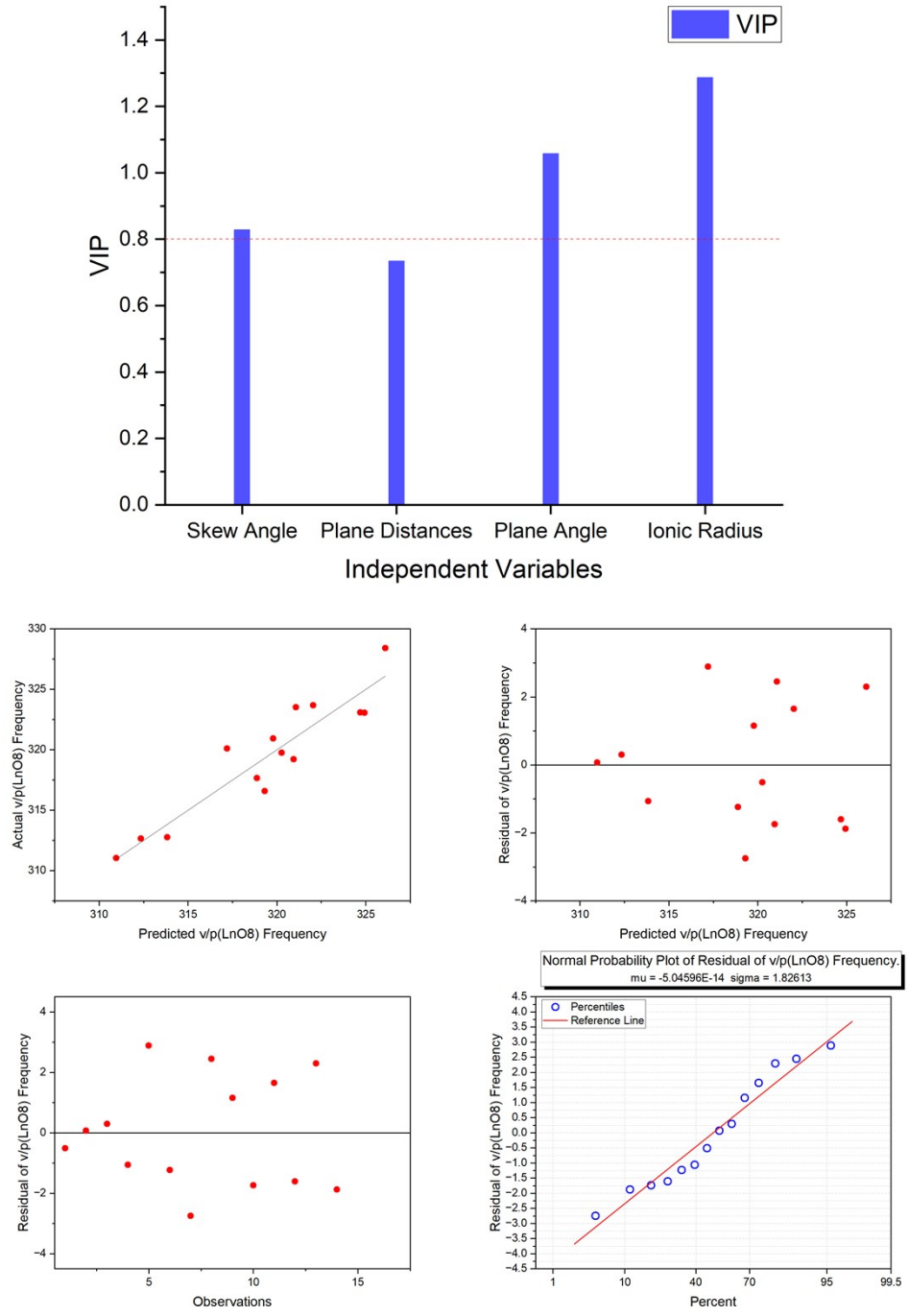

Figure S63. (**Top**) VIP plot and (**Bottom**) diagnostic plots for SAs, PAs, PDs, and ionic radii as independent variables and ν/ρ(LnO_8) frequencies as the dependent variable. The ν/ρ(LnO_8) frequencies were obtained from the fitted FIR spectra of complexes **1-14**.

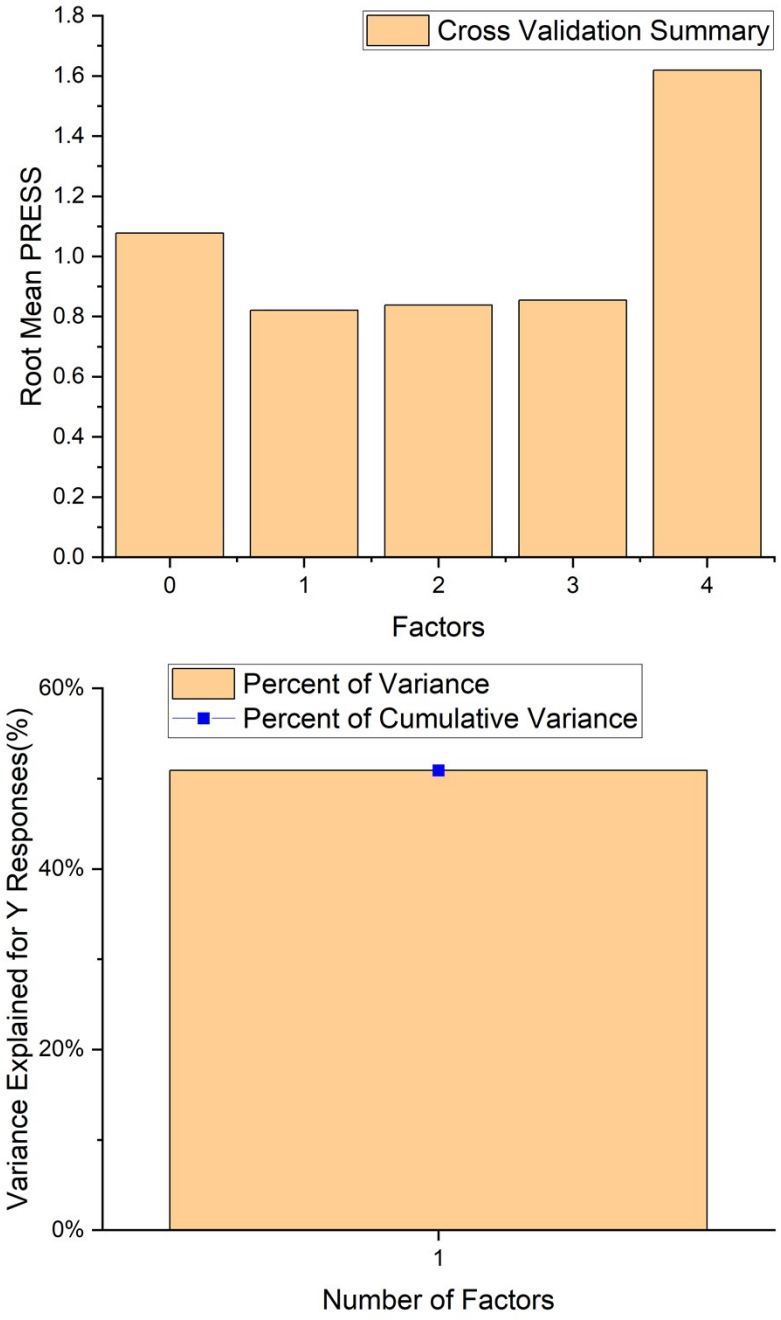

Figure S64. (Top) Root mean PRESS and (**Bottom**) Y-variance accountability plots for SAs, PAs, PDs, and ionic radii as independent variables with ν(Ln-O-W) frequencies as the dependent variable. The ν(Ln-O-W) frequencies were obtained from the fitted Raman spectra of complexes **1-14**.

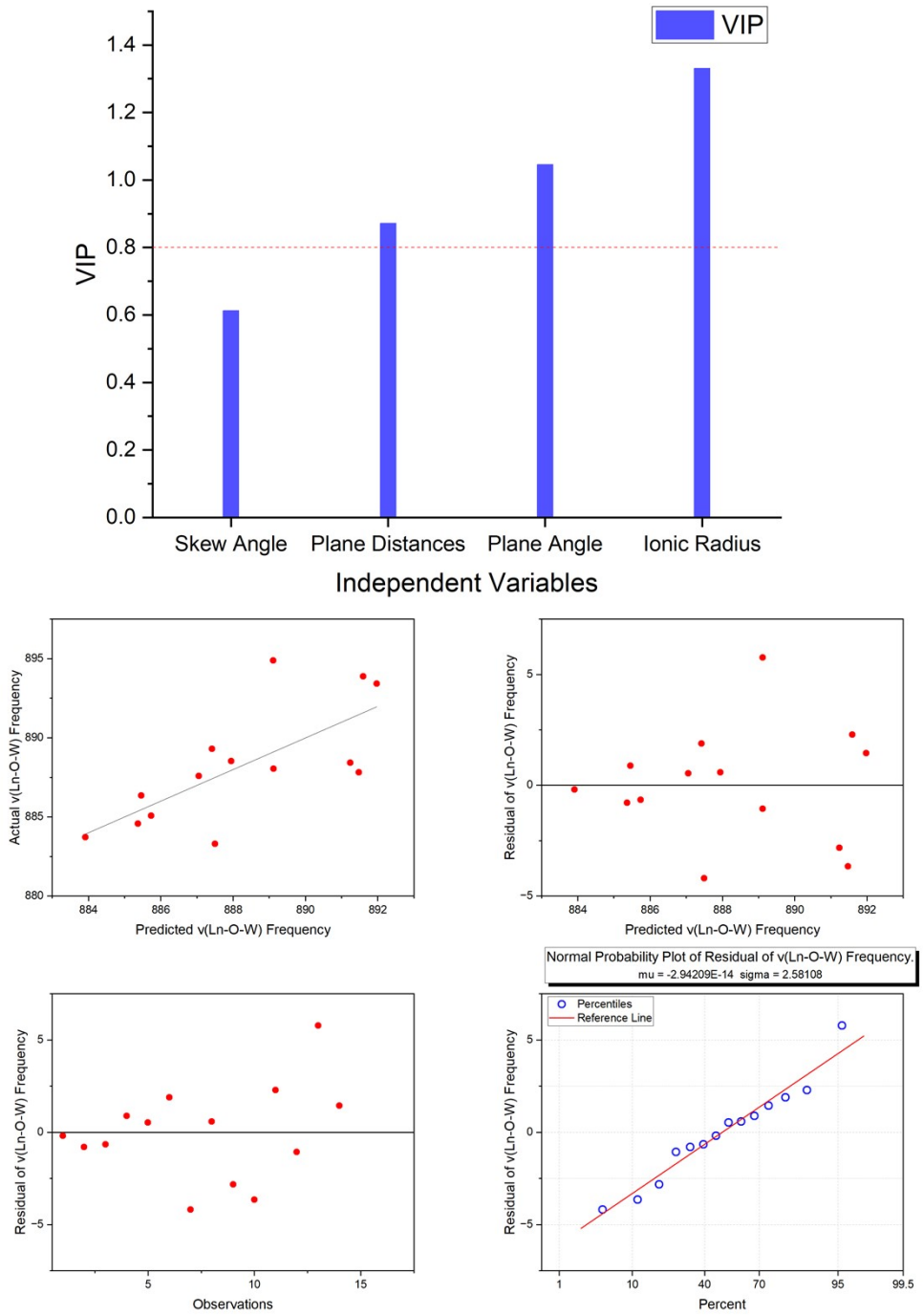

Figure S65. (**Top**) VIP plot and (**Bottom**) diagnostic plots for SAs, PAs, PDs, and ionic radii as independent variables and ν(Ln-O-W) frequencies as the dependent variable. The ν(Ln-O-W) frequencies were obtained from the fitted Raman spectra of complexes **1-14**.

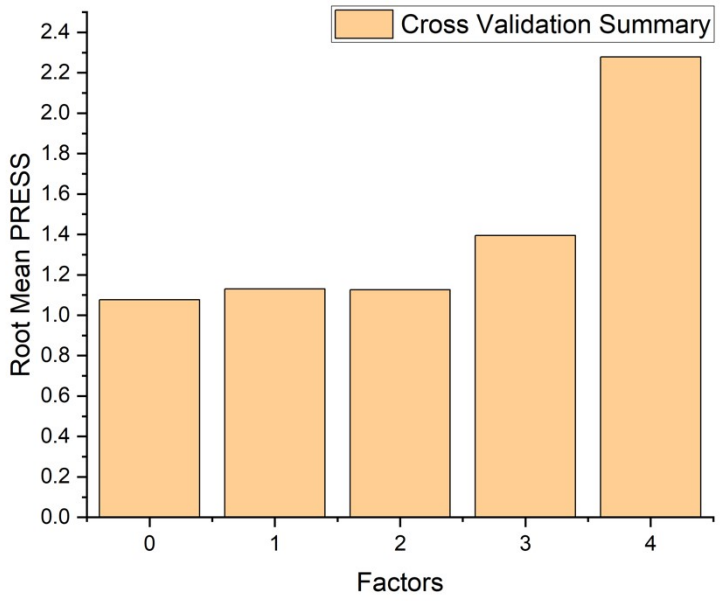

Figure S66. (Top) Root mean PRESS for SAs, PAs, PDs, and ionic radii as independent variables and the δ(W-O-W/ W=O/ Ln-O-W) Raman frequencies as the dependent variable. Full PLS analysis was not conducted due to the CV finding zero factors from the independent variables that had statistically significant effects on δ(W-O-W/ W=O/ Ln-O-W) Raman frequencies.

References

1. L. Kazanskii, A. Golubev, I. Baburina, E. Torchenkova and V. Spitsyn, *Bull. Acad. Sci. USSR, Div. Chem. Sci.*, 1978, **27**, 1956-1960.
2. P. Geladi and B. R. Kowalski, *Anal. Chim. Acta*, 1986, **185**, 1-17.
3. OriginPro, Version 2023b, Origin Lab Corporation, Northampton, MA, USA.
4. A. E. Gelfand, D. K. Dey and H. Chang, *Model Determination Using Predictive Distributions with Implementation via Sampling-Based Methods*, Technical Report No. 462, U.S. Office of Naval Research, 1992.